

Oralloy (93.15²³⁵U) Metal Annuli with Beryllium Core

John D. Bess
Leland M. Montierth
Raymond J. Reed
Nicholas J. Schira
John T. Mihalczo

September 2010



The INL is a U.S. Department of Energy National Laboratory
operated by Battelle Energy Alliance

Oralloy (93.15²³⁵U) Metal Annuli with Beryllium Core

John D. Bess
Leland Montierth
Raymond L. Reed¹
Nicholas J. Schira¹
John T. Mihalczo²

¹Washington Safety Management Solutions LLC

²Oak Ridge National Laboratory

September 2010

**Idaho National Laboratory
Idaho Falls, Idaho 83415**

<http://www.inl.gov>

Prepared for the
U.S. Department of Energy
Office of Nuclear Energy
Under DOE Idaho Operations Office
Contract DE-AC07-05ID14517

ORALLOY (93.15 ^{235}U) METAL ANNULI WITH BERYLLIUM CORE

Evaluator

John D. Bess
Idaho National Laboratory

Internal Reviewer
Leland M. Montierth

Independent Reviewers

Raymond L. Reed
Nicholas J. Schira
Washington Safety Management Solutions LLC

John T. Mihalczo
Oak Ridge National Laboratory

ORALLOY (93.15 ^{235}U) METAL ANNULI WITH BERYLLIUM CORE

IDENTIFICATION NUMBER: HEU-MET-FAST-059

SPECTRA

KEY WORDS: acceptable, annuli, beryllium-moderated, beryllium-reflected, critical experiment, cylinder, fast-spectrum, highly enriched, metal, oralloy, uranium

1.0 DETAILED DESCRIPTION

1.1 Overview of Experiment

A variety of critical experiments were constructed of enriched uranium metal (oralloy^a) during the 1960s and 1970s at the Oak Ridge Critical Experiments Facility (ORCEF) in support of criticality safety operations at the Y-12 Plant. The purposes of these experiments included the evaluation of storage, casting, and handling limits for the Y-12 Plant and providing data for verification of calculation methods and cross-sections for nuclear criticality safety applications. These included solid cylinders of various diameters, annuli of various inner and outer diameters, two and three interacting cylinders of various diameters, and graphite and polyethylene reflected cylinders and annuli.

Of the hundreds of delayed critical experiments, two were performed that consisted of uranium metal annuli surrounding a solid beryllium metal core. The outer diameter of the annuli was approximately 13 or 15 inches with an inner diameter of 7 inches. The diameter of the beryllium was 7 inches. The critical height of the configurations was approximately 5 and 4 inches, respectively. The uranium annulus consisted of multiple stacked rings, each with radial thicknesses of 1 inch and varying heights. The 15-inch experiment was performed on June 4, 1963, and the 13-inch experiment on July 12, 1963 by J. T. Mihalczo and D. L. Bentzinger (Ref. 1) with additional information in its corresponding logbook.^b

Unreflected and unmoderated experiments with the same set of highly enriched uranium metal parts were performed at the Oak Ridge Critical Experiments Facility in the 1960s and are evaluated in [HEU-MET-FAST-051](#). Thin graphite reflected (2 inches or less) experiments also using the same set of highly enriched uranium metal parts are evaluated in [HEU-MET-FAST-071](#). Polyethylene-reflected configurations are evaluated in [HEU-MET-FAST-076](#). A stack of highly enriched metal discs with a thick beryllium top reflector is evaluated in [HEU-MET-FAST-069](#).

Both detailed and simplified model specifications are provided in this evaluation. Both of these fast neutron spectra experiments were determined to be acceptable benchmark experiments. The calculated eigenvalues for both the detailed and the simple models are within approximately 0.6% of the benchmark values, but exceed the benchmark values by significantly greater than 3σ from the benchmark value because the uncertainty in the benchmark is very small: $<\pm 0.0004$ (1σ). There is significant variability between results using different neutron cross section libraries, the greatest being a Δk_{eff} of $\sim 0.67\%$.

These benchmark experiments were compared to similar bare HEU configurations (Appendix C). There is not any reduction in critical mass obtained by replacing the core of the uranium discs with beryllium reflector. The critical mass actually increases by 13.497 kg HEU for the 13-inch-diameter configuration and 3.258 kg HEU for the 15-inch-diameter configuration because the uranium material of greatest worth in the

^a Oralloy stands for Oak Ridge Alloy, and consists of HEU metal with an ^{235}U enrichment of more than 93%.

^b Experimental data for these experiments can be found on page 118 of ORNL logbook 12R (East Cell – Logbook 1) and pages 19-21, 55-57, and 60 of ORNL logbook 13R (East Cell – Logbook 2).

bare configurations is replaced with moderating/reflecting material. The calculated reactivity worth for the removal of the beryllium reflector from these two configurations is -8.5 ± 0.4 and -4.2 ± 0.2 dollars (\$), respectively.

1.2 Description of Experimental Configuration

These experiments were performed in the $35 \times 35 \times 30$ -ft-high East Cell of the ORCEF, and the assemblies of uranium were located approximately 11.7 ft from the five-ft-thick concrete west wall, 12.7 ft from the two-ft-thick concrete north wall, and 9.2 ft above the concrete floor.

The two internally-reflected, annular experiments consisted of a stack of annular uranium discs with a nominal inside diameter of ~7 inches, which was filled with beryllium metal discs with a nominal outer diameter of ~7 inches. The outer diameter of the uranium annuli for one experiment was ~13 inches with a height of ~5 inches (Configuration 1, Figure 1). The second experiment had an annuli outer diameter of ~15 inches with a height of ~4 inches (Configuration 2, Figure 2). The stack height of the beryllium discs was approximately the same as that of the uranium annuli in each experiment. A thin stainless steel (SS304) diaphragm separated the top and bottom halves of each experiment.

Detectors used for reactor period measurements were placed 10 to 15 feet away and consisted of BF_3 boron-lined ionization chambers. The reactivity worth was obtained from the difference in two measurements; one without the change and the other with the change. The inhour equation was then used to convert reactor period to reactivity. A neutron source was near the assemblies for startup only and was withdrawn ~4 feet away into a borated paraffin shield during the measurements. Measurements were performed at fission rates such that the neutrons coming out of the shield from the startup source were insignificant.^a

^a Personal communication with John T. Mihalczo, March 2010.

Revision: 0

Date: September 30, 2010



Figure 1.a. Oralloy Metal Annuli with Beryllium Core (Configuration 1).

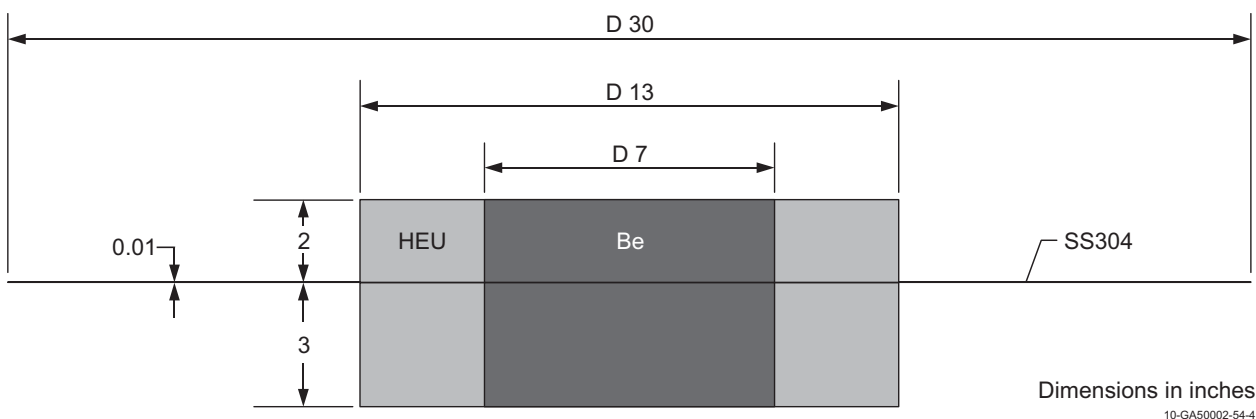


Figure 1.b. Oralloy Metal Annuli with Beryllium Core (Configuration 1, dimensions are nominal).



Figure 2.a. Oralloy Metal Annuli with Beryllium Core (Configuration 2).

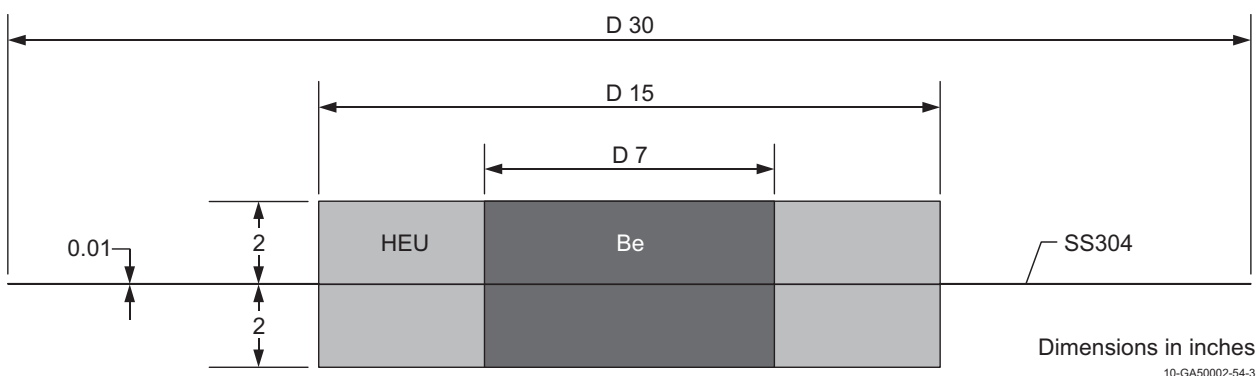


Figure 2.b. Oralloy Metal Annuli with Beryllium Core (Configuration 2, dimensions are nominal).

1.2.1 General Assembly Procedure – The experiments were each constructed on a vertical assembly machine (shown in Figure 3), which primarily consisted of a hydraulic lift (22-inch vertical motion) to support the lower section and a stationary upper section (The upper support shown in Figure 3 was not used in this experiment).

For unreflected experiments (i.e., no significant amounts of reflector material were placed around the periphery of the experiment), the lower support stand held the uranium metal of the lower section in place. The lower section was supported on 0.125-inch-thick aluminum edges, oriented vertically 120 degrees apart (visible in Figure 4). The upper section was supported by four vertical posts, which held a low-mass support consisting of two 30-inch-ID, 2-inch wide, 0.5-inch-thick, aluminum clamping rings bolted together and supported off vertical poles by aluminum tubing; see Figure 4. Note that Figure 4 shows an unreflected uranium metal assembly, but these internally reflected critical experiments were assembled on the same vertical lift with the same support structure as shown in this figure. The 30-inch-diameter clamping rings held a 0.010-inch-thick stainless steel (304L) diaphragm on which the upper uranium metal section was supported. The lower section was supported on a low-mass support stand (sometimes referred to as a support tower) mounted in the vertical position and also shown in Figure 4. The 0.5-inch-thick, 18-inch-diameter aluminum base of this support stand was bolted to the 1-inch-thick, 18-inch-diameter stainless steel table of the vertical lift as shown in Figure 4. The lower surface of the uranium was at a height of 36 inches above the aluminum base. Small aluminum pieces bolted to the 120° vertical members restrained lateral motion of the lower section. These low mass supports were used to minimize the reflection effects of support structure. The aluminum base of the support stand is type Al6061 and the stainless steel table is type 304L.^a Additional structural detail for the lower support stand and diaphragm clamping ring are given in Appendix D.

Experiments were assembled by mounting a fixed height of uranium metal parts on the lower section with beryllium reflector, after which uranium and reflector parts were added to the upper section until near delayed criticality was achieved. For these experiments, the lower section was raised until it made contact with the diaphragm and actually slightly lifted the upper section of material mounted on the diaphragm. The lifting of the top section slightly by the bottom section was used to compensate for the sag of the diaphragm due to the weight of the upper material. The lifting of the diaphragm was monitored to the nearest 0.001 inches and the lower section was moved up only until the diaphragm was level. Due to the thickness of the smallest uranium parts, the system could rarely be adjusted to exactly delayed criticality. For most assemblies the uranium mass of the upper section was adjusted until a self-sustaining fission chain reaction occurred with a measurable positive stable reactor period. For assemblies that were slightly subcritical, an additional hydrogenous reflector (small piece of Plexiglas) was added as a reflector to achieve a self-sustaining chain reaction. When the fission rate achieved a value from which a negative reactor period could be measured, the Plexiglas was quickly (within a fraction of a second)^b removed to measure the resulting negative reactor period.

1.2.2 Stack Height of Annuli and Discs – Assembly heights at different angular locations for the experiments were measured to within ± 0.001 inches by stacking them on a precision flat surface and measuring the distance between the upper surface of uranium and the precision flat surface. Multiple measurements were performed with all parts assembled in the same vertical order and orientation that they were in the critical experiment, which stacked uranium cylinders and annuli azimuthally such that the part numbers were always oriented towards the north wall. The part numbers were scribed on the upper surface of the part. This operation presented no criticality safety problems in hand stacking since the annuli were only one-inch-thick radially.

For the experiments with uranium metal on the lower support stand, the heights were measured with the uranium on the lower support stand as the assemblies were disassembled. That is, for a 15-inch-OD cylinder,

^a Personal communication with John T. Mihalczo, February 2010.

^b Personal communication with John T. Mihalczo in HEU-MET-FAST-076, June 2006.

the height of the outer annulus (13-15 inches) was measured at several locations azimuthally. After the height measurements for this annular ring were made, the annular ring was removed from the support stand and the height of the 11-13 inch annular ring measured. This process continued until the height of the central 7-inch diameter disc stack was measured. The stack height was measured directly with the lower support table in the withdrawn position since the top and bottom of the stacks are accessible. The micrometer read out to 0.001 inches and was repeatable at any azimuthal location. The standard deviation associated with the averages of the azimuthal measurements provides the uncertainty in the thickness.^a

Reported heights (Ref. 1) for the stacked annuli are given in Table 1. The series of stack height measurements recorded in the logbook are shown in Table 2. The beryllium reflector stack was also measured and the heights are reported in Table 2. The average stack heights were calculated and reported in the original logbooks. The standard deviation has been calculated using the original data.

^a Personal communication with John T. Mihalczo, March 2010.

Revision: 0

Date: September 30, 2010

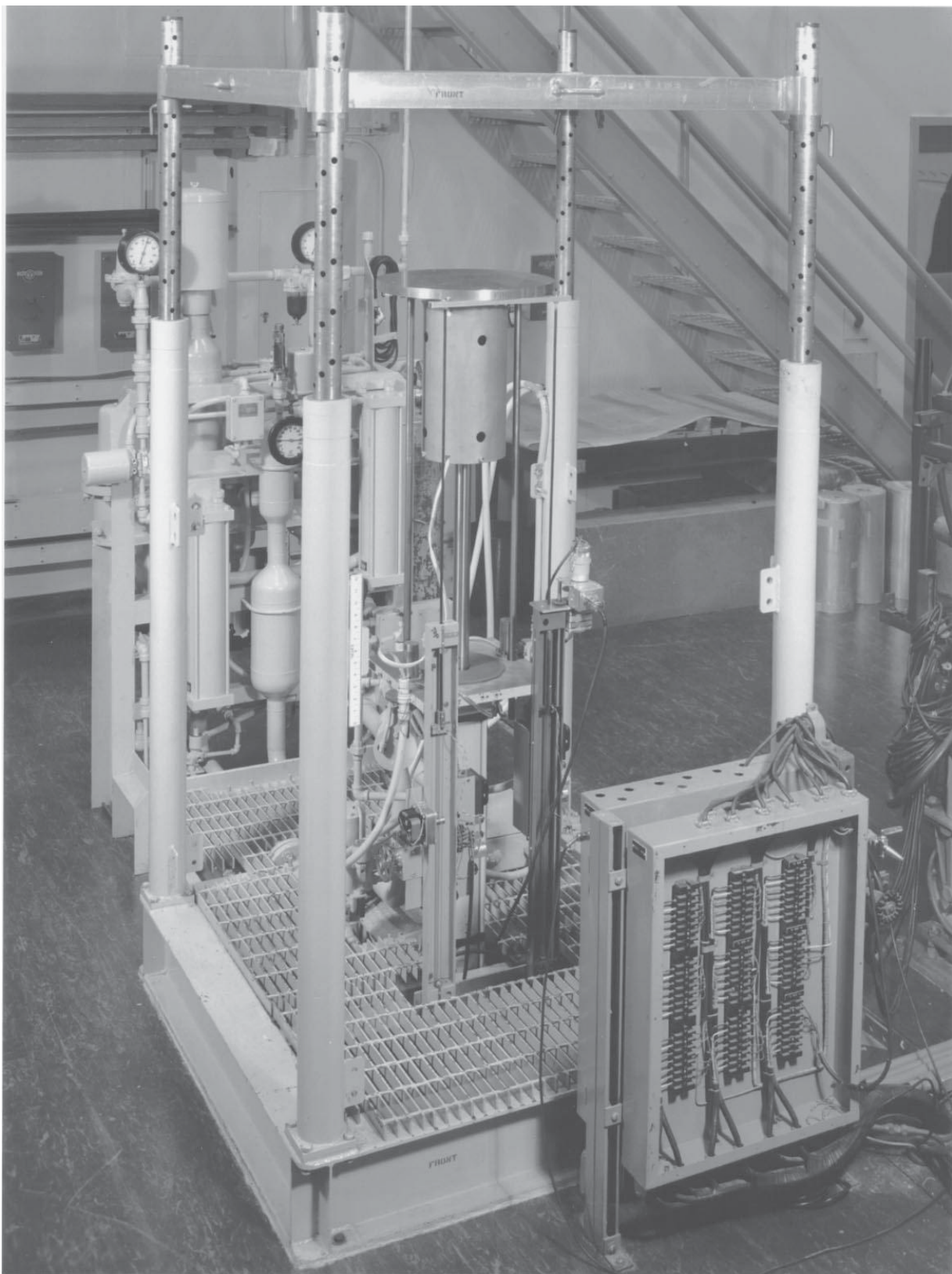


Figure 3. Photograph of the Vertical Assembly Machine with the Movable Table Up.
(The upper support shown in this photograph was not used in these measurements.)

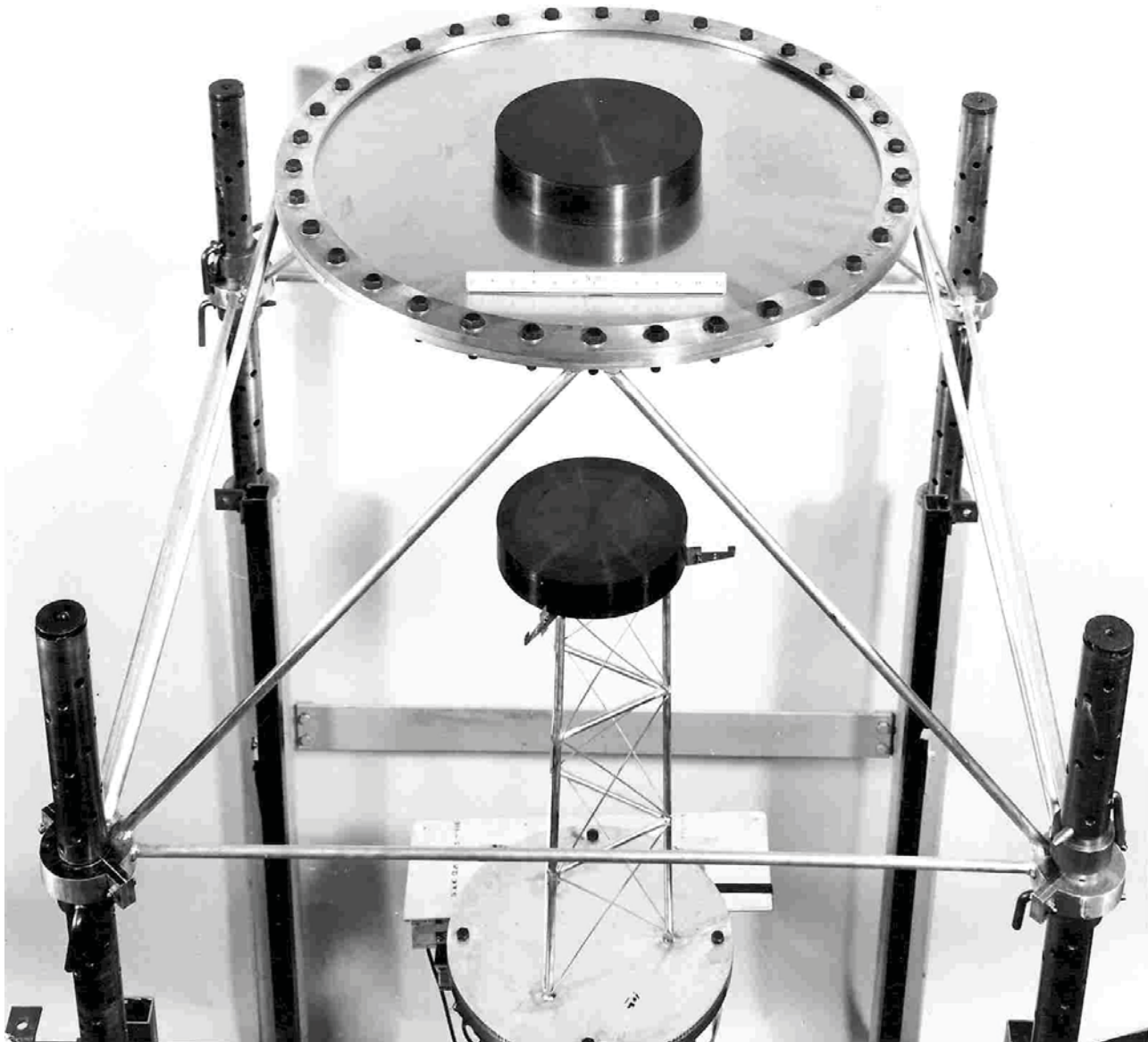


Figure 4. A Typical Uranium Metal Assembly of Two Interacting 11-inch-Diameter Cylinders at Close Spacing on the Vertical Assembly Machine.^a

(Similar supports were used in these measurements and are described in Appendix D.)

^a Photo 39380, Oak Ridge National Laboratory photo of a bare uranium assembly. This same support structure was used for internally Be moderated, unreflected uranium metal annuli and top-Be-reflected experiments.

Table 1. Reported Stack Height Measurements (Ref. 1).

Experiment	Description			Measured Height of Annular Rings (in.)			
	OD (in.)	ID (in.)	Material Inside Annulus	15-13 in.	13-11 in.	11-9 in.	9-7 in.
1 (Top)					1.8835	1.8740	1.9320
1 (Bottom)	13	7	Beryllium	--	3.0183	3.0108	3.0120
2 (Top)				1.9400	1.9440	2.0086	2.0040
2 (Bottom)	15	7	Beryllium	2.0066	2.0050	2.0040	2.0043

Table 2.a. Logbook Stack Height Measurements (in.).

Experiment	15-13 in.	13-11 in.	11-9 in.	9-7 in.	Beryllium
1 (Top) ^(a)	--	1.886	1.876	1.932	1.996
	--	1.884	1.876	1.932	1.995
	--	1.884	1.874	1.932	1.995
	--	1.882	1.873	1.932	1.994
	--	1.884	1.875	1.931	1.995
	--	1.883	1.8722	1.931	1.994
	--	--	--	--	1.994
Average	--	1.884	1.874	1.932	1.995
1σ	--	0.001	0.002	0.001	0.001
Experiment	15-13 in.	13-11 in.	11-9 in.	9-7 in.	Beryllium
1 (Bottom) ^(a)	--	3.018	3.011	3.011	3.006
	--	3.017	3.012	3.012	3.008
	--	3.018	3.012	3.012	3.007
	--	3.018	3.011	3.011	3.0075
	--	3.019	3.010	3.013	3.007
	--	3.020	3.009	3.013	3.011
	--	--	--	--	3.0095
Average	--	3.018	3.011	3.012	3.008
1σ	--	0.001	0.001	0.001	0.002

(a) Stack height measurements for the top and bottom halves of Configuration 1 were obtained from pages 57 and 60, respectively, from ORNL logbook 13R (East Cell – Logbook 2).

Table 2.b. Logbook Stack Height Measurements (in.).

Experiment	15-13 in.	13-11 in.	11-9 in.	9-7 in.	Beryllium
2 (Top) ^(a)	1.940	1.945	2.007	2.004	2.001
	1.938	1.944	2.012	2.005	2.001
	1.942	1.943	2.007	2.003	2.001
	1.939	1.944	2.007	2.003	2.001
	1.940	1.944	2.010	2.004	2.001
	1.940	1.944	2.0086	2.004	2.001
Average	1.940	1.944	2.009	2.004	2.001
1σ	0.001	0.001	0.002	0.001	0.000
Experiment	15-13 in.	13-11 in.	11-9 in.	9-7 in.	Beryllium
2 (Bottom) ^(a)	2.005	2.006	2.003	2.005	-- ^(b)
	2.006	2.004	2.005	2.003	--
	2.007	2.005	2.006	2.004	--
	2.008	2.005	2.003	2.006	--
	2.007	2.006	2.003	2.004	--
	2.007	2.005	2.004	2.004	--
	2.006	--	--	--	--
Average	2.007	2.005	2.004	2.004	-- ^(b)
1σ	0.001	0.001	0.001	0.001	--

(a) Stack height measurements for the bottom half of Configuration 2 were obtained from page 118 of ORNL logbook 12R (East Cell – Logbook 1), and the top half from page 21 of ORNL logbook 13R (East Cell – Logbook 2).

(b) Stack height measurements were not performed for the bottom half of Configuration 2 because it was a single 2-inch-thick beryllium disc.

1.2.3 Assembly Alignment

Radial Alignment of Upper Section: For assembly of the upper section, uranium metal was added to the top of the Type 304L stainless steel diaphragm. Uranium was positioned, with a ruler, the appropriate distance from the inside of the aluminum clamping ring, which held the 0.010-inch-thick stainless diaphragm. A layer of uranium metal for an 11-inch-diameter annulus typically consists of a 7-inch-ID / 9-inch-OD annulus, and a 9-inch-ID / 11-inch-OD annulus. About half of the material was added to the diaphragm and the location of the material was continuously adjusted with a precise high-quality level in one direction and then the level was rotated 90° on the top of the uranium. If the assembly was not exactly centered on the diaphragm, it would not be precisely level because of the sag in the diaphragm as it was loaded. Two precisely machined steel blocks (± 0.0001 inches) were used to squeeze the outside radial surface of the uranium metal until it was aligned. An edge of the machined block was then held at one outside radial location, squeezing the uranium together until no light was visible between the machined block and the uranium metal. This process was repeated 90° from the position of the original adjustment, rechecked again

Revision: 0

Date: September 30, 2010

at the original position, and small adjustments made if necessary. This process continued until the outside radii of the parts were precisely aligned and the upper section assembly was complete. The squeezing procedure was performed by one individual while another person observed the light coming through small gaps between the blocks and the uranium metal.^a The alignment of outer radii of the upper or lower section was less than ± 0.001 inches. Of course, if two positions 90° apart are adjusted, the positions at 180° and 270° can be off only by the difference in the diameters of the outside parts.

Radial Alignment of Lower Section: For the lower section, the uranium parts were centrally located on the lower support stand and the same procedure was used except that the leveling of the parts was accomplished by shimming with aluminum foil (various thicknesses of aluminum foil were available). The foil was placed between the three 120° upper edges of the lower support stand and the lowest parts.

Radial Alignment Accuracy Summary: Uncertainty in radial alignment of uranium metal parts on each half is ± 0.001 inch.

Lateral Alignment of Upper Section with the Lower Section: For these experiments, the alignment of the upper and lower sections was adjusted and verified using the Lateral Alignment Fixture shown in Figure 5. There were two identical fixtures used for lateral alignment between the upper section and the lower section. They were U-shaped and were machined out of 0.375-inch-thick aluminum. The end pieces were carefully machined by the Y-12 shops to be perpendicular to the long direction of the fixture and coplanar with each other. When leveled properly, the front face of the $4 \times 4 \times \frac{1}{2}$ -inch-thick end pieces were vertical and in the same plane to within ± 0.001 inch. In use, the lower side of the upper leg rested on the top surface of the clamping ring for the diaphragm. The fixture was perpendicular to the outer radial surface of the annuli and was moved inward until it touched the uranium of the top section. The leveling screws were adjusted until the fixture was level.

The second fixture was placed 90° apart from the first in a similar manner. Both fixtures were moved back slightly, and the lower section was raised until it was at the height of the lower leg of the U-shaped fixtures. Both fixtures were then nearly adjusted properly. Removal or additions of material from the upper section sometimes required small leveling adjustments. The fixtures were moved in until they touched uranium (either on the upper or the lower section). When lack of contact was observed at either of the front faces of the fixture, the lower section was lowered to the full-out position, and the position of the uranium on the lower support stand was adjusted. Finally, the lower lift table was raised and the alignment was checked.

The process was repeated several times as necessary. The final 0.005-inch adjustments were usually made by moving the upper section. This was a long and tedious procedure, which took one to two hours or more as needed but was always performed and resulted in uranium metal of the upper and lower sections being aligned within ± 0.005 inch.

Lateral Alignment Accuracy Summary: Upper and lower assembly uranium metal alignment uncertainty is ± 0.005 inch.

^a Personal communication with John T. Mihalczo, March 2010.

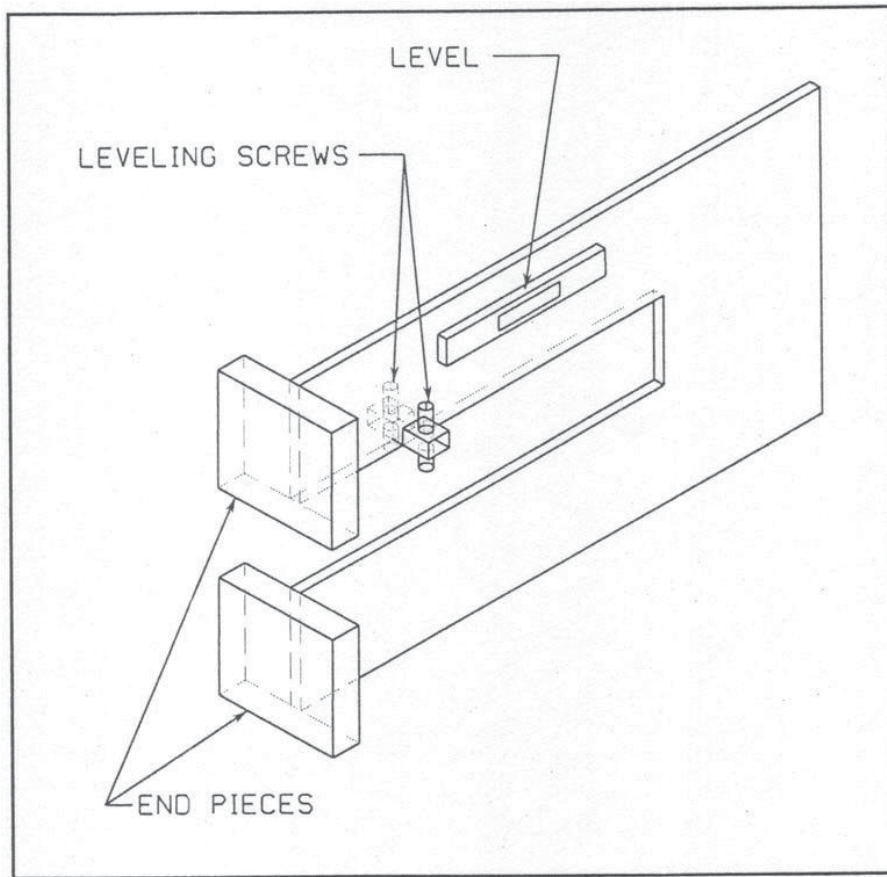


Figure 5. Sketch of Fixture for Lateral Alignment of Uranium.

1.2.4 Reactivity Effects of Support Structure – The support structure that was used to assemble these experiments was made up of the 0.010-inch-thick Type 304L stainless steel diaphragm, low-mass aluminum support stand, and two 30-inch-diameter, 2-inch-wide, 0.5-inch-thick diaphragm clamping rings bolted together. The support structure reactivity worth consisted primarily of the reactivity effects of the diaphragm, the diaphragm support rings, and the low-mass support stand. The reactivity worth of each of these three parts of the support structure was measured.

Additional figures depicting the assembly support structure are provided in Appendix D.

A positive reactivity effect means that the reactivity of the critical assembly increased due to the inclusion of that item in the assembly. Therefore, removing that particular item from the experiment resulted in a decrease in the neutron multiplication factor. A negative reactivity effect means that the reactivity of the assembly decreased due to the item's inclusion. The Type 304L stainless steel diaphragm in all experiments reduced the k_{eff} of the system since it separated uranium metal halves and introduced neutron absorbing material between them. The presence of the diaphragm support ring and low-mass support stand of the lower section resulted in a positive reactivity addition. The presence of the support ring and low-mass stand provided neutron reflection to the system. The combined reactivity effect of all other supports, such as the four vertical poles and tubing for the diaphragm support ring, was reported to be less than one cent and was not evaluated.

The reactivity of the support structure, when measured, was evaluated by assembling the system to delayed criticality or a known measured reactivity, adding additional support structure, and obtaining the reactivity of

the support structure from the measured reactor period for the assembly with and without the additional support structure. The effect of the lower support stand was evaluated using an inverted support stand, like that for the lower section, which was added to the top of the upper section. Care was taken in suspending it so that it would not compress the materials of the assembly. To estimate the effect of the diaphragm and clamping ring, their thicknesses were doubled and the reactivity change was measured. Where multiple instruments were used to measure the reactor period, the reactivity values obtained were averaged. These effects were measured for the components listed in Table 3. The reactivity worth of the entire support structure is obtained by adding the worth of the three components of the support structure: annular diaphragm rings, stainless steel diaphragm, and low-mass support stand. Multiple measurements for the reactivity effects of the support structure were unavailable. The measured worth of the diaphragm includes the separation distance between the two halves of the experiment.^a

Table 3. Reactivity Effects of Removing All Support Structure.

Experiment Configuration	Reactivity of Support Structure (cents)			
	Diaphragm	Rings	Low-Mass Support Structure	Total ^(b)
1 ^(a)	+11.25	-4.4	-12.2	-5.35
2	-- ^(c)	-- ^(c)	-- ^(c)	-8.92

- (a) These values were obtained by comparing the worth measurements between two slightly different configurations, where the difference is the portion of the support structure being evaluated. A total of four configurations were needed to evaluate the three worth measurements, where one of the configurations was that of the clean critical experiment.
- (b) These values are rounded to 5.4¢ and 8.9¢ in Ref. 1; the values reported here were obtained from the original logbook data.
- (c) The worth of individual components for Experiment 2 was not reported. The worth of all support structure was measured simultaneously.

The effective delayed-neutron fraction, β_{eff} , reported for a similar experiment in the series ([HEU-MET-FAST-069](#)) is 0.0066 ± 0.00033 ($\pm 5\%$), and should also apply to these two configurations.^b For Configuration 1, the full assembly was 21.8¢ above delayed critical (k_{eff} of 1.00144) and had an adjusted worth of 16.45¢ above delayed critical (k_{eff} of 1.00109) with all the support structure removed and 5.2¢ above delayed critical (k_{eff} of 1.00034) if all structural supports were removed except for the steel diaphragm. For Configuration 2, the full assembly was 2.96¢ above delayed critical (k_{eff} of 1.00020), and 5.96¢ below delayed critical (k_{eff} of 0.99961) when all the support structure was removed. The worth of individual components in the assembly of Configuration 2 was not reported.

The diaphragm bolts were not included in the experimental analysis of the support structure worth. The 304L stainless steel bolts are 0.5 in. (1.27 cm) in diameter and 1.5 in. (3.81 cm) long.^c

1.2.5 Uranium Components – The average dimensions and masses of the uranium metal parts for these experiments are given in Table 4 and come from the Y-12 database; the dimensions are measured to within 1×10^{-4} inches with an uncertainty of 5×10^{-5} inches and the masses of the parts are accurate to within 0.5

^a Personal communication with John T. Mihalczo, February 2010.^b Personal communication with John T. Mihalczo, December 2009.^c Personal communication with John T. Mihalczo, June-July 2010.

grams. All dimensional measurements for the parts were measured at 70° F at the Y-12 plant. The readout of the measuring device was calibrated to 0.0001 in. (0.000254 cm) using standards traceable back to the National Bureau of Standards (now NIST). An average of more than one measurement could result in the recording of a fifth digit.^a

The density of each part can be obtained by dividing the reported mass of the part by the volume, which is calculated using the values provided in Table 4.

The average gaps between uranium metal annular parts were obtained by subtracting the sum of the heights of the individual parts in a given stack from the measured stack height, and then dividing this value by the number of parts in the stack minus one. The reported vertical gap heights between the uranium annuli are in Table 5. The reported annular gap thicknesses between the uranium annuli are in Table 6.

^a Personal communication with John T. Mihalczo, March 2010.

Revision: 0

Date: September 30, 2010

Table 4. Measured Properties of Uranium Metal Annuli.

Part Number	Mass (g)	Height (in.)	Inner Diameter (in.)	Outer Diameter (in.)
2735	13409	0.9985	13.0020	14.9935
2736	2895	0.37635	7.0026	8.9960
2737	4336	0.5625	7.0015	8.9965
2738	7710	1.0012	7.00375	8.99575
2739	13461	0.9945	13.0027	14.9955
2740	11568	1.5000	7.0025	8.99625
2742	3617	0.3751	9.0015	10.9968
2743	3621	0.3740	9.0025	10.9965
2744	1223	0.12675	9.0065	10.9968
2745	9634	0.9990	9.0010	10.9965
2746	1238	0.12865	9.00175	10.9965
2747	14436	1.4999	9.0020	10.9968
2748	14462	1.5000	9.0025	10.9975
2749	4360	0.3774	11.0030	12.9955
2750	4336	0.37545	11.0015	12.9945
2751	5822	0.50355	11.0015	12.9958
2752	5811	0.50325	11.0025	12.9955
2753	5782	0.5013	11.0030	12.99675
2754	5826	0.5036	11.0040	12.9953
2755	6514	0.5635	11.0030	12.9960
2756	11567	1.0002	11.0036	12.9967
2757	11575	1.00155	11.0025	12.9960
2761	1706	0.1265	13.0010	14.99475
2762	7703	0.99925	7.00375	8.99625
2763	953	0.1243	7.0038	8.9958
2766	7605	0.5630	13.0010	14.9965
2773	962	0.1250	7.0015	8.9970
2774	1930	0.2500	7.0030	8.9965
2775	1917	0.2485	7.0040	8.99675
2776	9644	1.0015	9.0015	10.9965
2778	2411	0.2510	9.0020	10.9965
2779	2417	0.2510	9.0015	10.9970
2780	1440	0.12485	11.0020	12.99605
2784	5039	0.3725	13.0015	14.9945
2785	5043	0.3747	13.0029	14.9958
2829	2895	0.37625	7.00315	8.99625
2848	6748	0.5019	13.0031	14.9964

Table 5. Reported Vertical Gaps between Uranium Metal Annuli.

Experiment	Annular Ring	Average Void between Rings (in.)
1 (Top)	13-11 in.	0.0016
	11-9 in.	$\approx 0.0000^{(a)}$
	9-7 in.	$\approx 0.0000^{(a)}$
1 (Bottom)	13-11 in.	0.0016
	11-9 in.	0.0034
	9-7 in.	0.0032
2 (Top)	15-13 in.	0.0005
	13-11 in.	0.0008
	11-9 in.	0.0008
	9-7 in.	0.0009
2 (Bottom)	15-13 in.	0.0017
	13-11 in.	$\approx 0.0000^{(a)}$
	11-9 in.	0.0002
	9-7 in.	0.0016

(a) The sum of the heights of the individual parts was greater than the measured stack height.

Table 6. Reported Annular Gaps between Uranium Metal Annuli.

Experiment	Annular Ring or Void between Rings	Average Radial Voids (in.)	Average OD (in.)	Average ID (in.)
1 (Top)	13-11 in.	--	12.9958	11.0026
	11 in.	0.0028	--	--
	11-9 in.	--	10.9967	9.0023
	9 in.	0.0070	--	--
	9-7 in.	--	8.9963	7.0027
1 (Bottom)	13-11 in.	--	12.9958	11.0026
	11 in.	0.0055	--	--
	11-9 in.	--	10.9967	9.0023
	9 in.	0.0074	--	--
	9-7 in.	--	8.9963	7.0027
2 (Top)	15-13 in.	--	14.9953	13.0020
	13 in.	0.0028	--	--
	13-11 in.	--	12.9959	11.0029
	11 in.	0.0030	--	--
	11-9 in.	--	10.9968	9.0025
	9 in.	0.0075	--	--
	9-7 in.	--	8.9963	7.0031
2 (Bottom)	15-13 in.	--	14.9953	13.0020
	13 in.	0.0016	--	--
	13-11 in.	--	12.9959	11.0029
	11 in.	0.0014	--	--
	11-9 in.	--	10.9968	9.0025
	9 in.	0.0009	--	--
	9-7 in.	--	8.9963	7.0031

1.2.6 Beryllium Components – The nominal 7-inch-diameter internal moderators/reflectors are comprised of a stack of beryllium discs with nominal thicknesses (or heights) of 1/2, 1, 1.5, and/or 2 inches. The 5-inch stack of discs in Configuration 1 utilized all four discs. The 4-inch stack of discs in Configuration 2 did not use the 1-inch-high beryllium disc. Detailed dimensional data were not available. These beryllium discs were fabricated to nominally fit inside an annulus with 9 in. (22.86 cm) outer diameter and 7 in. (17.78 cm) inner diameter and the diameter of the discs should be within 0.001 in. (0.00254 cm) of the average of the oralloy metal discs in HEU-MET-FAST-069, which is 6.996444 inches (17.7709671 cm), and they should have the same machining uncertainty.^a The beryllium discs were also measured at Y-12

^a Personal communications with John T. Mihalczo, October 2009 and July 2010.

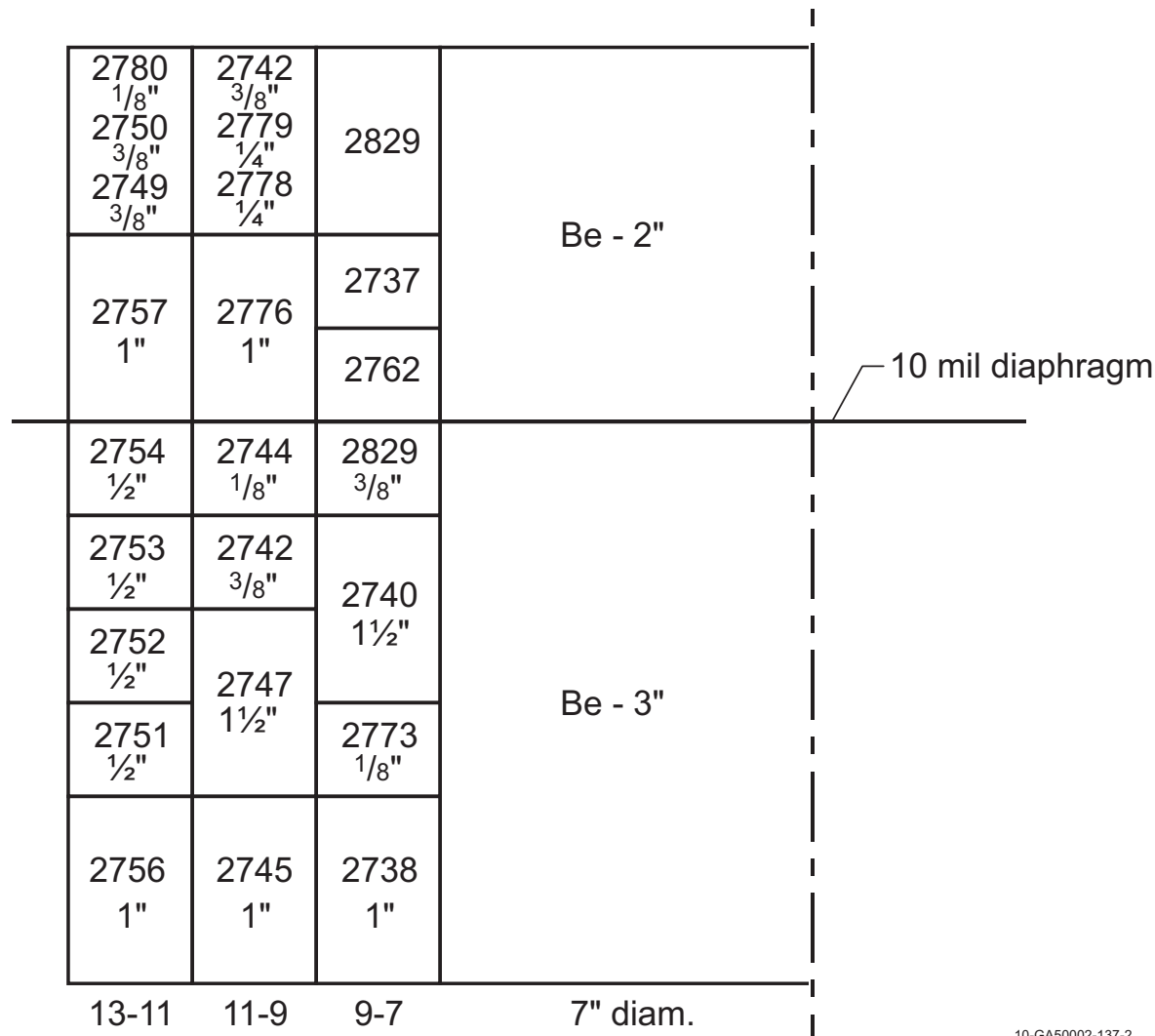
Revision: 0

Date: September 30, 2010

with a measuring device that was accurate to 0.0001 in. (0.000254 cm) and traceable back to the National Bureau of Standards.^a The record of the measurements of the beryllium discs is no longer available.

Gap heights were not reported, but could be obtained by comparing the heights of the discs with their stack height measurements reported in Table 2.

1.2.7 Experimental Configurations – The experimental assemblies comprised of the uranium annuli and beryllium discs provided in the logbooks, with the part locations identified, are shown in Figures 6 and 7 for Configurations 1 and 2, respectively. For Configuration 1, two of the parts are specified in both the top and bottom halves of the experiment. In the top half of Configuration 1, Figure 6, part 2742 is actually part 2743, and part 2829 is part 2736.^b

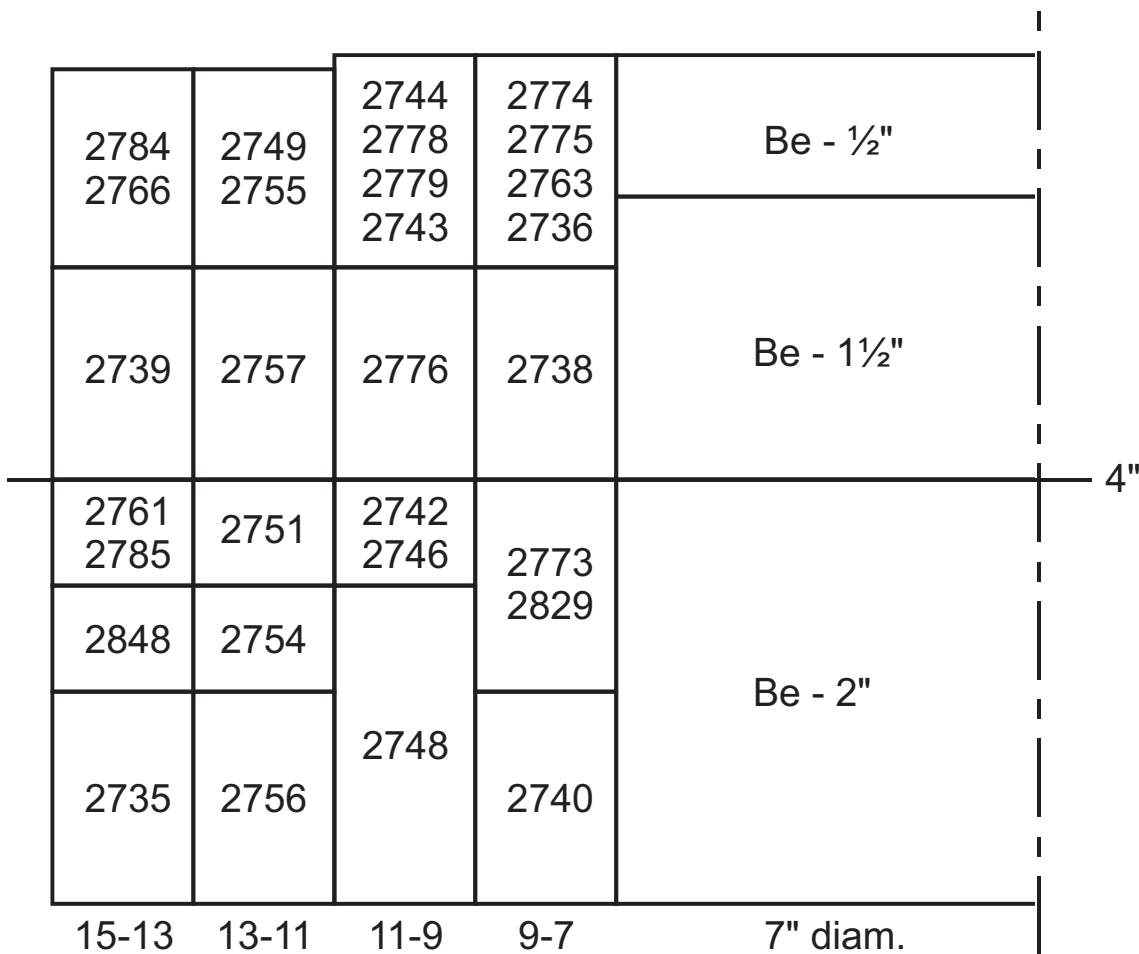


10-GA50002-137-2

Figure 6. Sketch of Experimental Configuration 1 (Thirteen-Inch Annulus).
Redrawn from pages 52 and 57 of ORNL logbook 13R (East Cell – Logbook 2).

^a Personal communication with John T. Mihalczo, March 2010.

^b Personal communication with John T. Mihalczo, October 2009.



10-GA50002-137-1

Figure 7. Sketch of Experimental Configuration 2 (Fifteen-Inch Annulus).
Obtained from page 21 of ORNL logbook 13R (East Cell – Logbook 2).

1.3 Description of Material Data

1.3.1 Uranium Components – The uranium metal parts for these critical experiments were carefully cast and machined at the Oak Ridge Y-12 Plant in the early 1960s. Each uranium metal part was a separate casting which was then machined. Dimensions, masses, uranium isotopes, and impurity content were measured after machining. Uranium part masses and dimensions can be found in Table 4. The total uranium mass is 141.591 and 168.138 kg for Configurations 1 and 2, respectively, which is the sum of the individual part masses.

The uranium isotopes obtained from Y-12 spectrographic analyses are given in Table 7. The average isotopic contents of the uranium are 0.97 wt.% ^{234}U , 93.15 wt.% ^{235}U and 0.24 wt.% ^{236}U with an average impurity content of ~500 ppm. The uncertainty in the measured values for ^{234}U , ^{235}U , and ^{236}U are 5×10^{-3} wt.%. The ^{238}U values were obtained by subtracting the sum of the other three from 100%.

The impurities from the 11 spectrographic analyses performed are given in Table 8 for uranium parts; only average and variation information exist.^a These 11 randomly sampled uranium parts include discs and annular parts. As such, the information presented is a representative average of the impurity content in all uranium parts. These values are consistent with the nominal impurity content of highly enriched uranium metal at the Oak Ridge Y-12 Plant at the time the parts were made (i.e., 99.95 g of U per 100 g of material). Oxygen and nitrogen content was assumed by the experimentalist to be 20 and 30 ppm, respectively, consistent with highly enriched uranium produced at the time of these experiments.^b

The HEU parts were coated annually in a very thin film of lightweight fluorocarbon oil to decrease oxidation removal. This oil has negligible effect upon the experiment conditions. After oiling, the parts were wiped with a dry rag to remove most of the oil. The oralloy parts were then handled by leather gloves, which further reduced the oil on the surface.^c

^a J. T. Mihalczo, "Graphite and Polyethylene Reflected Uranium-Metal Cylinders and Annuli," Union Carbide Corporation Nuclear Division, Oak Ridge Y-12 Plant, Y-DR-81 (1972).

^b HEU-MET-FAST-076.

^c Personal communication with John T. Mihalczo, June-July 2010.

Table 7. Uranium Disc Isotopic Content.^(a)

Part Number	²³⁴ U (wt.%)	²³⁵ U (wt.%)	²³⁶ U (wt.%)	²³⁸ U (wt.%) ^(b)
2735	0.98	93.12	0.25	5.65
2736	1.01	93.17	0.21	5.61
2737	0.99	93.08	0.29	5.64
2738	0.98	93.15	0.24	5.63
2739	0.96	93.16	0.25	5.63
2740	0.97	93.17	0.24	5.62
2742	0.98	93.14	0.23	5.65
2743	0.98	93.14	0.23	5.65
2744	0.98	93.14	0.23	5.65
2745	0.96	93.20	0.22	5.62
2746	1.00	93.09	0.22	5.69
2747	0.98	93.16	0.19	5.67
2748	1.00	93.09	0.22	5.69
2749	0.98	93.19	0.25	5.58
2750	0.95	93.12	0.25	5.68
2751	0.98	93.13	0.24	5.65
2752	0.98	93.13	0.24	5.65
2753	0.95	93.12	0.25	5.68
2754	0.96	93.10	0.28	5.66
2755	0.96	93.10	0.28	5.66
2756	0.93	93.18	0.25	5.64
2757	0.96	93.20	0.23	5.61
2761	0.96	93.12	0.27	5.65
2762	0.97	93.13	0.27	5.63
2763	0.96	93.18	0.25	5.61
2766	0.98	93.16	0.27	5.59
2773	0.97	93.17	0.24	5.62
2774	0.99	93.08	0.29	5.64
2775	0.98	93.15	0.24	5.63
2776	0.96	93.16	0.23	5.65
2778	0.96	93.16	0.23	5.65
2779	0.96	93.16	0.23	5.65
2780	0.98	93.13	0.25	5.64
2784	0.99	93.11	0.26	5.64
2785	0.98	93.14	0.24	5.64
2829	0.99	93.10	0.24	5.67
2848	0.99	93.18	0.24	5.59

(a) Mass spectrographic analysis, unless noted otherwise.

(b) By difference from 100% pure uranium.

Table 8. Measured Impurity Content of Uranium Metal Cylinders, Annuli, and Plates.^(a)

Element ^(a)	Parts per Million by Weight (ppm) ^(b)	Variation (ppm)	Standard Deviation (ppm) ^(c)
Ag	8	3-25	3.2
Ba	< 0.01 ^(d)	-	0.005
Bi	164	81-311	52.9
C	< 10	-	2.4
Ca	0.1	-	0.05
Cd	< 1	-	0.5
Co	5	2-15	1.9
Cr	7	4-12	1.9
Cu	25	10-40	8
K	< 0.2	0.2-0.8	0.1
Li	< 2	-	1
Mg	3	2-3	1.7
Mn	56	25-89	17.1
Mo	< 1	< 1 – 1	0.5
Na	27	15-50	7.7
Ni	100	-	10
Sb	38	10-80	17.4
Ti	1	-	0.5

- (a) Mass spectrographic analysis except for oxygen and nitrogen using data in J. T. Mihalczo, "Graphite and Polyethylene Reflected Uranium-Metal Cylinders and Annuli," Union Carbide Corporation Nuclear Division, Oak Ridge Y-12 Plant, Y-DR-81 (April 28, 1972). Oxygen and nitrogen content was assumed by the principal experimentalist to be 20 and 30 ppm, respectively, consistent with highly enriched uranium produced at the time of these experiments. Total impurity content is consistent with stated values at that time of 500 ppm which gives 99.95 grams of U per 100 grams of material. Minor differences in the impurities exist between values listed in Table 8 and the impurity values provided in [HEU-MET-FAST-051](#).
- (b) Except for the values shown as less than the detection limit, impurity data are average values from 11 randomly sampled uranium parts.
- (c) Personal communication, J. A. Mullens to John Mihalczo in [HEU-MET-FAST-076](#), June 2004.
- (d) Less than (<) indicates lower detection limit and not necessarily that the impurity is present.

1.3.2 Beryllium Components – The measured mass of the beryllium stack is 5.787 and 4.628 kg with an average calculated density of 1.8353 and 1.8346 g/cm³ for Configurations 1 and 2, respectively. The beryllium discs were machined at the Y-12 Plant from material obtained from Brush Beryllium^a and had the reported average, or expected, impurities shown in Table 9 and would have been machined and measured with the same accuracy and precision as the uranium discs.^b The individual masses of each beryllium disc are reported in the logbook^c and summarized in Table 10.

^a K. A. Walsh, et al., *Beryllium Chemistry and Processing*, ASM International, Materials Park, OH, pp. 9-11 (2009).^b Personal communication with John T. Mihalczo, November 2009.^c Page 1 of ORNL logbook 13R (East Cell – Logbook 2).

Table 9. Material Density and Impurities of Unmachined Beryllium.^(a)

Density (g/cm ³)	1.854 ^(b)
Impurity	wt.%
BeO	1.93
Al	0.06
C	0.12
Fe	0.13
Mg	0.02
Bi	0.05
B	0.001
Cd	0.0002
Dy	0.0001
Br	0.00005
Gd	0.0001
Ni	0.0001
Sm	0.0001
Total	2.31165

(a) Personal communication with John T. Mihalczo, October 2009. These are the properties of the raw material delivered to Y-12 for fabrication into discs.

(b) The reported material density is greater than the density calculated with the measured mass and approximate dimensions of the beryllium discs used in the experiment. The density of pure beryllium is reported to be 1.8477 g/cm³ with a commercial grade density between 1.82 and 1.85 g/cm³, which would be typical of material obtained from Brush Beryllium (K. A. Walsh, et al., *Beryllium Chemistry and Processing*, ASM International, Materials Park, OH, p. 27 (2009)).

Table 10. Individual Masses of Beryllium Discs.

Thickness (in)	Mass (g)
2	2314
1.5	1741
1	1159
½	573

1.3.3 Temperature – Room and assembly temperature measurements were not recorded during the course of the experiments. The ORCEF operated in a controlled environment.^a The fission rate in the

^a Personal communication with John T. Mihalczo, February 2010.

Revision: 0

Date: September 30, 2010

measurements corresponded to usually much less than 0.01 watts, so there was no appreciable heating of the experiment components. The dimensions of the uranium were measured at 70 °F and the experiments were performed at 72 °F. The reactivity coefficient for a temperature change for these assemblies is approximately $-1\text{e}^{\circ}\text{C}$.^a

1.4 Supplemental Experimental Measurements

No additional supplemental experimental measurements were performed.

^a Personal communication with John T. Mihalczo, March 2010.

Revision: 0

Date: September 30, 2010

2.0 EVALUATION OF EXPERIMENTAL DATA

Monte Carlo n-Particle (MCNP) version 5.1.51 calculations were utilized to estimate the biases and uncertainties associated with the experimental results in this evaluation. MCNP is a general-purpose, continuous-energy, generalized-geometry, time-dependent, coupled n-particle Monte Carlo transport code.^a The Evaluated Neutron Data File library, ENDF/B-VII.0,^b was utilized in analysis of the experiment and benchmark model biases and uncertainties. The statistical uncertainty in k_{eff} and Δk_{eff} is 0.00002 and 0.00003, respectively. Calculations were performed with 1,050 generations with 1,000,000 neutrons per generation. The k_{eff} estimates did not include the first 50 generations and are the result of 1,000,000,000 neutron histories.

The detailed benchmark model provided in Section 3 was utilized with perturbations of the model parameters to estimate uncertainties in k_{eff} due to uncertainties in parameter values defining the benchmark configuration. Where applicable, comparison of the upper and lower perturbation k_{eff} values to evaluate the uncertainty in the k_{eff} eigenvalue were utilized to minimize correlation effects, if any, induced by comparing all perturbations to the original benchmark model configuration, as discussed elsewhere.^c

Unless specifically stated otherwise, all uncertainty values in this section correspond to 1σ . When the changes in k_{eff} between the base case and the perturbed model, or two perturbed models, is less than the statistical uncertainty of the Monte Carlo results, the changes in the variable are amplified, if possible, and the calculations repeated. The resulting calculated change is then scaled back corresponding to the actual uncertainty, assuming that it is linear, which should be adequate for these changes in k_{eff} . Linearity was evaluated and found to apply, within statistical uncertainty, to the scaled perturbations.

Uncertainties less than or equal to 0.00005 are treated as negligible. When calculated uncertainties in Δk_{eff} are less than or equal to their statistical uncertainties, and an increased parameter scaling cannot be performed, the statistical uncertainties are added to the calculated uncertainty to assess the magnitude of the total uncertainty; however, the absolute magnitude of any uncertainty combined in this way is much less than 0.00005 Δk_{eff} , therefore they are treated as negligible.

Room return effects with its associated uncertainty are addressed in Section 3.1.3.1.

The total evaluated uncertainty in k_{eff} for this experiment is provided in Table 13. The square root of the sum of the squares of all the individual uncertainties assessed in this section is used to obtain the total uncertainty to be applied towards the benchmark eigenvalue.

When evaluating parameters such as part diameters, heights, and masses, all parts of a given type are perturbed at the same time: e.g., the diameter of all HEU annuli are simultaneously increased or decreased. Then the calculated uncertainty is reduced by the square root of the number of components perturbed. All uncertainties are treated as 100% random, without any systematic component. Systematic uncertainties were either not reported, or believed to be negligible. The measurement uncertainties are approximately the same as the uncertainty in the standards that were used for measurement calibration. However, even if all uncertainties were treated as 100% systematic, the total uncertainty in the experiment would not increase significantly.

^a X-5 Monte Carlo Team, "MCNP – a General Monte Carlo n-Particle Transport Code, version 5," LA-UR-03-1987, Los Alamos National Laboratory (2003).

^b M. B. Chadwick, et al., "ENDF/B-VII.0: Next Generation Evaluated Nuclear Data Library for Nuclear Science and Technology," *Nucl. Data Sheets*, **107**: 2931-3060 (2006).

^c D. Mennerdahl, "Statistical Noise for Nuclear Criticality Safety Specialists," *Trans. Am. Nucl. Soc.*, **101**: 465-466 (2009).

2.1 Experimental Measurements

2.1.1 Temperature – These experiments were performed at a room temperature of ~295 K. Part measurements were performed at a room temperature of ~294 K. The uncertainty in each of these two temperatures is unknown. Any variations in temperature for the experiments and room environment were small. Heating effects in the experiment components were negligible. The temperature reactivity coefficient is approximately $-1\text{f}^{\circ}\text{C}$. It is assumed that a temperature variation of 2 °C (1σ) adequately describes the temperature uncertainty. A temperature uncertainty of $\pm 2\text{ }^{\circ}\text{C}$ in k_{eff} results in a Δk_{eff} of ± 0.00013 for both configurations.

2.1.2 Experiment Reproducibility – The experimenter indicated that to completely dismantle a system and reassemble it on a different day, the reactivity differences are $\sim 2\text{f}$ or less. The experimenter indicated that reproducibility of experiments performed with the vertical lift is even better. The corresponding uncertainty of $\pm 0.00013 \Delta k_{\text{eff}}$ is treated as a 1σ for both configurations.

The uncertainty in the actual measurement of the reactivity, which is determined by positive period measurements, is considered very accurate. There is some uncertainty in fitting data and evaluation of the period. Careful measurements and rigorous fitting procedures can yield estimate uncertainties of ~ 0.2 pcm, which is negligible.^a It is assumed that uncertainty in the actual measurement of the reactivity is already included in the reproducibility uncertainty already discussed in the previous paragraph.

2.1.3 Measured Reactivity of Support Structure Removal – Reactivity values for the worth of the support structure are given in Table 3. Multiple measurements to assess the uncertainty in the support structure worth were not performed. Previous benchmarks in this series ([HEU-MET-FAST-051](#), [HEU-MET-FAST-071](#), and [HEU-MET-FAST-076](#)) assumed a 1σ standard deviation of 10% of each measured value of the support structure worth and the delayed critical measurement worth was sufficient. A slightly more rigorous approach is utilized in this evaluation.

The individual worth measurements were obtained using modified experiments from the clean critical experimental configuration. Each of these configurations would have a repeatability uncertainty of $\sim 2\text{f}$ (as discussed in the previous section). Therefore the uncertainty in the adjustment for the removal of the assembly support structure from the experiment configuration would be obtained by taking the square root of the number of measured worths, multiplied by the square root of the number of experiment configurations needed to evaluate a given measured worth, and multiplied by the reproducibility uncertainty for a single configuration. A total of four experiments were needed to evaluate the worth of Configuration 1, and two experiments for Configuration 2: $\sqrt{3} \times \sqrt{2} \times 2\text{f}$ and $\sqrt{1} \times \sqrt{2} \times 2\text{f}$, respectively. The uncertainty in the repeatability of the clean critical experiment is already evaluated in Section 2.1.2.

The calculated k_{eff} uncertainty associated with the uncertainty in the measured reactivity for support structure removal is 0.00032 for Configuration 1 and 0.00018 for Configuration 2.

2.1.4 Effective Delayed Neutron Fraction, β_{eff} – This parameter was reported by the experimenter to be 0.0066. Typically the uncertainty in β_{eff} is around 5%, which results in a Δk_{eff} of approximately ± 0.00005 and ± 0.00002 for Configurations 1 and 2, respectively, which is considered negligible (≤ 0.00005). This uncertainty was obtained by taking the difference between the experimental eigenvalue calculated for the actual experiment using the reported delayed neutron fraction, and an eigenvalue calculated using the delayed neutron fraction increased by an additional 5%.

^a Personal communication with Dick McKnight, July 2010.

Revision: 0

Date: September 30, 2010

Calculations were performed to verify the reported value of 0.0066 using ENDF/B-VII.0, JEFF-3.1, and JENDL-3.3. MCNP Monte Carlo calculations performed for the detailed benchmark model (both configurations) in Section 3 and results provided in Section 4 were repeated with neutron production from delayed neutrons disabled (TOTNU card set to “no”). Comparison of the calculated eigenvalues, using the equation below,^a provides estimated β_{eff} values. Averages of the calculated results from the three cross section sets are 0.00652 ± 0.00003 and 0.00644 ± 0.00004 , for Configurations 1 and 2, respectively, and are within the typical uncertainty of the reported value.

$$\beta_{eff} = 1 - \frac{k_{prompt}}{k_{eff}}.$$

2.2 Geometrical Properties

The measurement uncertainties in the stack heights can be calculated using the standard deviation of the average from multiple measurements, which are typically about ± 0.001 inches (± 0.00254 cm). The manufacturing tolerances of the Y-12 parts are ± 0.0001 inches (± 0.000254 cm). When multiple measurements of the dimensions of a part were taken, the average was typically within ± 0.00005 inches (± 0.000127 cm) of all the individual measurements.^b

There may be effects on the system k_{eff} values associated with correlations between uncertainties in stack heights, gap thicknesses, and the height of the individual parts in an assembly. However, except for the k_{eff} uncertainty associated with the uranium stack height uncertainties, the individual evaluated uncertainties in k_{eff} are negligible. Therefore, a possible increase in the uncertainty in k_{eff} due to correlation, if any, between the individual uncertainties is considered negligible.

2.2.1 Uranium Annuli - There are a total of 24 uranium annuli in Configuration 1 and 29 uranium annuli in Configuration 2. When evaluating the uncertainty for a given parameter, all uranium components are simultaneously modified. The calculated change in the eigenvalue for the perturbation of a given parameter is scaled by the square root of the number of annuli, N, to represent the randomness of the actual variation amongst the individual pieces.

2.2.1.1 Diameter

The diameters of each uranium annulus was measured after machining at the Y-12 Plant to an accuracy of 0.0001 inches (0.000254 cm) at several locations (~8) and then averaged. All measurements were at 70° Fahrenheit and are traceable back to the National Bureau of Standards. The uncertainty in the diameter of each of the annuli is reported as ± 0.00005 inches (± 0.000127 cm). To find the effect of this diametral uncertainty on the k_{eff} value, the diameters of the annuli (Table 4) were adjusted by a factor of 100 times the reported uncertainty. In order to keep the uranium mass of each experiment constant, the density of each of the uranium parts was adjusted accordingly. Effectively the entire uranium volume in the system was expanded and contracted while maintaining the total uranium mass constant. Outer and inner diameters were simultaneously increased by 0.0127 cm to find an upper perturbation k_{eff} value and then simultaneously decreased to find a lower perturbation k_{eff} value. Half of the difference between the upper and lower perturbation k_{eff} values was used to represent the variation in k_{eff} due to perturbing the annuli diameters by 0.0127 cm. The calculated difference in k_{eff} is 0.00055 and 0.00046 for Configurations 1 and 2, respectively. The 1σ uncertainty in k_{eff} associated with the uncertainty in the diameter of the uranium annuli is found from the following formula, where Δk_{eff} is one-half the difference between the upper and lower perturbation k_{eff}

^a R. K. Meulekamp and S. C. van der Marck, “Calculating the Effective Delayed Neutron Fraction with Monte Carlo,” *Nucl. Sci. Eng.*, **152**, 142-148 (2006).

^b Personal communication with John T. Mihalczo, March 2010.

values, N is the number of uranium annuli in each configuration, and the factor of square root of two is present because the inner and outer diameters were simultaneously perturbed:

$$\frac{\Delta k_{\text{eff}}}{100\sqrt{2}\sqrt{N}}.$$

The calculated k_{eff} uncertainty associated with the uncertainty in the diameters of the uranium annuli is <0.00001 for both configurations, which is negligible (≤ 0.00005).

2.2.1.2 Height

The height of each uranium annulus was measured after machining at the Y-12 Plant to an accuracy of 0.0001 inches (0.000254 cm) at several radial locations (~8) and then averaged. All measurements were at 70° Fahrenheit and are traceable back to the National Bureau of Standards. The uncertainty in the height of each uranium annulus is reported as ± 0.00005 inches (± 0.000127 cm). To find the effect of this uncertainty on the k_{eff} value, the heights of the annuli (Table 4) were adjusted by a factor of 10 times the reported uncertainty, while reducing the effective gap thicknesses between each component. The measured stack height, where possible, was conserved. When the increase in the combined heights of the individual parts was greater than the stack height, the parts were modeled in contact, with no gaps, and the effective stack height was increased. In order to keep the uranium mass of each experiment constant, the density of each of the uranium parts was adjusted accordingly. Effectively the entire uranium volume in the system was expanded and contracted while maintaining the total uranium mass constant. Heights were simultaneously increased by 0.00127 cm to find an upper perturbation k_{eff} value and then simultaneously decreased to find a lower perturbation k_{eff} value. Half of the difference between the upper and lower perturbation k_{eff} values was used to represent the variation in k_{eff} due to perturbing the annuli heights by 0.00127 cm. The calculated difference in k_{eff} is 0.00007 and 0.00006 for Configurations 1 and 2, respectively. The 1σ uncertainty in k_{eff} associated with the uncertainty in the heights of the uranium annuli is found from the following formula, where Δk_{eff} is one-half the difference between the upper and lower perturbation k_{eff} values, N is the number of uranium annuli in each configuration, and 10 is the parameter scaling factor:

$$\frac{\Delta k_{\text{eff}}}{10\sqrt{N}}.$$

The calculated k_{eff} uncertainty associated with the uncertainty in the individual heights of the uranium annuli is <0.00001 for both configurations, which is negligible (≤ 0.00005).

2.2.1.3 Stack Height

The stack heights of the uranium annuli placed above and below the stainless steel diaphragm were measured with a standard deviation of the average of ± 0.001 in. (± 0.00254 cm) for most measurements, which is also the uncertainty of the measurement device for taking stack height measurements. To find the effect of this uncertainty on the k_{eff} value, the stack height of these annuli (Table 2) was adjusted by increasing the effective gap thicknesses between each component. The stack height was increased by 0.0254 cm (a factor of 10 times the reported uncertainty) to find an upper perturbation k_{eff} value. The difference between the upper perturbation k_{eff} value and the benchmark model k_{eff} value was used to represent the variation in k_{eff} due to perturbing the disc stack height by 0.0254 cm. The calculated difference in k_{eff} is -0.00190 and -0.00224 for Configurations 1 and 2, respectively. The 1σ uncertainty in k_{eff} associated with the uncertainty in the measured stack height of the uranium annuli is found from the following formula, where Δk_{eff} is the difference between the upper perturbation and benchmark model k_{eff} values, N is the number of uranium

annuli stacks in each configuration, 10 is the parameter scaling factor, and X represents the fraction of annuli stacks that had an uncertainty twice that of the nominal value (see Table 2):

$$\frac{\Delta k_{\text{eff}}}{10\sqrt{N}}(1+X).$$

There are six stacks in Configuration 1 and eight stacks in Configuration 2. In both configurations, the top 9-11 inch annulus had an uncertainty twice that of the nominal uncertainty. This increase in the uncertainty estimate was accounted for by the factor $(1 + X)$ in the above equation. The fraction, X, is 1/6 and 1/8 for Configurations 1 and 2, respectively. The calculated k_{eff} uncertainty associated with the uncertainty in the uranium annuli stack height is 0.00009 for both configurations.

2.2.2 Beryllium Discs - There are a total of four beryllium discs in Configuration 1 and three beryllium discs in Configuration 2. When evaluating the uncertainty for a given parameter, all beryllium components are simultaneously modified. The calculated change in the eigenvalue for the perturbation of a given parameter is scaled by the square root of the number of discs, N, to represent the randomness of the actual variation amongst the individual pieces.

2.2.2.1 Diameter

The diameter of each beryllium disc is stated to be approximately the same as the average diameter of the uranium discs in [HEU-MET-FAST-069](#), which is 6.996444 inches (17.7709671 cm). The uncertainty in the diameter of each of the uranium parts is reported as ± 0.00005 inches (± 0.000127 cm). However, twice that uncertainty is assumed to apply to the beryllium discs because of the lack of reported information. To find the effect of this diametral uncertainty on the k_{eff} value, the diameters of the discs were adjusted by a factor of 100 times the assumed uncertainty. In order to keep the beryllium mass of each experiment constant, the density of each of the beryllium discs was adjusted accordingly. Effectively the entire beryllium volume in the system was expanded and contracted while maintaining the total beryllium mass constant. Diameters were simultaneously increased by 0.0254 cm to find an upper perturbation k_{eff} value and then simultaneously decreased to find a lower perturbation k_{eff} value. Half of the difference between the upper and lower perturbation k_{eff} values was used to represent the variation in k_{eff} due to perturbing the diameters by 0.0254 cm. The calculated difference in k_{eff} is 0.00007 and 0.00005 for Configurations 1 and 2, respectively. The 1σ uncertainty in k_{eff} associated with the uncertainty in the diameter of the beryllium discs is found from the following formula, where Δk_{eff} is one-half the difference between the upper and lower perturbation k_{eff} values, N is the number of beryllium discs in each configuration, and 100 is the parameter scaling factor:

$$\frac{\Delta k_{\text{eff}}}{100\sqrt{N}}.$$

The calculated k_{eff} uncertainty associated with the uncertainty in the diameters of the beryllium discs is <0.00001 for both configurations, which is negligible (≤ 0.00005).

2.2.2.2 Height

Nominal heights were reported for the beryllium discs. The uncertainty in the height of each uranium disc is reported as ± 0.00005 inches (± 0.000127 cm). However, twice that uncertainty is assumed to apply to the beryllium discs because of the lack of reported information. To find the effect of this uncertainty on the k_{eff} value, the heights of the discs (Table 10) were adjusted by a factor of 10 times the assumed uncertainty, while reducing the effective gap thicknesses between each component. The measured stack height, where possible, was conserved. When the increase in the combined heights of the individual parts was greater than

the stack height, the parts were modeled in contact, with no gaps, and the effective stack height was increased. In order to keep the beryllium mass of each experiment constant, the density of each of the beryllium discs was adjusted accordingly. Effectively the entire beryllium volume in the system was expanded and contracted while maintaining the total beryllium mass constant. Heights were simultaneously increased by 0.00254 cm to find an upper perturbation k_{eff} value and then simultaneously decreased to find a lower perturbation k_{eff} value. Half of the difference between the upper and lower perturbation k_{eff} values was used to represent the variation in k_{eff} due to perturbing the heights by 0.00254 cm. The calculated difference in k_{eff} is 0.00006 for both configurations. The 1σ uncertainty in k_{eff} associated with the uncertainty in the heights of the beryllium discs is found from the following formula, where Δk_{eff} is one-half the difference between the upper and lower perturbation k_{eff} values, N is the number of beryllium discs in each configuration, and 10 is the parameter scaling factor:

$$\frac{\Delta k_{\text{eff}}}{10\sqrt{N}}.$$

The calculated k_{eff} uncertainty associated with the uncertainty in the individual heights of the beryllium discs is <0.00001 for both configurations, which is negligible (≤ 0.00005).

2.2.2.3 Stack Height

There are two stacks in Configuration 1 and one stack in Configuration 2. The single stack in Configuration 2 had no uncertainty in the stack height measurement and only a single beryllium disc was used for the lower half of the experiment. However, the uncertainty of the measurement device for taking stack height measurements is ± 0.001 in. (± 0.00254 cm).

The stack heights of the beryllium discs placed above and below the stainless steel diaphragm were measured with a standard deviation of the average of less than ± 0.002 in. (± 0.00508 cm). To find the effect of this uncertainty on the k_{eff} value, the stack height (Table 2) was adjusted by increasing the effective gap thicknesses between each component. The stack height was increased by 0.0508 cm (a factor of 10 times the maximum measurement uncertainty) to find an upper perturbation k_{eff} value. The difference between the upper perturbation k_{eff} value and the benchmark model k_{eff} value was used to represent the variation in k_{eff} due to perturbing the stack height by 0.0508 cm. The calculated difference in k_{eff} is 0.00055 and 0.00004 for Configurations 1 and 2, respectively. The 1σ uncertainty in k_{eff} associated with the uncertainty in the measured stack height of the beryllium discs is found from the following formula for Configuration 1, where Δk_{eff} is the difference between the upper perturbation and benchmark model k_{eff} values, N is the number (two) of beryllium disc stacks, 10 is the parameter scaling factor, and X represents the fraction of disc stacks (1/2) that had an uncertainty half that of the nominal value:

$$\frac{\Delta k_{\text{eff}}}{10\sqrt{N}}(1-X).$$

The 1σ uncertainty in k_{eff} associated with the uncertainty in the measured stack height of the beryllium discs is found from the following formula for Configuration 2, where Δk_{eff} is the difference between the upper perturbation and benchmark model k_{eff} values and 20 is the parameter scaling factor (assuming a stack height uncertainty of ± 0.001 in. (± 0.00254 cm)), which is equivalent to the uncertainty in the device for stack height measurements:

$$\frac{\Delta k_{\text{eff}}}{20}.$$

The calculated k_{eff} uncertainty associated with the uncertainty in the beryllium disc stack height is 0.00002 for Configuration 1 and <0.00001 for Configuration 2, both of which are negligible (≤ 0.00005).

2.2.3 Lateral Assembly Alignment – Lateral alignment measurements were made to within ± 0.005 inches (± 0.0127 cm). To find the effect of this uncertainty on the k_{eff} value, the lower half of each configuration was moved laterally (in a model) by a factor of 10 times the reported uncertainty. The lower halves were moved (in a model) a distance of 0.127 cm in the horizontal direction to find an upper perturbation k_{eff} value. The difference between the upper perturbation k_{eff} value and the benchmark model k_{eff} value was used to represent the variation in k_{eff} due to perturbing the lateral assembly alignment by 0.127 cm. The calculated difference in k_{eff} is -0.00005 and -0.00006 for Configurations 1 and 2, respectively. The 1σ uncertainty associated with the uncertainty in the lateral alignment is found from the following formula, where Δk_{eff} is the difference between the upper perturbation and benchmark model k_{eff} values, and 10 is the parameter scaling factor:

$$\frac{\Delta k_{\text{eff}}}{10\sqrt{3}}.$$

This uncertainty is treated as a bounding uncertainty with uniform probability; therefore, the final uncertainty is divided by the square root of three. The calculated k_{eff} uncertainty associated with the uncertainty in the lateral assembly alignment is <0.00001 for both configurations, which is negligible (≤ 0.00005).

2.2.4 Vertical Assembly Alignment – The uncertainty of axial symmetry was not considered in this evaluation since it is embedded within the uranium and beryllium diameter uncertainties.

2.2.5 Gaps between Parts – The uncertainty in gap heights was not considered in this evaluation since it is embedded within the uranium and beryllium disc stack height and diameter uncertainties.

For the benchmark model and uncertainty analysis, the total height of the gaps between the beryllium discs was obtained by taking the difference between the measured stack height and the summation of the heights of the beryllium discs in each stack. The total gap height was then divided by the number of discs minus one, to represent the number of gaps between the beryllium discs. There is no gap between the top beryllium disc stack and the stainless steel diaphragm. The gap heights for the beryllium discs were calculated to be 0.0 and 0.008 in. (0.0 and 0.02032 cm) for the top and bottom stacks, respectively, of Configuration 1. The stack height above the diaphragm had a measured value less than the sum of the heights of the individual parts; thus the experimenter treated the gap thickness with an effective height of zero. The gap between the discs in the top stack of beryllium discs in Configuration 2 is 0.001 in. (0.0254 cm). There was only a single beryllium disc below the steel diaphragm in Configuration 2.

The total height of the gaps between the stacks of uranium annuli was obtained by taking the difference between the measured stack height and the summation of the heights of the uranium annuli in each stack. The total gap height was then divided by the number of annuli minus one, to represent the number of gaps between the uranium annuli. There is no gap between the bottom of the top uranium annuli stacks and the stainless steel diaphragm. The gap heights for Configurations 1 and 2 can be seen in their respective figures in Section 3.2 (Figures 10 and 11, respectively).

The tallest stack of uranium annuli or beryllium discs in the lower section of each configuration was modeled “in contact with” the bottom of the stainless steel diaphragm. The gaps between the diaphragm and the remaining stacks were adjusted such that the bottoms of all the lower stacks were collocated on the same plane. This effectively models each of these stacks as having been “raised” as a single configuration on a planar surface (as was performed in the actual experiment).

The measured worth of the diaphragm includes the separation distance between the two halves of the experiment. Therefore, when the diaphragm is removed from the model, the parts adjacent to the diaphragm are brought closer together and the thickness of 0.010 in. (0.0254 cm) that represents the diaphragm thickness would be eliminated.^a

It should be noted that the gaps calculated using the experimental data do not necessarily match exactly with those in Table 5; most, however, are approximately the same within rounding of digits. The exceptions include the 9-11" bottom annulus for both Configuration 1 and 2. The differences are much less than the measurement uncertainty of the individual parts and the stacked height and most likely evolve from experimenter miscalculation of the actual number of gaps in each stack of annuli because the stack height reported in both Reference 1 and the logbook are identical. It is unclear for what purpose the annular gaps in Table 6 were presented other than to demonstrate the close fit of the annuli, effectively producing a "solid" annulus of HEU material.

2.2.6 Assembly Separation – The uncertainty for the separation of the upper and lower assemblies is based upon accuracy of measurement when bringing the two experiment halves into contact, ± 0.001 in. (± 0.00254 cm). This uncertainty, however, would be included within the measurement uncertainty of the worth of the stainless steel diaphragm.

2.3 Compositional Variations

2.3.1 Uranium Annuli - There are a total of 24 uranium annuli in Configuration 1 and 29 uranium annuli in Configuration 2. When evaluating the uncertainty for a given parameter, all uranium components are simultaneously modified. The calculated change in the eigenvalue for the perturbation of a given parameter is scaled by the square root of the number of annuli, N, to represent the randomness of the actual variation amongst the individual pieces.

2.3.1.1 Mass

The uranium mass of each part measured at the Y-12 Plant is traceable back to the Bureau of Standards to less than 0.5 gram accuracy and then rounded to the nearest gram. The uncertainty for the mass of each uranium annuli is ± 0.5 g. A mass measurement of multiple uranium annuli was not performed. To find the effect of this uncertainty on the k_{eff} value, the masses of the annuli (Table 4) were adjusted by a factor of 10 times the reported uncertainty. In order to keep the uranium volume of the experiment constant, the density of each of the uranium annuli was adjusted accordingly. Uranium masses were simultaneously increased by 5 g to find an upper perturbation k_{eff} value and then simultaneously decreased to find a lower perturbation k_{eff} value. Half of the difference between the upper and lower perturbation k_{eff} values was used to represent the variation in k_{eff} due to perturbing the annuli masses by 5 g. The calculated difference in k_{eff} is 0.00060 and 0.00070 for Configurations 1 and 2, respectively. The 1σ uncertainty in k_{eff} associated with the uncertainty in the mass of the uranium annuli is found from the following formula, where Δk_{eff} is one-half the difference between the upper and lower perturbation k_{eff} values, N is the number of uranium annuli in each configuration, and 10 is the parameter scaling factor:

$$\frac{\Delta k_{\text{eff}}}{10\sqrt{N}}.$$

The calculated k_{eff} uncertainty associated with the uncertainty in the mass of the uranium annuli is 0.00001 for both configurations, which is negligible (≤ 0.00005).

^a Personal communication with John T. Mihalczo, February 2010.

Revision: 0

Date: September 30, 2010

2.3.1.2 Isotopic Content

Based on the accuracy of isotopic ratios from the mass spectrometry laboratory at the Y-12 Plant, uncertainty for the uranium isotopic content is ± 0.005 wt.% for ^{234}U , ^{235}U , and ^{236}U . The ^{238}U content was obtained by subtracting the sum of the ^{234}U , ^{235}U , and ^{236}U contents from one. The effect of this uncertainty on the k_{eff} values was determined by adjusting the isotopic content (Table 7) of the uranium parts by a factor of 10 times the reported maximum uncertainty. An upper perturbation k_{eff} value was found by simultaneously increasing the isotopic contents of ^{234}U , ^{235}U , and ^{236}U by 0.05 wt.% and adjusting the ^{238}U isotopic content accordingly. The isotopic contents of ^{234}U , ^{235}U , and ^{236}U were then simultaneously decreased by 0.05 wt.%, again with the ^{238}U content adjusted, to find the lower perturbation k_{eff} value. Half of the difference between the upper and lower perturbation k_{eff} values was used to represent the variation in k_{eff} due to perturbing the isotopic content by 0.05 wt.%. The calculated difference in k_{eff} is 0.00047 and 0.00049 for Configurations 1 and 2, respectively. The 1σ uncertainty in k_{eff} associated with the uncertainty in the isotopic content of the uranium annuli is found from the following formula, where Δk_{eff} is one-half the difference between the upper and lower perturbation k_{eff} values, N is the number of uranium annuli in each configuration, and 10 is the parameter scaling factor:

$$\frac{\Delta k_{\text{eff}}}{10\sqrt{N}}.$$

The calculated k_{eff} uncertainty associated with the uncertainty in the isotopic content of the uranium discs is 0.00001 for both configurations, which is negligible (≤ 0.00005). Since uncertainty in ^{234}U , ^{235}U , and ^{236}U are not perfectly correlated (if one value is off by 0.05 wt.%), the variability in ^{238}U is probably overestimated. However, the effect of uncertainty in isotopic content of uranium is a small contributor to the overall uncertainty in k_{eff} .

A second study was performed to evaluate the effect of increasing the ^{235}U content by 0.05 wt.% and decreasing the ^{234}U and ^{236}U contents by 0.025 wt.% apiece (maintaining the ^{238}U content constant) to obtain an upper perturbation k_{eff} value. The reverse adjustments in wt.% were performed to obtain a lower perturbation k_{eff} value. Half of the difference between the upper and lower perturbation k_{eff} values was used to represent the variation in k_{eff} due to perturbing the isotopic content. The calculated difference in k_{eff} is 0.00012 and 0.00013 for Configurations 1 and 2, respectively. The 1σ uncertainty in k_{eff} associated with the uncertainty in the isotopic content of the uranium annuli is found from the previous formula. The calculated k_{eff} uncertainty associated with the uncertainty in the isotopic content of the uranium discs is < 0.00001 for both configurations, which is negligible (≤ 0.00005).

Typically, the isotopic content of all components in a system would be varied individually so as to isolate any parts with significant merit. As this is a small system and relatively large perturbations of the combined isotopic content yield a negligible change in k_{eff} , all isotopic contents were adjusted simultaneously.

2.3.1.3 Impurities

The uranium impurities listed in Table 8 are given as the average of a spectrographic analysis from randomly sampled components for each impurity (assuming the values to be normally distributed) or listed as less than a minimum value. In the latter case, they are less than the detectable limit. The impurity content, as specified in Table 8, is accepted as the nominal composition. For impurities below a detectable limit, the content is selected as half the detectable limit and the other half representing the 1σ uncertainty; therefore the uncertainty represents a 100% uncertainty in the detection limit. A summary of the nominal impurity composition is found in Table 11. The oxygen and nitrogen content was included at the experimentalist-specified quantities of 20 and 30 ppm, respectively. A 1σ uncertainty of half their value was assumed.

Table 11. Impurity Content of Uranium Metal Discs.

Element	Parts per Million by Weight (ppm)	Standard Deviation (ppm)
Ag	8	3.2
Ba	0.005	0.005
Bi	164	52.9
C	5	2.4
Ca	0.1	0.05
Cd	0.5	0.5
Co	5	1.9
Cr	7	1.9
Cu	25	8
K	0.1	0.1
Li	1	1
Mg	3	1.7
Mn	56	17.1
Mo	0.5	0.5
Na	27	7.7
Ni	100	10
Sb	38	17.4
Ti	1	0.5
O	20	10
N	30	15

The impurities were simultaneously increased by 3σ to find an upper perturbation k_{eff} value and then simultaneously decreased to find a lower perturbation k_{eff} value. Impurity limits were not reduced below a quantity of zero. The weight fraction of the uranium metal was adjusted, as appropriate, to compensate for the adjustments in impurity content. Half of the difference between the upper and lower perturbation k_{eff} values was used to represent the variation in k_{eff} due to perturbing the uranium impurity. The calculated difference in k_{eff} is 0.00017 and 0.00016 for Configurations 1 and 2, respectively. The 1σ uncertainty in k_{eff} associated with the impurity content of the uranium annuli is found from the following formula, where Δk_{eff} is one-half the difference between the upper and lower perturbation k_{eff} values and 3 is the parameter scaling factor:

$$\frac{\Delta k_{eff}}{3}.$$

The calculated k_{eff} uncertainty associated with the uncertainty in the impurity content of the uranium annuli is 0.00006 for Configuration 1 and 0.00005 for Configuration 2.

2.3.2 Beryllium Discs - The density of the beryllium is not directly evaluated as an uncertainty in this benchmark evaluation. The beryllium discs were weighed with the same precision as the uranium discs. Therefore the mass is believed to be a more accurate measurement than the reported density. While the dimensions of the beryllium discs were not recorded in detail but machined with the same precision as the uranium discs, the larger assumed uncertainty in these measurements account for additional density variation. The mass densities of the beryllium discs vary between 1.819 and 1.842 g/cm³ with an average mass density of 1.832 g/cm³ (HEU-MET-FAST-069). The reported density of 1.854 g/cm³ in Table 6 for the original stock material is believed to be incorrect. However, since the material was later machined at Y-12 and subsequently weighed and measured, the calculated mass density values are believed to appropriately represent the beryllium discs used in this experiment.

There are a total of four beryllium discs in Configuration 1 and three beryllium discs in Configuration 2. When evaluating the uncertainty for a given parameter, all beryllium components are simultaneously modified. The calculated change in the eigenvalue for the perturbation of a given parameter is scaled by the square root of the number of discs, N, to represent the randomness of the actual variation amongst the individual pieces.

The uncertainties in the mass and dimensions of the beryllium discs were evaluated and determined to be negligible.

2.3.2.1 Mass

The uncertainty for the mass of each beryllium disc is ± 0.5 g. To find the effect of this uncertainty on the k_{eff} value, the mass of the discs were adjusted by a factor of 10 times the measurement uncertainty. Beryllium masses (Table 10) were simultaneously increased by 5 g to find an upper perturbation k_{eff} value and then simultaneously decreased to find a lower perturbation k_{eff} value. Half of the difference between the upper and lower perturbation k_{eff} values was used to represent the variation in k_{eff} due to perturbing the disc masses by 5 g. The calculated difference in k_{eff} is 0.00024 and 0.00014 for Configurations 1 and 2, respectively. The 1σ uncertainty in k_{eff} associated with the uncertainty in the mass of the beryllium discs is found from the following formula, where Δk_{eff} is one-half the difference between the upper and lower perturbation k_{eff} values, N is the number of beryllium discs, and 10 is the parameter scaling factor:

$$\frac{\Delta k_{\text{eff}}}{10\sqrt{N}}.$$

The calculated k_{eff} uncertainty associated with the uncertainty in the mass of the beryllium discs is 0.00001 for both configurations, which is negligible (≤ 0.00005).

2.3.2.2 Impurities

The beryllium impurities listed in Table 9 are given as the average impurity quantities. The impurity content, as specified in Table 12, is accepted as the nominal composition. The amount of oxygen contained in the BeO impurity is computed and also treated as an impurity (Table 12). To find the effect of this uncertainty on the k_{eff} value, the impurity content is adjusted by a factor of 100% of the average quantity. This uncertainty is then treated as a bounding uncertainty with uniform probability; therefore, the final uncertainty is divided by the square root of three.

Table 12. Nominal Beryllium Impurities.

Impurity	wt.%
O	1.23458
Al	0.06
C	0.12
Fe	0.13
Mg	0.02
Bi	0.05
B	0.001
Cd	0.0002
Dy	0.0001
Br	0.00005
Gd	0.0001
Ni	0.0001
Sm	0.0001
Total	1.61623 ^(a)

(a) The total quantity of impurities does not add up to the original amount of 2.31165 wt.% because the beryllium in BeO is not included.

The impurities were simultaneously doubled to find an upper perturbation k_{eff} value and then simultaneously removed to find a lower perturbation k_{eff} value. The weight fraction of the beryllium metal was adjusted, as appropriate, to compensate for the adjustments in impurity content. Half of the difference between the upper and lower perturbation k_{eff} values was used to represent the variation in k_{eff} due to perturbing the beryllium impurity by 100%. The calculated difference in k_{eff} is 0.00056 and 0.00032 for Configurations 1 and 2, respectively. The 1σ uncertainty associated with the impurity content of the beryllium discs is found from the following formula, where Δk_{eff} is one-half the difference between the upper and lower perturbation k_{eff} values:

$$\frac{\Delta k_{\text{eff}}}{\sqrt{3}}.$$

The calculated k_{eff} uncertainty associated with the uncertainty in the impurity content of the beryllium discs is 0.00032 for Configuration 1 and 0.00018 for Configuration 2.

2.4 Total Experimental Uncertainty

The total k_{eff} uncertainty for each experiment was calculated by taking the square root of the sum of the squares of all the individual uncertainties discussed in this section; they are summarized in Table 13. The uncertainties make these acceptable benchmark experiments. Case 1 represents Configuration 1, the 13" annulus, and Case 2 represents Configuration 2, the 15" annulus.

Table 13.a. Total Experimental Uncertainty.

Perturbed Parameter	Parameter Value	1σ Uncertainty	Case 1 Δk_{eff} (13" Annulus)
Temperature (K)	294	± 2	0.00013
Experiment reproducibility (ϕ)	--	± 2	0.00013
Measured reactivity worth (ϕ)	--	$\pm \sqrt{3} \times \sqrt{2} \times 2$	0.00032
β_{eff}	0.0066	$\pm 5\%$	Negligible
Uranium diameter (cm)	Table 16	± 0.000127	Negligible
Uranium height (cm)	Table 16	± 0.000127	Negligible
Uranium stack height (cm)	Table 2	+0.00254	0.00009
Beryllium diameter (cm)	Figure 10	± 0.000254	Negligible
Beryllium height (cm)	Figure 10	± 0.000254	Negligible
Beryllium stack height (cm)	Table 2	+0.00508	Negligible
Lateral assembly alignment (cm)	0	± 0.0127	Negligible
Vertical assembly alignment (cm)		Not Applicable – See Section 2.2.4	
Gaps between parts (cm)		Not Applicable – See Section 2.2.5	
Assembly separation (cm)		Not Applicable – See Section 2.2.6	
Uranium mass (g)	Table 4	± 0.5	Negligible
Uranium isotopic content (wt.%)	Table 7	± 0.005	Negligible
Uranium impurities (ppm)	Table 11		0.00006
Beryllium mass (g)	Table 10	± 0.5	Negligible
Beryllium impurities (wt.%)	Table 12		0.00032
Total	--	--	0.00050

Table 13.b. Total Experimental Uncertainty.

Perturbed Parameter	Parameter Value	1σ Uncertainty	Case 2 Δk_{eff} (15" Annulus)
Temperature (K)	294	± 2	0.00013
Experiment reproducibility (ϕ)	--	± 2	0.00013
Measured reactivity worth (ϕ)	--	$\pm \sqrt{1} \times \sqrt{2} \times 2$	0.00018
β_{eff}	0.0066	$\pm 5\%$	Negligible
Uranium diameter (cm)	Table 16	± 0.000127	Negligible
Uranium height (cm)	Table 16	± 0.000127	Negligible
Uranium stack height (cm)	Table 2	+0.00254	0.00009
Beryllium diameter (cm)	Figure 11	± 0.000254	Negligible
Beryllium height (cm)	Figure 11	± 0.000254	Negligible
Beryllium stack height (cm)	Table 2	+0.00508	Negligible
Lateral assembly alignment (cm)	0	± 0.0127	Negligible
Vertical assembly alignment (cm)		Not Applicable – See Section 2.2.4	
Gaps between parts (cm)		Not Applicable – See Section 2.2.5	
Assembly separation (cm)		Not Applicable – See Section 2.2.6	
Uranium mass (g)	Table 4	± 0.5	Negligible
Uranium isotopic content (wt.%)	Table 7	± 0.005	Negligible
Uranium impurities (ppm)		Table 11	Negligible
Beryllium mass (g)	Table 10	± 0.5	Negligible
Beryllium impurities (wt.%)		Table 12	0.00018
Total	--	--	0.00033

3.0 BENCHMARK SPECIFICATIONS

3.1 Description of Models

Two benchmark models were developed to represent each of the HEU metal annuli with beryllium core experiments. Figures 8 and 9 show the 13- and 15-inch annuli experiments, respectively (Configurations 1 and 2, respectively). The detailed benchmark model represents, as much as possible, the experiment described in Reference 1. Some approximation is necessary to estimate the height of gaps between the individual components of the experiment and reproduce the measured stack heights; however, any uncertainty in the gap height would be negligible (see Sections 2.2.1.3, 2.2.2.3, and 2.2.5). The simple benchmark model reduces the experiment to a basic cylindrical structure comprised of two single materials: HEU and beryllium.

The experimental assembly, including the stainless steel diaphragm and the room itself, are not included in the benchmark models.

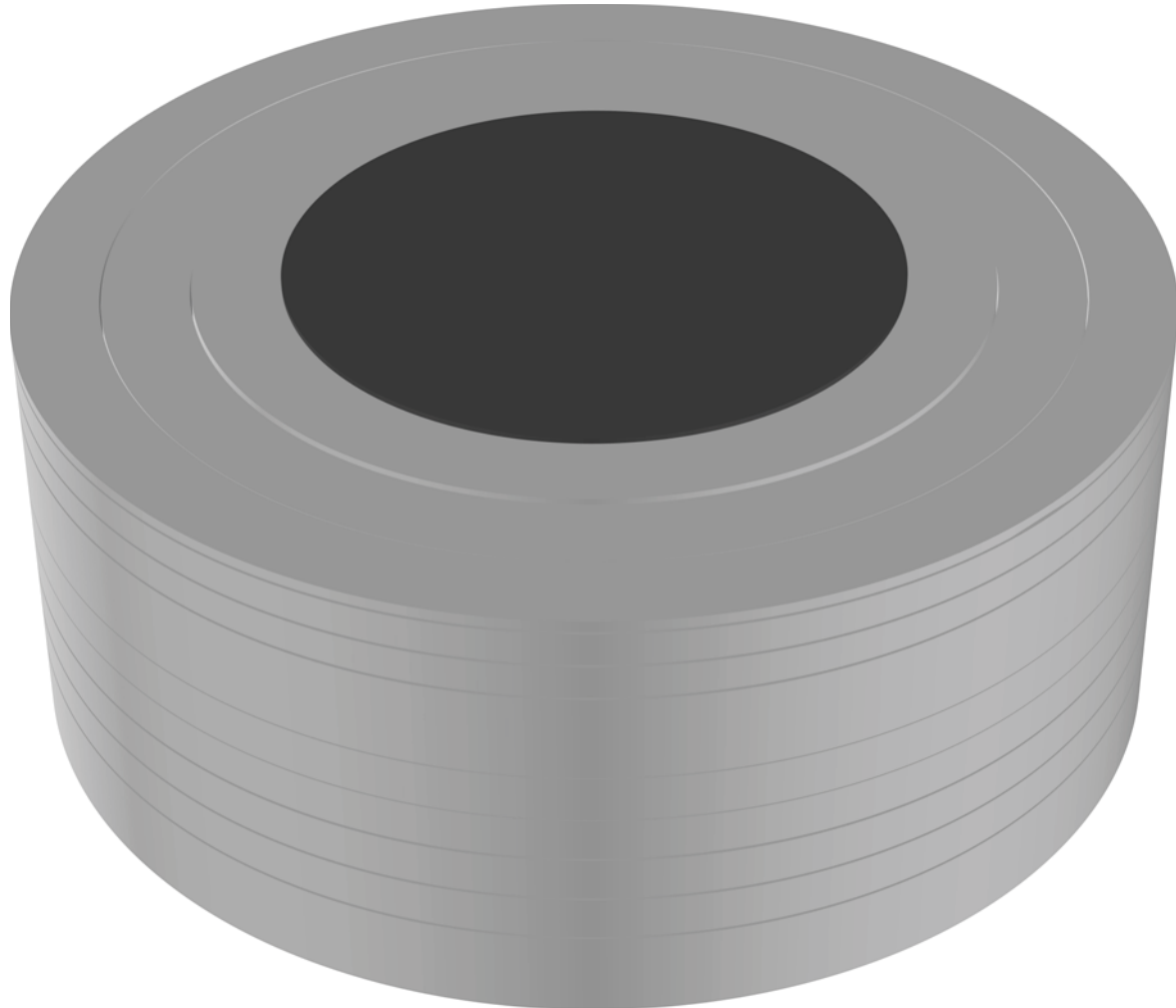


Figure 8. Stack of HEU Annuli (13-Inch-Diameter) with Beryllium Core.

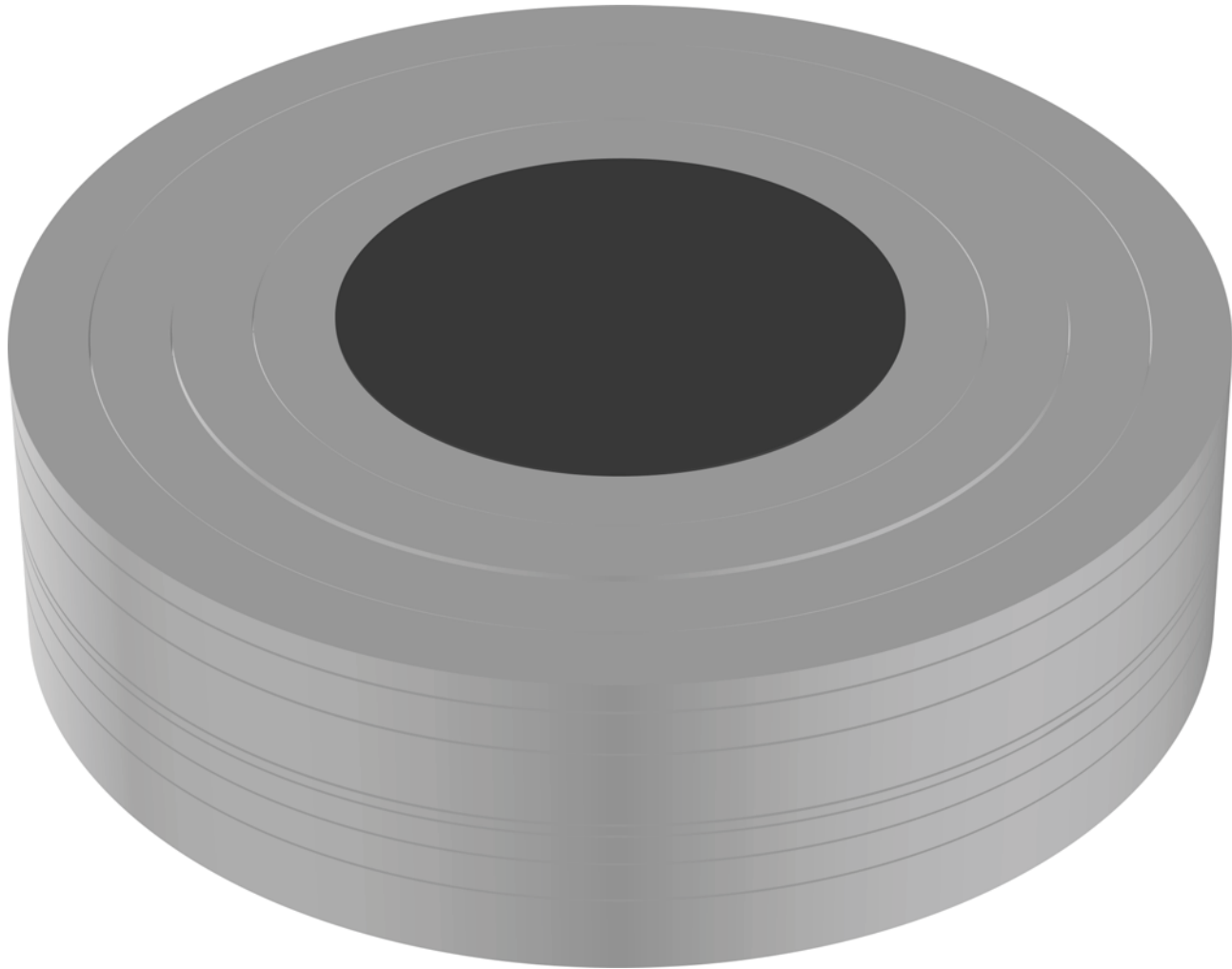


Figure 9. Stack of HEU Annuli (15-Inch-Diameter) with Beryllium Core.

3.1.1 Detailed Models – The detailed benchmark models are comprised of stacks of uranium metal annuli. There are three sets of rings in Configuration 1 and four sets in Configuration 2. The center core of the annuli contains a stack of beryllium discs. Small gaps exist between adjacent components of the experiment and each component has unique dimensions and composition that reproduce, as closely as possible, the actual component dimensions and compositions (see Figures 10 and 11). A discussion of the gaps between discs is provided in Section 2.2.5.

Very small gaps exist between the components of the experiment, as the top and bottom surfaces of the discs are not perfectly smooth. However, it is not easy to exactly model the imperfect surfaces of the experiment components. The measured stack height and individual heights of each part are preserved in the detailed benchmark model. To preserve the stack height, small gaps must be placed between the discs. These gap heights are exaggerated in Figures 10 and 11 so that the gap heights can be easily noticed. The effect of eliminating the gaps between parts is quite small compared to effects such as adjusting the overall stacked height dimension of the experiment.

3.1.2 Simple Models – The simple benchmark models consist of a single HEU metal annulus with an inner diameter of 17.78 cm (7 in.) and an outer diameter of 33.02 cm (13 in.) or 38.1 cm (15. in.) for Configurations 1 and 2, respectively. The core of the annulus is a beryllium cylinder with a diameter of

17.78 cm (7 in.) and a height matching that of the uranium annulus in each configuration. The respective heights of the annuli in Configurations 1 and 2 are 12.7 cm (5 in.) and 10.16 cm (4 in.). There are no gaps present between the uranium and beryllium parts. Total mass for the beryllium and uranium is conserved in the simple model. The simple model dimensions are chosen to correspond to the nominal experimental dimensions.

3.1.3 Bias Assessment

3.1.3.1 Room Return

The properties and dimensions of the room in which the experiment was performed were not provided in Reference 1, but they are well known and available from many other East Cell, ORCEF experiment reports. The dimensions were obtained from a similar benchmark report: [HEU-MET-FAST-076](#). Room return effects were estimated using the room and experiment placement dimensions provided in Section 1.2 and assuming that the other concrete wall, floor, and ceiling thicknesses are 2 feet. The concrete was modeled as Oak Ridge Concrete with a density of 2.3 g/cm^3 and the room containing air with a density of 1.2 kg/m^3 . The use of either Oak Ridge Concrete or Magnuson Concrete would provide similar results as shown in [HEU-MET-FAST-076](#). Both concretes were prepared using crushed limestone instead of sand due to the unavailability of sand at the time.^a

The effective bias in neglecting room return effects was determined to be $-0.00055 \pm 0.00003 \Delta k_{\text{eff}}$ for Configuration 1 and $-0.00021 \pm 0.00003 \Delta k_{\text{eff}}$ for Configuration 2. Their respective worth is equivalent to $-8.3 \pm 0.6\%$ and $-3.2 \pm 0.5\%$ using a β_{eff} of 0.0066 ± 0.00033 (assumed uncertainty of 5%). Room return calculations for [HEU-MET-FAST-069](#) using both MCNP5 and KENO-IV were found to be comparable within 2σ . No additional room return calculations were performed to evaluate these benchmark experiments.

3.1.3.2 Support Structure Removal

The benchmark models do not include the support structure of the experimental assembly or the stainless steel diaphragm. Removal of the support structure materials was included in the experimental assessment of the reported eigenvalue and the uncertainty in their worth is discussed in Section 2.2.2.

The diaphragm bolts were not included in the experimental analysis of the support structure worth.^b A calculation was performed to evaluate a “ring” of steel material where the bolts would have been located in the actual experiment. The calculated bias was negligible.

3.1.3.3 Temperature

The temperature reactivity coefficient is reported by the experimenter to be approximately $-1\text{e}^{-\text{C}}$. The parts were measured at $\sim 294 \text{ K}$ and the original experiments were performed at $\sim 295 \text{ K}$. The uncertainty in either of these two temperatures is unknown. The benchmark models use dimensions as measured at room temperature conditions, $\sim 294 \text{ K}$, and ENDF/B-VII.0 cross sections evaluated at 300 K . No bias for temperature effects was included in the benchmark model, however an uncertainty in the temperature of the experiments and evaluation are provided in Section 2.1.1.

^a Personal communication with John T. Mihalczo, February 2010.

^b Personal communication with John T. Mihalczo, June 2010.

3.1.3.4 Model Simplification

Additional simplifications were performed to facilitate the application of a simple model in place of the detailed model. Simplifications include the removal of impurities from the uranium and beryllium discs (for the impurity of BeO, only the oxygen in BeO is removed, and the beryllium is assumed to be beryllium metal), development of a cylinder of beryllium with uniform material properties, and development of an annular cylinder of uranium with uniform material properties. The inner diameter of the annulus and diameter of the beryllium cylinder are adjusted to 17.78 cm (7 in.) for both simplifications. The adjusted heights of the annuli and discs in Configurations 1 and 2 are 12.7 cm (5 in.) and 10.16 cm (4 in.), respectively. There are no gaps between the individual discs or annuli in a stack, as they are modeled as a single homogenous cylinder or annulus. These adjustments in dimensions were performed to match the approximate measurement descriptions for the experiment. The density of the individual stacks was computed using the total measured mass of each stack divided by the total adjusted volume. The mass density of the beryllium and uranium cylinders is 1.8353 and 18.3355 g/cm³, respectively, for Configuration 1. These same two densities are respectively 1.8346 and 18.5568 g/cm³ for Configuration 2. These densities are less than those for the individual parts due to the incorporation of gaps into the total volume. The weight fraction of isotopes in the uranium disc stack was weighted by the mass of the individual discs in the stack. Results for these simplifications are shown in Table 14. MCNP was utilized to estimate the biases; the statistical uncertainty in Δk_{eff} is 0.00003.

The effect of incorporating all of these simplifications into a single benchmark model was assessed using ENDF/B-VII.0, JEFF-3.1,^a and JENDL-3.3^b neutron cross section libraries. Results, including the total simplification bias, are shown in Table 15. There is a significant difference in eigenvalues between the simple and detailed benchmark models caused by the increase in neutron leakage from the system (Appendix B). There are two competing effects when homogenizing the benchmark models: removal of the interstitial gaps between parts, and increasing the surface area to volume ratio while conserving mass. The removal of the gaps increases k_{eff} by eliminating any streaming paths while the homogenization of the model to meet the nominal dimensions of the experiment provided by the experimenter reduces k_{eff} . Because the gaps between parts are very small, their contribution to the bias is minimal compared to the effect of increasing the total leakage from the system.

Table 14. Calculated Biases for Individual Model Simplifications.

Simplification	Configuration 1			Configuration 2		
	Δk_{eff}	\pm	σ	Δk_{eff}	\pm	σ
Removal of beryllium impurities	-0.00046	\pm	0.00003	-0.00030	\pm	0.00003
Removal of uranium impurities	-0.00020	\pm	0.00003	-0.00012	\pm	0.00003
Homogenized stack of beryllium discs and removal of beryllium impurities	-0.00150	\pm	0.00003	-0.00119	\pm	0.00003
Homogenized stack of uranium discs And removal of uranium impurities	-0.00644	\pm	0.00003	-0.00613	\pm	0.00003

^a A. Koning, R. Forrest, M. Kellett, R. Mills, H. Henriksson, and Y. Rugama, "The JEFF-3.1 Nuclear Data Library," JEFF Report 21, Organisation for Economic Co-operation and Development, Paris (2006).

^b K. Shibata, et al., "Japanese Evaluated Nuclear Data Library Version 3 Revision-3: JENDL-3.3," *J. Nucl. Sci. Tech.*, 39(11): 1125-1136 (November 2002).

Table 15. Calculated Biases for Combined Model Simplifications.

Neutron Cross Section Library	Configuration 1			Configuration 2		
	Δk_{eff}	\pm	σ	Δk_{eff}	\pm	σ
ENDF/B-VII.0	-0.00758	\pm	0.00003	-0.00423	\pm	0.00003
JEFF-3.1	-0.00747	\pm	0.00003	-0.00424	\pm	0.00003
JENDL-3.3	-0.00792	\pm	0.00003	-0.00426	\pm	0.00003
Average	-0.00766	\pm	0.00020	-0.00424	\pm	0.00003
Model simplification with room return effects (total bias)	-0.00821	\pm	0.00024	-0.00445	\pm	0.00003

Because there is a significant bias, due to increased neutron leakage, when simplifying these two benchmark models, the uncertainty in the simple model will be increased. One third of the effective bias in the simple model will be applied as additional uncertainty to each configuration. The simplification uncertainty for Configurations 1 and 2, respectively, is ± 0.00274 and $\pm 0.00148 \Delta k_{\text{eff}}$.

3.1.3.5 Total Bias Adjustment (Detailed Models)

The detailed benchmark model represents the experiments except for room return effects. Therefore the total bias adjustment for the detailed benchmark models is that reported for room return effects in Section 3.1.3.1, which is -0.00055 ± 0.00003 and $-0.00021 \pm 0.00003 \Delta k_{\text{eff}}$ for Configurations 1 and 2, respectively.

3.1.3.6 Total Bias Adjustment (Simple Models)

The total bias for the simple models is the combination of the average bias for all simplifications except room return effects (Table 15) and the bias for neglecting room return effects (Section 3.1.3.1). The total bias values for the simple benchmark models are -0.00821 ± 0.00274 and $-0.00445 \pm 0.00148 \Delta k_{\text{eff}}$ for Configurations 1 and 2, respectively.

3.2 Dimensions

3.2.1 Detailed Models – The detailed benchmark models are shown in Figures 10 and 11 for Configurations 1 and 2, respectively. They are labeled with part identifiers and dimensions. Part dimensions are summarized in Table 16.

HEU-MET-FAST-059

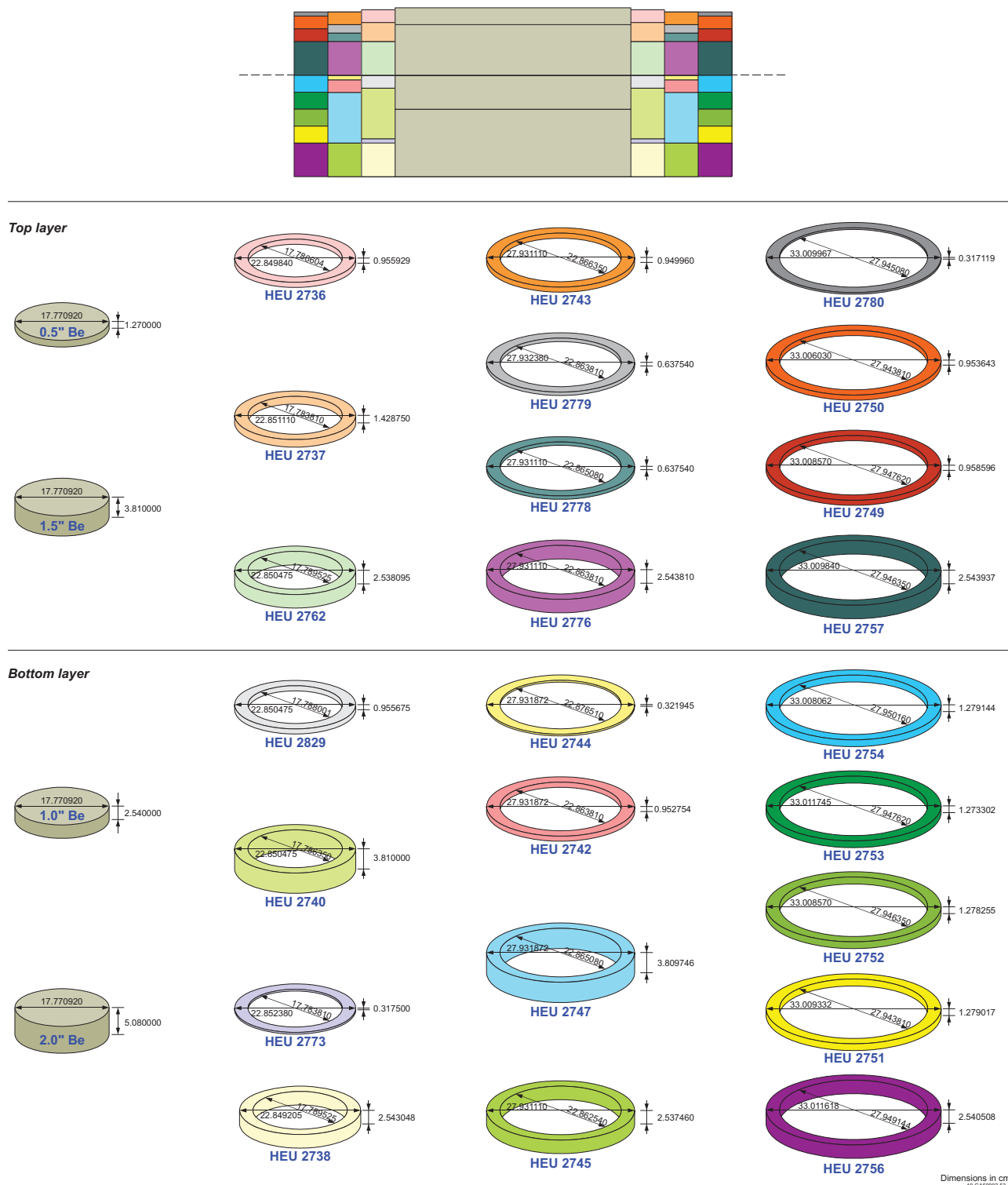


Figure 10.a. Detailed Benchmark Model of Configuration 1.

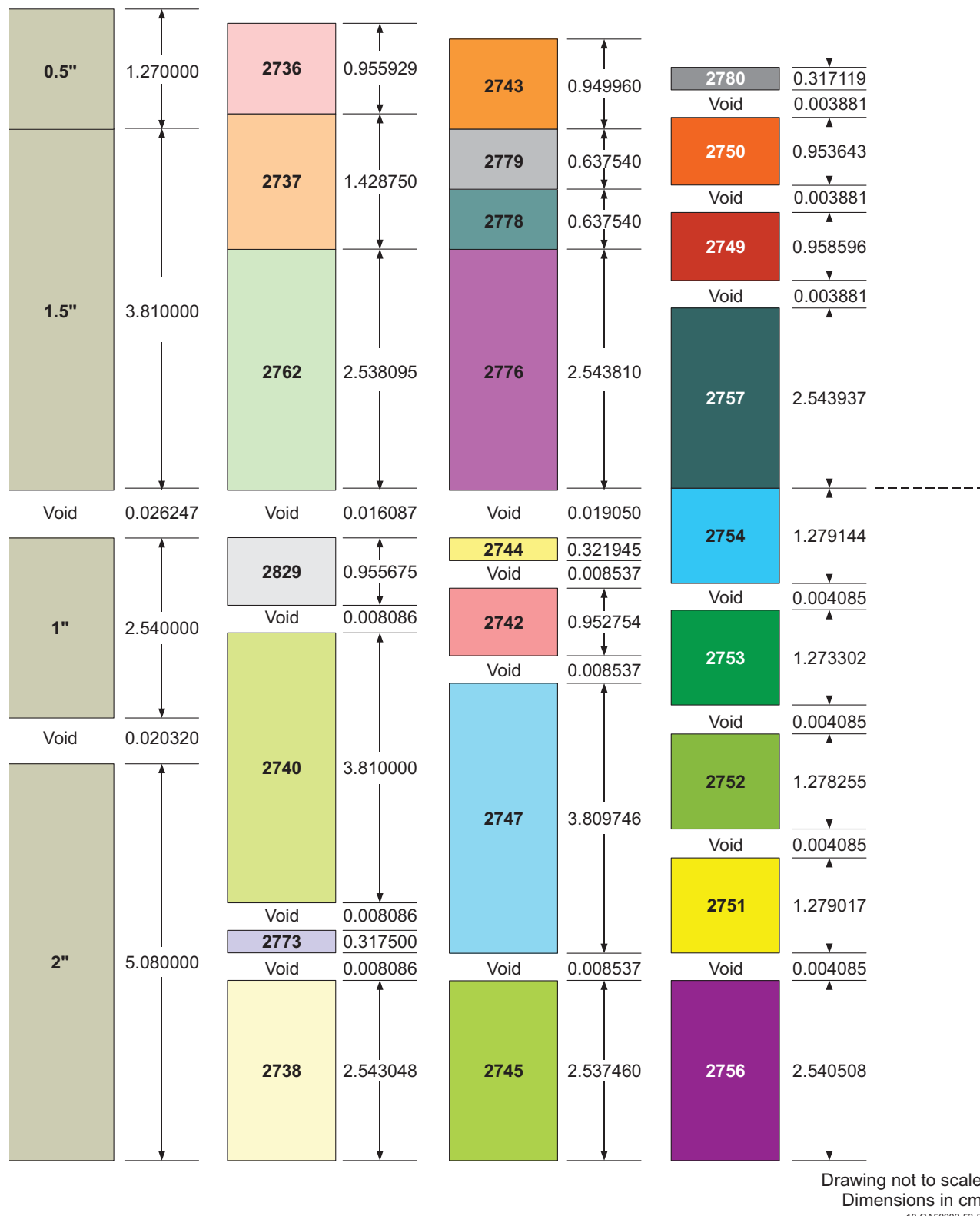


Figure 10.b. Detailed Benchmark Model of Configuration 1.
(Note that gap heights are quite small and visually exaggerated for the benefit of the reader.)

HEU-MET-FAST-059

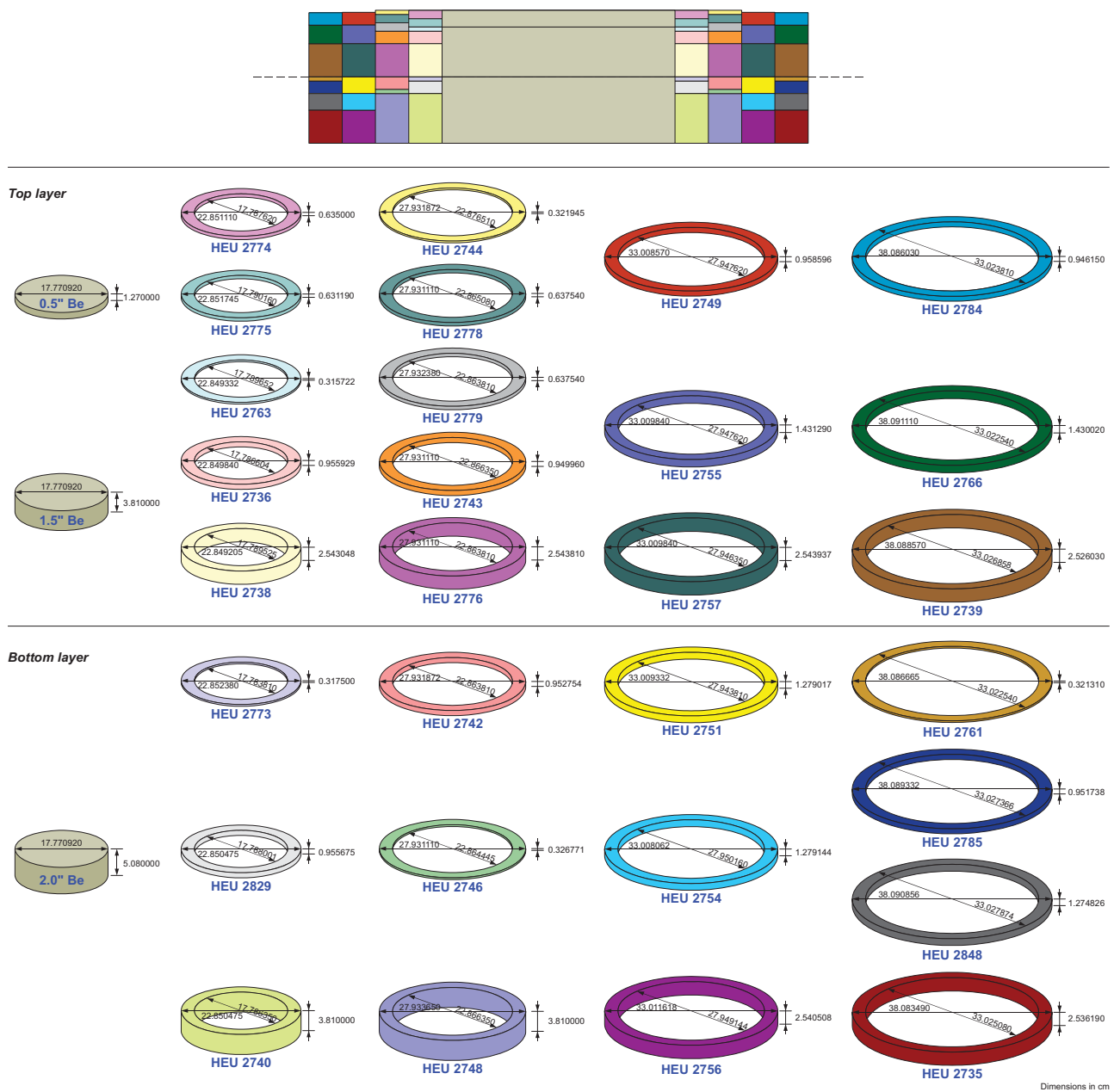


Figure 11.a. Detailed Benchmark Model of Configuration 2.

HEU-MET-FAST-059

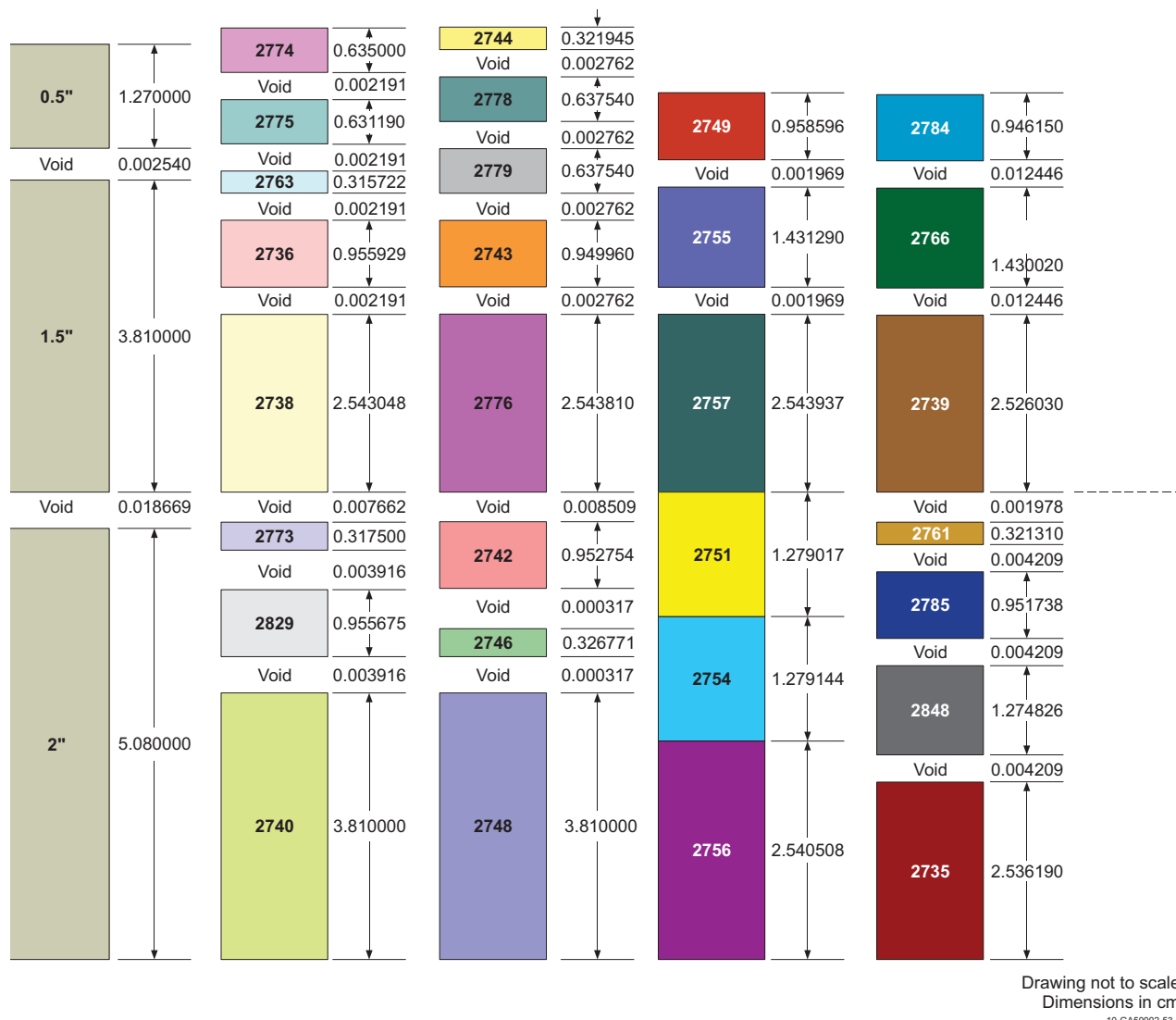


Figure 11.b. Detailed Benchmark Model of Configuration 2.
(Note that gap heights are quite small and visually exaggerated for the benefit of the reader.)

Table 16. Dimensions (cm) of Benchmark Model Parts.

Part Number	Inside Diameter	Outside Diameter	Height
2735	33.025080	38.083490	2.536190
2736	17.786604	22.849840	0.955929
2737	17.783810	22.851110	1.428750
2738	17.789525	22.849205	2.543048
2739	33.026858	38.088570	2.526030
2740	17.786350	22.850475	3.810000
2742	22.863810	27.931872	0.952754
2743	22.866350	27.931110	0.949960
2744	22.876510	27.931872	0.321945
2745	22.862540	27.931110	2.537460
2746	22.864445	27.931110	0.326771
2747	22.865080	27.931872	3.809746
2748	22.866350	27.933650	3.810000
2749	27.947620	33.008570	0.958596
2750	27.943810	33.006030	0.953643
2751	27.943810	33.009332	1.279017
2752	27.946350	33.008570	1.278255
2753	27.947620	33.011745	1.273302
2754	27.950160	33.008062	1.279144
2755	27.947620	33.009840	1.431290
2756	27.949144	33.011618	2.540508
2757	27.946350	33.009840	2.543937
2761	33.022540	38.086665	0.321310
2762	17.789525	22.850475	2.538095
2763	17.789652	22.849332	0.315722
2766	33.022540	38.091110	1.430020
2773	17.783810	22.852380	0.317500
2774	17.787620	22.851110	0.635000
2775	17.790160	22.851745	0.631190
2776	22.863810	27.931110	2.543810
2778	22.865080	27.931110	0.637540
2779	22.863810	27.932380	0.637540
2780	27.945080	33.009967	0.317119
2784	33.023810	38.086030	0.946150
2785	33.027366	38.089332	0.951738
2829	17.788001	22.850475	0.955675
2848	33.027874	38.090856	1.274826

3.2.1.1 Uranium Annuli

The diameters, positions, and heights of the uranium annuli in the benchmark model are shown in Figures 10 and 11. Gaps between the uranium discs and other components of the experiment are also shown in the figures.

3.2.1.2 Beryllium Discs

The diameters, positions, and heights of the beryllium discs in the benchmark model are shown in Figures 10 and 11. Gaps between the beryllium discs and other components of the experiment are also shown in the figures.

3.2.2 Simple Models – The simple benchmark models are shown in Figures 12 and 13 for Configurations 1 and 2, respectively. They are labeled with dimensions and material types. The simple model dimensions are chosen to correspond to the nominal experiment dimensions.

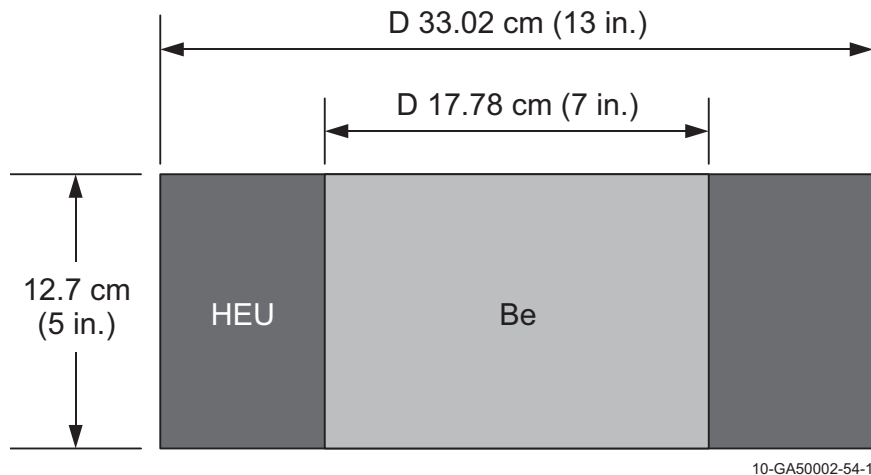


Figure 12. Simple Benchmark Model of Configuration 1.

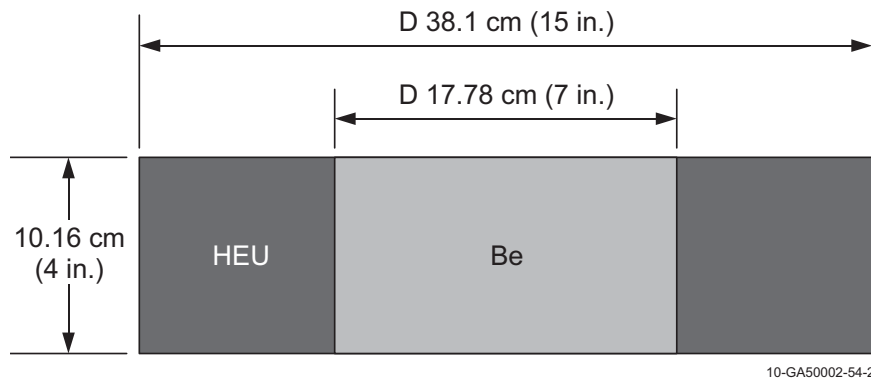


Figure 13. Simple Benchmark Model of Configuration 2.

3.2.2.1 Uranium Annulus

For Configuration 1, the uranium annulus has a height of 12.7 cm (5 in.), inner diameter of 17.78 cm (7 in.), and an outer diameter of 33.02 cm (13 in.).

For Configuration 2, the uranium annulus has a height of 10.16 cm (4 in.), inner diameter of 17.78 cm (7 in.), and an outer diameter of 38.1 cm (15. in.).

3.2.2.2 Beryllium Cylinder

For both configurations, the diameter of the beryllium cylinder is 17.78 cm (7 in.). The height of the beryllium cylinder is 12.7 cm (5 in.) for Configuration 1 and 10.16 cm (4 in.) for Configuration 2.

3.3 Material Data

3.3.1 Detailed Models - Material mass densities were obtained by taking the mass of the uranium, or beryllium, components divided by the volume they occupy in the benchmark model.

3.3.1.1 Uranium Annuli

The atom densities of the various uranium annuli are in Table 17, where part identifiers match the identifiers shown in Figures 10 and 11.

Table 17. Uranium Annuli Atom Densities (a/b-cm)
for the Detailed Benchmark Models.

Part Number	^{234}U	^{235}U	^{236}U	^{238}U	Ag
2735	4.7169E-04	4.4629E-02	1.1931E-04	2.6736E-03	8.3586E-07
2736	4.8680E-04	4.4715E-02	1.0036E-04	2.6584E-03	8.3702E-07
2737	4.7780E-04	4.4731E-02	1.3877E-04	2.6762E-03	8.3813E-07
2738	4.7317E-04	4.4783E-02	1.1489E-04	2.6725E-03	8.3848E-07
2739	4.6537E-04	4.4968E-02	1.2016E-04	2.6832E-03	8.4185E-07
2740	4.6863E-04	4.4821E-02	1.1497E-04	2.6694E-03	8.3900E-07
2742	4.7324E-04	4.4785E-02	1.1012E-04	2.6824E-03	8.3860E-07
2743	4.7545E-04	4.4994E-02	1.1064E-04	2.6949E-03	8.4251E-07
2744	4.7461E-04	4.4915E-02	1.1044E-04	2.6902E-03	8.4103E-07
2745	4.6359E-04	4.4815E-02	1.0534E-04	2.6682E-03	8.3862E-07
2746	4.8204E-04	4.4682E-02	1.0515E-04	2.6966E-03	8.3711E-07
2747	4.7245E-04	4.4720E-02	9.0820E-05	2.6874E-03	8.3721E-07
2748	4.8285E-04	4.4757E-02	1.0533E-04	2.7012E-03	8.3853E-07
2749	4.7313E-04	4.4799E-02	1.1967E-04	2.6486E-03	8.3841E-07
2750	4.5842E-04	4.4743E-02	1.1961E-04	2.6947E-03	8.3800E-07
2751	4.7310E-04	4.4767E-02	1.1488E-04	2.6816E-03	8.3836E-07
2752	4.7278E-04	4.4737E-02	1.1480E-04	2.6798E-03	8.3780E-07
2753	4.5759E-04	4.4662E-02	1.1940E-04	2.6898E-03	8.3648E-07
2754	4.6438E-04	4.4843E-02	1.3429E-04	2.6918E-03	8.4005E-07
2755	4.6364E-04	4.4771E-02	1.3408E-04	2.6875E-03	8.3870E-07
2756	4.4929E-04	4.4823E-02	1.1975E-04	2.6788E-03	8.3896E-07
2757	4.6342E-04	4.4798E-02	1.1008E-04	2.6625E-03	8.3830E-07
2761	4.6350E-04	4.4768E-02	1.2925E-04	2.6819E-03	8.3845E-07
2762	4.6870E-04	4.4808E-02	1.2935E-04	2.6745E-03	8.3911E-07
2763	4.6147E-04	4.4601E-02	1.1915E-04	2.6513E-03	8.3479E-07
2766	4.7348E-04	4.4817E-02	1.2934E-04	2.6553E-03	8.3902E-07
2773	4.6726E-04	4.4689E-02	1.1463E-04	2.6616E-03	8.3654E-07
2774	4.7883E-04	4.4828E-02	1.3907E-04	2.6819E-03	8.3994E-07
2775	4.7378E-04	4.4841E-02	1.1504E-04	2.6760E-03	8.3957E-07
2776	4.6302E-04	4.4740E-02	1.0999E-04	2.6792E-03	8.3759E-07
2778	4.6197E-04	4.4639E-02	1.0974E-04	2.6731E-03	8.3569E-07
2779	4.6289E-04	4.4728E-02	1.0996E-04	2.6784E-03	8.3735E-07
2780	4.7200E-04	4.4663E-02	1.1938E-04	2.6706E-03	8.3640E-07
2784	4.7962E-04	4.4916E-02	1.2489E-04	2.6864E-03	8.4133E-07
2785	4.7235E-04	4.4701E-02	1.1469E-04	2.6726E-03	8.3702E-07
2829	4.7734E-04	4.4698E-02	1.1474E-04	2.6878E-03	8.3732E-07
2848	4.7656E-04	4.4663E-02	1.1455E-04	2.6456E-03	8.3597E-07

Table 17 (cont'd). Uranium Annuli Atom Densities (a/b-cm)
for the Detailed Benchmark Models.

Part Number	Ba	Bi	C	Ca	Cd
2735	4.1035E-10	8.8445E-06	4.6917E-06	2.8121E-08	5.0130E-08
2736	4.1091E-10	8.8568E-06	4.6982E-06	2.8160E-08	5.0200E-08
2737	4.1146E-10	8.8686E-06	4.7044E-06	2.8197E-08	5.0267E-08
2738	4.1163E-10	8.8722E-06	4.7064E-06	2.8209E-08	5.0287E-08
2739	4.1329E-10	8.9079E-06	4.7253E-06	2.8322E-08	5.0489E-08
2740	4.1189E-10	8.8778E-06	4.7093E-06	2.8227E-08	5.0319E-08
2742	4.1169E-10	8.8735E-06	4.7070E-06	2.8213E-08	5.0295E-08
2743	4.1361E-10	8.9149E-06	4.7290E-06	2.8345E-08	5.0530E-08
2744	4.1289E-10	8.8993E-06	4.7207E-06	2.8295E-08	5.0441E-08
2745	4.1170E-10	8.8738E-06	4.7072E-06	2.8214E-08	5.0296E-08
2746	4.1096E-10	8.8578E-06	4.6987E-06	2.8163E-08	5.0206E-08
2747	4.1101E-10	8.8588E-06	4.6993E-06	2.8166E-08	5.0212E-08
2748	4.1166E-10	8.8728E-06	4.7067E-06	2.8211E-08	5.0291E-08
2749	4.1160E-10	8.8715E-06	4.7060E-06	2.8207E-08	5.0283E-08
2750	4.1140E-10	8.8672E-06	4.7037E-06	2.8193E-08	5.0259E-08
2751	4.1157E-10	8.8710E-06	4.7057E-06	2.8205E-08	5.0280E-08
2752	4.1130E-10	8.8650E-06	4.7025E-06	2.8186E-08	5.0247E-08
2753	4.1065E-10	8.8511E-06	4.6952E-06	2.8142E-08	5.0168E-08
2754	4.1240E-10	8.8888E-06	4.7152E-06	2.8262E-08	5.0382E-08
2755	4.1174E-10	8.8746E-06	4.7076E-06	2.8217E-08	5.0301E-08
2756	4.1187E-10	8.8774E-06	4.7091E-06	2.8225E-08	5.0316E-08
2757	4.1155E-10	8.8704E-06	4.7054E-06	2.8203E-08	5.0277E-08
2761	4.1162E-10	8.8720E-06	4.7062E-06	2.8208E-08	5.0286E-08
2762	4.1194E-10	8.8790E-06	4.7099E-06	2.8230E-08	5.0326E-08
2763	4.0982E-10	8.8332E-06	4.6857E-06	2.8085E-08	5.0066E-08
2766	4.1190E-10	8.8780E-06	4.7094E-06	2.8227E-08	5.0320E-08
2773	4.1068E-10	8.8518E-06	4.6955E-06	2.8144E-08	5.0171E-08
2774	4.1235E-10	8.8877E-06	4.7146E-06	2.8258E-08	5.0375E-08
2775	4.1217E-10	8.8838E-06	4.7125E-06	2.8246E-08	5.0353E-08
2776	4.1119E-10	8.8628E-06	4.7014E-06	2.8179E-08	5.0234E-08
2778	4.1026E-10	8.8427E-06	4.6907E-06	2.8115E-08	5.0120E-08
2779	4.1108E-10	8.8603E-06	4.7000E-06	2.8171E-08	5.0220E-08
2780	4.1061E-10	8.8503E-06	4.6947E-06	2.8139E-08	5.0163E-08
2784	4.1303E-10	8.9025E-06	4.7224E-06	2.8305E-08	5.0459E-08
2785	4.1092E-10	8.8568E-06	4.6982E-06	2.8160E-08	5.0200E-08
2829	4.1106E-10	8.8600E-06	4.6999E-06	2.8170E-08	5.0218E-08
2848	4.1040E-10	8.8457E-06	4.6923E-06	2.8125E-08	5.0137E-08

Table 17 (cont'd). Uranium Annuli Atom Densities (a/b-cm)
for the Detailed Benchmark Models.

Part Number	Co	Cr	Cu	K	Li
2735	9.5620E-07	1.5173E-06	4.4339E-06	2.8826E-08	1.6237E-06
2736	9.5752E-07	1.5194E-06	4.4401E-06	2.8866E-08	1.6260E-06
2737	9.5879E-07	1.5214E-06	4.4460E-06	2.8904E-08	1.6281E-06
2738	9.5919E-07	1.5220E-06	4.4478E-06	2.8916E-08	1.6288E-06
2739	9.6304E-07	1.5281E-06	4.4657E-06	2.9032E-08	1.6354E-06
2740	9.5979E-07	1.5230E-06	4.4506E-06	2.8934E-08	1.6298E-06
2742	9.5933E-07	1.5222E-06	4.4485E-06	2.8920E-08	1.6291E-06
2743	9.6381E-07	1.5294E-06	4.4692E-06	2.9055E-08	1.6367E-06
2744	9.6211E-07	1.5267E-06	4.4614E-06	2.9004E-08	1.6338E-06
2745	9.5936E-07	1.5223E-06	4.4486E-06	2.8921E-08	1.6291E-06
2746	9.5763E-07	1.5196E-06	4.4406E-06	2.8869E-08	1.6262E-06
2747	9.5774E-07	1.5197E-06	4.4411E-06	2.8872E-08	1.6264E-06
2748	9.5925E-07	1.5221E-06	4.4481E-06	2.8918E-08	1.6289E-06
2749	9.5911E-07	1.5219E-06	4.4474E-06	2.8914E-08	1.6287E-06
2750	9.5865E-07	1.5212E-06	4.4453E-06	2.8899E-08	1.6279E-06
2751	9.5906E-07	1.5218E-06	4.4472E-06	2.8912E-08	1.6286E-06
2752	9.5841E-07	1.5208E-06	4.4442E-06	2.8892E-08	1.6275E-06
2753	9.5691E-07	1.5184E-06	4.4372E-06	2.8847E-08	1.6249E-06
2754	9.6098E-07	1.5249E-06	4.4561E-06	2.8970E-08	1.6319E-06
2755	9.5945E-07	1.5224E-06	4.4490E-06	2.8924E-08	1.6293E-06
2756	9.5974E-07	1.5229E-06	4.4504E-06	2.8933E-08	1.6298E-06
2757	9.5899E-07	1.5217E-06	4.4469E-06	2.8910E-08	1.6285E-06
2761	9.5916E-07	1.5220E-06	4.4477E-06	2.8915E-08	1.6288E-06
2762	9.5992E-07	1.5232E-06	4.4512E-06	2.8938E-08	1.6301E-06
2763	9.5497E-07	1.5153E-06	4.4282E-06	2.8789E-08	1.6217E-06
2766	9.5981E-07	1.5230E-06	4.4507E-06	2.8935E-08	1.6299E-06
2773	9.5698E-07	1.5185E-06	4.4375E-06	2.8849E-08	1.6251E-06
2774	9.6086E-07	1.5247E-06	4.4556E-06	2.8966E-08	1.6317E-06
2775	9.6044E-07	1.5240E-06	4.4536E-06	2.8954E-08	1.6309E-06
2776	9.5817E-07	1.5204E-06	4.4431E-06	2.8885E-08	1.6271E-06
2778	9.5600E-07	1.5170E-06	4.4330E-06	2.8820E-08	1.6234E-06
2779	9.5790E-07	1.5200E-06	4.4418E-06	2.8877E-08	1.6266E-06
2780	9.5682E-07	1.5183E-06	4.4368E-06	2.8844E-08	1.6248E-06
2784	9.6246E-07	1.5272E-06	4.4630E-06	2.9014E-08	1.6344E-06
2785	9.5752E-07	1.5194E-06	4.4401E-06	2.8866E-08	1.6260E-06
2829	9.5787E-07	1.5199E-06	4.4417E-06	2.8876E-08	1.6266E-06
2848	9.5632E-07	1.5175E-06	4.4345E-06	2.8829E-08	1.6239E-06

Table 17 (cont'd). Uranium Annuli Atom Densities (a/b-cm)
for the Detailed Benchmark Models.

Part Number	Mg	Mn	Mo	Na	Ni
2735	1.3911E-06	1.1488E-05	5.8736E-08	1.3236E-05	1.9203E-05
2736	1.3930E-06	1.1504E-05	5.8818E-08	1.3255E-05	1.9230E-05
2737	1.3949E-06	1.1519E-05	5.8896E-08	1.3272E-05	1.9255E-05
2738	1.3955E-06	1.1524E-05	5.8920E-08	1.3278E-05	1.9263E-05
2739	1.4011E-06	1.1570E-05	5.9157E-08	1.3331E-05	1.9341E-05
2740	1.3963E-06	1.1531E-05	5.8957E-08	1.3286E-05	1.9275E-05
2742	1.3957E-06	1.1526E-05	5.8929E-08	1.3280E-05	1.9266E-05
2743	1.4022E-06	1.1580E-05	5.9204E-08	1.3342E-05	1.9356E-05
2744	1.3997E-06	1.1559E-05	5.9100E-08	1.3318E-05	1.9322E-05
2745	1.3957E-06	1.1526E-05	5.8931E-08	1.3280E-05	1.9267E-05
2746	1.3932E-06	1.1505E-05	5.8824E-08	1.3256E-05	1.9232E-05
2747	1.3934E-06	1.1507E-05	5.8831E-08	1.3258E-05	1.9234E-05
2748	1.3956E-06	1.1525E-05	5.8924E-08	1.3279E-05	1.9264E-05
2749	1.3954E-06	1.1523E-05	5.8915E-08	1.3277E-05	1.9262E-05
2750	1.3947E-06	1.1518E-05	5.8887E-08	1.3270E-05	1.9252E-05
2751	1.3953E-06	1.1523E-05	5.8912E-08	1.3276E-05	1.9261E-05
2752	1.3943E-06	1.1515E-05	5.8872E-08	1.3267E-05	1.9248E-05
2753	1.3921E-06	1.1497E-05	5.8780E-08	1.3246E-05	1.9217E-05
2754	1.3981E-06	1.1546E-05	5.9031E-08	1.3303E-05	1.9299E-05
2755	1.3958E-06	1.1527E-05	5.8936E-08	1.3281E-05	1.9268E-05
2756	1.3963E-06	1.1531E-05	5.8954E-08	1.3285E-05	1.9274E-05
2757	1.3952E-06	1.1522E-05	5.8908E-08	1.3275E-05	1.9259E-05
2761	1.3954E-06	1.1524E-05	5.8919E-08	1.3277E-05	1.9263E-05
2762	1.3965E-06	1.1533E-05	5.8965E-08	1.3288E-05	1.9278E-05
2763	1.3893E-06	1.1473E-05	5.8661E-08	1.3219E-05	1.9179E-05
2766	1.3964E-06	1.1532E-05	5.8959E-08	1.3286E-05	1.9276E-05
2773	1.3922E-06	1.1498E-05	5.8784E-08	1.3247E-05	1.9219E-05
2774	1.3979E-06	1.1544E-05	5.9023E-08	1.3301E-05	1.9297E-05
2775	1.3973E-06	1.1539E-05	5.8997E-08	1.3295E-05	1.9288E-05
2776	1.3940E-06	1.1512E-05	5.8858E-08	1.3264E-05	1.9243E-05
2778	1.3908E-06	1.1486E-05	5.8724E-08	1.3234E-05	1.9199E-05
2779	1.3936E-06	1.1509E-05	5.8841E-08	1.3260E-05	1.9237E-05
2780	1.3920E-06	1.1496E-05	5.8775E-08	1.3245E-05	1.9216E-05
2784	1.4002E-06	1.1563E-05	5.9121E-08	1.3323E-05	1.9329E-05
2785	1.3930E-06	1.1504E-05	5.8818E-08	1.3255E-05	1.9230E-05
2829	1.3935E-06	1.1508E-05	5.8839E-08	1.3259E-05	1.9237E-05
2848	1.3913E-06	1.1490E-05	5.8744E-08	1.3238E-05	1.9206E-05

Table 17 (cont'd). Uranium Annuli Atom Densities (a/b-cm)
for the Detailed Benchmark Models.

Part Number	Sb	Ti	O	N	Mass Density (g/cm ³)
2735	3.5176E-06	2.3539E-07	1.4088E-05	2.4139E-05	18.7150
2736	3.5225E-06	2.3571E-07	1.4108E-05	2.4173E-05	18.7408
2737	3.5272E-06	2.3603E-07	1.4127E-05	2.4205E-05	18.7658
2738	3.5287E-06	2.3612E-07	1.4133E-05	2.4215E-05	18.7736
2739	3.5428E-06	2.3707E-07	1.4189E-05	2.4312E-05	18.8490
2740	3.5309E-06	2.3627E-07	1.4141E-05	2.4230E-05	18.7853
2742	3.5292E-06	2.3616E-07	1.4135E-05	2.4218E-05	18.7763
2743	3.5456E-06	2.3726E-07	1.4201E-05	2.4331E-05	18.8639
2744	3.5394E-06	2.3684E-07	1.4176E-05	2.4288E-05	18.8307
2745	3.5293E-06	2.3617E-07	1.4135E-05	2.4219E-05	18.7768
2746	3.5229E-06	2.3574E-07	1.4110E-05	2.4175E-05	18.7430
2747	3.5233E-06	2.3577E-07	1.4111E-05	2.4178E-05	18.7452
2748	3.5289E-06	2.3614E-07	1.4133E-05	2.4216E-05	18.7747
2749	3.5284E-06	2.3610E-07	1.4131E-05	2.4213E-05	18.7720
2750	3.5267E-06	2.3599E-07	1.4125E-05	2.4201E-05	18.7629
2751	3.5282E-06	2.3609E-07	1.4131E-05	2.4211E-05	18.7709
2752	3.5258E-06	2.3593E-07	1.4121E-05	2.4195E-05	18.7583
2753	3.5203E-06	2.3556E-07	1.4099E-05	2.4157E-05	18.7289
2754	3.5353E-06	2.3657E-07	1.4159E-05	2.4260E-05	18.8087
2755	3.5296E-06	2.3619E-07	1.4136E-05	2.4221E-05	18.7786
2756	3.5307E-06	2.3626E-07	1.4141E-05	2.4229E-05	18.7844
2757	3.5279E-06	2.3608E-07	1.4130E-05	2.4210E-05	18.7697
2761	3.5286E-06	2.3612E-07	1.4132E-05	2.4214E-05	18.7730
2762	3.5313E-06	2.3630E-07	1.4143E-05	2.4233E-05	18.7878
2763	3.5131E-06	2.3509E-07	1.4070E-05	2.4108E-05	18.6910
2766	3.5309E-06	2.3628E-07	1.4142E-05	2.4230E-05	18.7858
2773	3.5205E-06	2.3558E-07	1.4100E-05	2.4159E-05	18.7302
2774	3.5348E-06	2.3654E-07	1.4157E-05	2.4257E-05	18.8063
2775	3.5332E-06	2.3643E-07	1.4151E-05	2.4246E-05	18.7980
2776	3.5249E-06	2.3587E-07	1.4118E-05	2.4189E-05	18.7536
2778	3.5169E-06	2.3534E-07	1.4086E-05	2.4134E-05	18.7112
2779	3.5239E-06	2.3581E-07	1.4114E-05	2.4182E-05	18.7483
2780	3.5199E-06	2.3554E-07	1.4098E-05	2.4155E-05	18.7271
2784	3.5407E-06	2.3693E-07	1.4181E-05	2.4297E-05	18.8375
2785	3.5225E-06	2.3571E-07	1.4108E-05	2.4173E-05	18.7409
2829	3.5238E-06	2.3580E-07	1.4113E-05	2.4181E-05	18.7477
2848	3.5181E-06	2.3542E-07	1.4090E-05	2.4142E-05	18.7173

3.3.1.2 Beryllium Discs

The atom densities of the four beryllium discs are shown in Table 18, where part identifiers match the identifiers shown in Figures 10 and 11.

Table 18. Beryllium Disc Atom Densities (a/b-cm) for the Detailed Benchmark Models.

Part ID → Material ↓	0.5"	1"	1.5"	2"
Be	1.1959E-01	1.2094E-01	1.2112E-01	1.2073E-01
Al	2.4360E-05	2.4636E-05	2.4672E-05	2.4594E-05
B	1.0133E-06	1.0248E-06	1.0262E-06	1.0230E-06
Bi	2.6209E-06	2.6507E-06	2.6545E-06	2.6461E-06
Br	6.8547E-09	6.9325E-09	6.9425E-09	6.9205E-09
C	1.0944E-04	1.1069E-04	1.1084E-04	1.1049E-04
Cd	1.9490E-08	1.9711E-08	1.9740E-08	1.9677E-08
Dy	6.7412E-09	6.8176E-09	6.8275E-09	6.8059E-09
Fe	2.5500E-05	2.5790E-05	2.5827E-05	2.5745E-05
Gd	6.9662E-09	7.0453E-09	7.0554E-09	7.0331E-09
Mg	9.0141E-06	9.1164E-06	9.1295E-06	9.1006E-06
Ni	1.8665E-08	1.8877E-08	1.8904E-08	1.8844E-08
O	8.4529E-04	8.5488E-04	8.5611E-04	8.5340E-04
Sm	7.2855E-09	7.3681E-09	7.3787E-09	7.3554E-09
Mass Density (g/cm ³)	1.8190	1.8397	1.8423	1.8365

3.3.2 Simple Models**3.3.2.1 Uranium Annulus**

The atomic composition of the uranium annulus is in Table 19 for Configuration 1 and Table 20 for Configuration 2. The average isotopic weight fraction of the uranium annulus was obtained by taking the sum of the mass-weighted isotopic weight fraction of each uranium annulus in each configuration. The density of the uranium annulus in each simple configuration is obtained by dividing the total uranium mass by the volume of the modeled annulus; the density is then multiplied by the factor 0.999508795 to account for the removal of impurities (Table 11).

Table 19. Uranium Annulus Composition (Configuration 1).

Material	Wt.%	Atom Density (a/b-cm)
^{234}U	0.968	4.5628E-04
^{235}U	93.154	4.3740E-02
^{236}U	0.237	1.1092E-04
^{238}U	5.641	2.6151E-03
Mass Density (g/cm ³)	--	18.3355

Table 20. Uranium Annulus Composition (Configuration 2).

Material	Wt.%	Atom Density (a/b-cm)
^{234}U	0.973	4.6422E-04
^{235}U	93.146	4.4264E-02
^{236}U	0.244	1.1543E-04
^{238}U	5.638	2.6453E-03
Mass Density (g/cm ³)	--	18.5568

3.3.2.2 Beryllium Cylinder

The atomic composition of the beryllium cylinder is in Table 21 for Configuration 1 and Table 22 for Configuration 2. The mass density of the beryllium cylinder is 1.8353 and 1.8346 g/cm³ for Configurations 1 and 2, respectively. The beryllium density is obtained by dividing the total beryllium mass by the volume of the modeled cylinder; the density is then multiplied by the factor 0.9838377 to account for the removal of impurities (Table 12). The beryllium reported in the impurity BeO is retained in the simple benchmark model as beryllium metal. The oxygen is considered an impurity and removed.

Table 21. Beryllium Cylinder Composition (Configuration 1).

Material	Atom Density (a/b-cm)
Be	1.2065E-01 ^(a)

(a) Includes beryllium from BeO.

Table 22. Beryllium Cylinder
Composition (Configuration 2).

Material	Atom Density (a/b-cm)
Be	1.2061E-01 ^(a)

(a) Includes beryllium from BeO.

3.4 Temperature Data

The temperature of all benchmark models is at room temperature, 294 K.

3.5 Experimental and Benchmark Model k_{eff}

The experimental k_{eff} value for the full assembly is 1.0014 ± 0.0005 and 1.0002 ± 0.0003 for Configurations 1 and 2, respectively. The adjusted experimental eigenvalue for just the stack of uranium annuli and beryllium discs is 1.0011 ± 0.0005 and 0.9996 ± 0.0003 for Configurations 1 and 2, respectively.

3.5.1 Detailed Models – The expected k_{eff} value for the detailed benchmark models of Configurations 1 and 2, respectively, adjusted for room return effects, is 1.0005 ± 0.0005 and 0.9994 ± 0.0003 .

3.5.2 Simple Models – The expected k_{eff} value for the simple benchmark models of Configurations 1 and 2, respectively, adjusted for room return effects and model simplifications, is 0.9929 ± 0.0028 and 0.9952 ± 0.0016 .

4.0 RESULTS OF SAMPLE CALCULATIONS

Results were calculated using MCNP5 and ENDF/B-VII.0, JEFF-3.1, and JENDL-3.3 neutron cross section libraries with the input decks and specifications provided in Appendix A. A comparison of the neutron spectral data between the detailed and simple models is provided in Appendix B. The cross section data for ^{16}O is used for ^{18}O in the input decks.

4.1 Detailed Benchmark Models

The calculated results for the detailed benchmark model are reported in Tables 23 and 24 for Configurations 1 and 2, respectively. There is variability in the calculated results for the different libraries, with ENDF/B-VII.0 and JEFF-3.1 both calculating below the expected benchmark value and JENDL-3.3 above. The greatest difference between MCNP results with different cross sections is $\sim 0.67\% \Delta k_{\text{eff}}$. The differences are much greater than the evaluated uncertainty for the benchmark experiment. The number of sigmas between the benchmark eigenvalue and the calculated eigenvalues is between 3 and 11 for Configuration 1, and between 7 and 17 for Configuration 2, due to the small amount of uncertainty in the benchmark experiment itself.

Table 23. Comparison of Detailed Benchmark Eigenvalues (Configuration 1).

Analysis Code	Neutron Cross Section Library	Calculated			Benchmark			$\frac{C-E}{E}(\%)$
		k_{eff}	\pm	σ	k_{eff}	\pm	σ	
MCNP5	ENDF/B-VII.0	0.99711	\pm	0.00002	1.0005	\pm	0.0005	-0.34
	JEFF-3.1	0.99519	\pm	0.00002				-0.53
	JENDL-3.3	1.00193	\pm	0.00002				0.14

Table 24. Comparison of Detailed Benchmark Eigenvalues (Configuration 2).

Analysis Code	Neutron Cross Section Library	Calculated			Benchmark			$\frac{C-E}{E}(\%)$
		k_{eff}	\pm	σ	k_{eff}	\pm	σ	
MCNP5	ENDF/B-VII.0	0.99680	\pm	0.00002	0.9994	\pm	0.0003	-0.26
	JEFF-3.1	0.99451	\pm	0.00002				-0.49
	JENDL-3.3	1.00125	\pm	0.00002				0.19

4.2 Simple Benchmark Models

The calculated results for the simple benchmark model are reported in Tables 25 and 26 for Configurations 1 and 2, respectively. Comments discussed in the previous section regarding the detailed benchmark model also apply to the simple benchmark model. The calculated eigenvalues are within $\sim 3\sigma$ of the benchmark eigenvalues due to the increased uncertainty assigned with the simplification of the benchmark models.

Table 25. Comparison of Simple Benchmark Eigenvalues (Configuration 1).

Analysis Code	Neutron Cross Section Library	Calculated			Benchmark			$\frac{C-E}{E}(\%)$
		k_{eff}	\pm	σ	k_{eff}	\pm	σ	
MCNP5	ENDF/B-VII.0	0.98953	\pm	0.00002	0.9929	\pm	0.0028	-0.34
	JEFF-3.1	0.98772	\pm	0.00002				-0.52
	JENDL-3.3	0.99401	\pm	0.00002				0.11

Table 26. Comparison of Simple Benchmark Eigenvalues (Configuration 2).

Analysis Code	Neutron Cross Section Library	Calculated			Benchmark			$\frac{C-E}{E}(\%)$
		k_{eff}	\pm	σ	k_{eff}	\pm	σ	
MCNP5	ENDF/B-VII.0	0.99257	\pm	0.00002	0.9952	\pm	0.0016	-0.26
	JEFF-3.1	0.99027	\pm	0.00002				-0.49
	JENDL-3.3	0.99699	\pm	0.00002				0.18

5.0 REFERENCES

1. J. T. Mihalczo and D. L. Bentzinger, "Two Delayed Critical Uranium (93.2) Metal Cylindrical Annuli with Central Be Moderation," *Trans. Am. Nucl. Soc.*, **77**, 246-247 (1997).

APPENDIX A: TYPICAL INPUT LISTINGS

The MCNP5 calculations were performed using the continuous energy, ENDF/B-VII.0 neutron cross section data and were performed with 1,050 generations with 1,000,000 neutrons per generation. The k_{eff} estimates did not include the first 50 generations and are the result of 1,000,000,000 neutron histories. The statistical uncertainty in k_{eff} is 0.00002.

A.1 MCNP Input Listings

A.1.1 Thirteen-Inch-Diameter Annulus (Configuration 1)

A.1.1.1 Detailed Model

```
ORALLOY (93.15 235U) METAL ANNULI WITH BERYLLIUM CORE (DETAILED - 13")
c
c John Darrell Bess - Idaho National Laboratory
c Last Updated: January 5, 2010
c
c Cell Cards ****
c ----- Be Discs -----
1   1  1.2176E-01   1  -2  -9      imp:n=1 $ 2"
2   2  1.2197E-01   3  -4  -9      imp:n=1 $ 1"
3   3  1.2215E-01   5  -6  -9      imp:n=1 $ 1.5"
4   4  1.2060E-01   7  -8  -9      imp:n=1 $ 0.5"
c
c ----- 7"-9" HEU Annulus -----
5   5  4.8155E-02  10  -11 24  -31  imp:n=1 $ Part 2738
6   6  4.8043E-02  12  -13 25  -32  imp:n=1 $ Part 2773
7   7  4.8185E-02  14  -15 26  -33  imp:n=1 $ Part 2740
8   8  4.8088E-02  16  -17 27  -34  imp:n=1 $ Part 2829
9   9  4.8191E-02  18  -19 28  -35  imp:n=1 $ Part 2762
10  10 4.8134E-02  20  -21 29  -36  imp:n=1 $ Part 2737
11  11 4.8071E-02  22  -23 30  -37  imp:n=1 $ Part 2736
c
c ----- 9"-11" HEU Annulus -----
12  12 4.8163E-02  38  -39 54  -62  imp:n=1 $ Part 2745
13  13 4.8082E-02  40  -41 55  -63  imp:n=1 $ Part 2747
14  14 4.8161E-02  42  -43 56  -64  imp:n=1 $ Part 2742
15  15 4.8301E-02  44  -45 57  -65  imp:n=1 $ Part 2744
16  16 4.8103E-02  46  -47 58  -66  imp:n=1 $ Part 2776
17  17 4.7994E-02  48  -49 59  -67  imp:n=1 $ Part 2778
18  18 4.8090E-02  50  -51 60  -68  imp:n=1 $ Part 2779
19  19 4.8386E-02  52  -53 61  -69  imp:n=1 $ Part 2743
c
c ----- 11"-13" HEU Annulus -----
20  20 4.8182E-02  70  -71 88  -97  imp:n=1 $ Part 2756
21  21 4.8148E-02  72  -73 89  -98  imp:n=1 $ Part 2751
22  22 4.8115E-02  74  -75 90  -99  imp:n=1 $ Part 2752
23  23 4.8040E-02  76  -77 91  -100 imp:n=1 $ Part 2753
24  24 4.8244E-02  78  -79 92  -101 imp:n=1 $ Part 2754
25  25 4.8145E-02  80  -81 93  -102 imp:n=1 $ Part 2757
26  26 4.8151E-02  82  -83 94  -103 imp:n=1 $ Part 2749
27  27 4.8127E-02  84  -85 95  -104 imp:n=1 $ Part 2750
28  28 4.8035E-02  86  -87 96  -105 imp:n=1 $ Part 2780
c
c ----- Void Spaces-----
29   0  1  -8  -106 #1 #2 #3 #4 #5 #6 #7 #8 #9 #10 #11 #12 #13 #14#15 #16 #17 #18
           #19 #20 #21 #22 #23 #24 #25 #26 #27 #28 imp:n=1 $ Gaps
30   0  -1:8:106                                     imp:n=0 $ The Great Void

c Surface Cards ****
c ----- Be Discs -----
c ----- Horizontal Planes -----
1   pz  -7.666567 $ Bottom
2   pz  -2.586567 $ 2"
3   pz  -2.566247 $ Gap
```

HEU-MET-FAST-059

```
4   pz  -0.026247 $ 1"
5   pz  0.000000 $ Gap (Diaphragm Location)
6   pz  3.810000 $ 1.5"
7   pz  3.810000 $ Gap
8   pz  5.080000 $ 0.5" (Top)
c ----- Outer Radii -----
9   cz  8.885460 $ All Be
c
c ----- 7"-9" HEU Annulus -----
c ----- Horizontal Planes -----
10  pz  -7.666567 $ Bottom
11  pz  -5.123519 $ Part 2738
12  pz  -5.115433 $ Gap
13  pz  -4.797933 $ Part 2773
14  pz  -4.789847 $ Gap
15  pz  -0.979847 $ Part 2740
16  pz  -0.971762 $ Gap
17  pz  -0.016087 $ Part 2829
18  pz  0.000000 $ Gap (Diaphragm Location)
19  pz  2.538095 $ Part 2762
20  pz  2.538095 $ Gap
21  pz  3.966845 $ Part 2737
22  pz  3.966845 $ Gap
23  pz  4.922774 $ Part 2736 (Top)
c ----- Inner Radii -----
24  cz  8.894763 $ Part 2738
25  cz  8.891905 $ Part 2773
26  cz  8.893175 $ Part 2740
27  cz  8.894001 $ Part 2829
28  cz  8.894763 $ Part 2762
29  cz  8.891905 $ Part 2737
30  cz  8.893302 $ Part 2736
c ----- Outer Radii -----
31  cz  11.424603 $ Part 2738
32  cz  11.426190 $ Part 2773
33  cz  11.425238 $ Part 2740
34  cz  11.425238 $ Part 2829
35  cz  11.425238 $ Part 2762
36  cz  11.425555 $ Part 2737
37  cz  11.424920 $ Part 2736
c
c ----- 9"-11" HEU Annulus -----
c ----- Horizontal Planes -----
38  pz  -7.666567 $ Bottom
39  pz  -5.129107 $ Part 2745
40  pz  -5.120569 $ Gap
41  pz  -1.310823 $ Part 2747
42  pz  -1.302286 $ Gap
43  pz  -0.349532 $ Part 2742
44  pz  -0.340995 $ Gap
45  pz  -0.019050 $ Part 2744
46  pz  0.000000 $ Gap (Diaphragm Location)
47  pz  2.543810 $ Part 2776
48  pz  2.543810 $ Gap
49  pz  3.181350 $ Part 2778
50  pz  3.181350 $ Gap
51  pz  3.818890 $ Part 2779
52  pz  3.818890 $ Gap
53  pz  4.768850 $ Part 2743 (Top)
c ----- Inner Radii -----
54  cz  11.431270 $ Part 2745
55  cz  11.432540 $ Part 2747
56  cz  11.431905 $ Part 2742
57  cz  11.438255 $ Part 2744
58  cz  11.431905 $ Part 2776
59  cz  11.432540 $ Part 2778
60  cz  11.431905 $ Part 2779
61  cz  11.433175 $ Part 2743
c ----- Outer Radii -----
62  cz  13.965555 $ Part 2745
63  cz  13.965936 $ Part 2747
64  cz  13.965936 $ Part 2742
```

NEA/NSC/DOC/(95)03/II
Volume II

HEU-MET-FAST-059

65 cz 13.965939 \$ Part 2744
66 cz 13.965555 \$ Part 2776
67 cz 13.965555 \$ Part 2778
68 cz 13.966190 \$ Part 2779
69 cz 13.965555 \$ Part 2743
c
c ----- 11"-13" HEU Annulus -----
c ----- Horizontal Planes -----
70 pz -7.666567 \$ Bottom
71 pz -5.126059 \$ Part 2756
72 pz -5.121974 \$ Gap
73 pz -3.842957 \$ Part 2751
74 pz -3.838871 \$ Gap
75 pz -2.560616 \$ Part 2752
76 pz -2.556531 \$ Gap
77 pz -1.283229 \$ Part 2753
78 pz -1.279144 \$ Gap
79 pz 0.000000 \$ Part 2754
80 pz 0.000000 \$ Gap (Diaphragm Location)
81 pz 2.543937 \$ Part 2757
82 pz 2.547818 \$ Gap
83 pz 3.506414 \$ Part 2749
84 pz 3.510294 \$ Gap
85 pz 4.463937 \$ Part 2750
86 pz 4.467818 \$ Gap
87 pz 4.784937 \$ Part 2780 (Top)
c ----- Inner Radii -----
88 cz 13.974572 \$ Part 2756
89 cz 13.971905 \$ Part 2751
90 cz 13.973175 \$ Part 2752
91 cz 13.973810 \$ Part 2753
92 cz 13.975080 \$ Part 2754
93 cz 13.973175 \$ Part 2757
94 cz 13.973810 \$ Part 2749
95 cz 13.971905 \$ Part 2750
96 cz 13.972540 \$ Part 2780
c ----- Outer Radii -----
97 cz 16.505809 \$ Part 2756
98 cz 16.504666 \$ Part 2751
99 cz 16.504285 \$ Part 2752
100 cz 16.505873 \$ Part 2753
101 cz 16.504031 \$ Part 2754
102 cz 16.504920 \$ Part 2757
103 cz 16.504285 \$ Part 2749
104 cz 16.503015 \$ Part 2750
105 cz 16.504984 \$ Part 2780
c
106 cz 16.510000 \$ Boundary
c

c Data Cards *****
c --- Material Cards -----
c ----- Be Discs -----
c ----- 2" -----
m1 4009.00c 1.2073E-01 13027.00c 2.4594E-05 5010.00c 2.0358E-07
5011.00c 8.1942E-07 83209.00c 2.6461E-06 35079.00c 3.5080E-09
35081.00c 3.4125E-09 6000.00c 1.1049E-04 48106.00c 2.4596E-10
48108.00c 1.7513E-10 48110.00c 2.4577E-09 48111.00c 2.5187E-09
48112.00c 4.7481E-09 48113.00c 2.4046E-09 48114.00c 5.6533E-09
48116.00c 1.4738E-09 66156.00c 4.0835E-12 66158.00c 6.8059E-12
66160.00c 1.5926E-10 66161.00c 1.2870E-09 66162.00c 1.7362E-09
66163.00c 1.6947E-09 66164.00c 1.9179E-09 26054.00c 1.5048E-06
26056.00c 2.3622E-05 26057.00c 5.4554E-07 26058.00c 7.2602E-08
64152.00c 1.4066E-11 64154.00c 1.5332E-10 64155.00c 1.0409E-09
64156.00c 1.4397E-09 64157.00c 1.1007E-09 64158.00c 1.7470E-09
64160.00c 1.5374E-09 12024.00c 7.1886E-06 12025.00c 9.1006E-07
12026.00c 1.0020E-06 28058.00c 1.2828E-08 28060.00c 4.9415E-09
28061.00c 2.1480E-10 28062.00c 6.8489E-10 28064.00c 1.7442E-10
8016.00c 8.5308E-04 8017.00c 3.2429E-07 62144.00c 2.2581E-10
62147.00c 1.1026E-09 62148.00c 8.2675E-10 62149.00c 1.0165E-09
62150.00c 5.4283E-10 62152.00c 1.9676E-09 62154.00c 1.6734E-09
c Total 1.2176E-01

Revision: 0

Date: September 30, 2010

NEA/NSC/DOC/(95)03/II
Volume II

HEU-MET-FAST-059

```

mt1      Be.00t  OBeO.00t
c
c ----- 1" -----
m2      4009.00c 1.2094E-01   13027.00c 2.4636E-05   5010.00c 2.0393E-07
      5011.00c 8.2083E-07   83209.00c 2.6507E-06   35079.00c 3.5141E-09
      35081.00c 3.4184E-09   6000.00c 1.1069E-04   48106.00c 2.4639E-10
      48108.00c 1.7543E-10   48110.00c 2.4619E-09   48111.00c 2.5230E-09
      48112.00c 4.7563E-09   48113.00c 2.4087E-09   48114.00c 5.6630E-09
      48116.00c 1.4764E-09   66156.00c 4.0906E-12   66158.00c 6.8176E-12
      66160.00c 1.5953E-10   66161.00c 1.2892E-09   66162.00c 1.7392E-09
      66163.00c 1.6976E-09   66164.00c 1.9212E-09   26054.00c 1.5074E-06
      26056.00c 2.3663E-05   26057.00c 5.4648E-07   26058.00c 7.2727E-08
      64152.00c 1.4091E-11   64154.00c 1.5359E-10   64155.00c 1.0427E-09
      64156.00c 1.4422E-09   64157.00c 1.1026E-09   64158.00c 1.7500E-09
      64160.00c 1.5401E-09   12024.00c 7.2010E-06   12025.00c 9.1164E-07
      12026.00c 1.0037E-06   28058.00c 1.2851E-08   28060.00c 4.9500E-09
      28061.00c 2.1517E-10   28062.00c 6.8607E-10   28064.00c 1.7472E-10
      8016.00c 8.5455E-04    8017.00c 3.2485E-07   62144.00c 2.2620E-10
      62147.00c 1.1045E-09   62148.00c 8.2817E-10   62149.00c 1.0183E-09
      62150.00c 5.4377E-10   62152.00c 1.9710E-09   62154.00c 1.6762E-09
c      Total      1.2197E-01
mt2      Be.00t  OBeO.00t
c
c ----- 1.5" -----
m3      4009.00c 1.2112E-01   13027.00c 2.4672E-05   5010.00c 2.0422E-07
      5011.00c 8.2201E-07   83209.00c 2.6545E-06   35079.00c 3.5191E-09
      35081.00c 3.4233E-09   6000.00c 1.1084E-04   48106.00c 2.4674E-10
      48108.00c 1.7568E-10   48110.00c 2.4655E-09   48111.00c 2.5267E-09
      48112.00c 4.7632E-09   48113.00c 2.4122E-09   48114.00c 5.6712E-09
      48116.00c 1.4785E-09   66156.00c 4.0965E-12   66158.00c 6.8275E-12
      66160.00c 1.5976E-10   66161.00c 1.2911E-09   66162.00c 1.7417E-09
      66163.00c 1.7000E-09   66164.00c 1.9240E-09   26054.00c 1.5096E-06
      26056.00c 2.3697E-05   26057.00c 5.4727E-07   26058.00c 7.2832E-08
      64152.00c 1.4111E-11   64154.00c 1.5381E-10   64155.00c 1.0442E-09
      64156.00c 1.4442E-09   64157.00c 1.1042E-09   64158.00c 1.7526E-09
      64160.00c 1.5423E-09   12024.00c 7.2114E-06   12025.00c 9.1295E-07
      12026.00c 1.0052E-06   28058.00c 1.2869E-08   28060.00c 4.9571E-09
      28061.00c 2.1548E-10   28062.00c 6.8706E-10   28064.00c 1.7497E-10
      8016.00c 8.5578E-04    8017.00c 3.2532E-07   62144.00c 2.2653E-10
      62147.00c 1.1061E-09   62148.00c 8.2937E-10   62149.00c 1.0197E-09
      62150.00c 5.4455E-10   62152.00c 1.9738E-09   62154.00c 1.6787E-09
c      Total      1.2215E-01
mt3      Be.00t  OBeO.00t
c
c ----- 0.5" -----
m4      4009.00c 1.1959E-01   13027.00c 2.4360E-05   5010.00c 2.0164E-07
      5011.00c 8.1163E-07   83209.00c 2.6209E-06   35079.00c 3.4747E-09
      35081.00c 3.3801E-09   6000.00c 1.0944E-04   48106.00c 2.4363E-10
      48108.00c 1.7346E-10   48110.00c 2.4343E-09   48111.00c 2.4947E-09
      48112.00c 4.7030E-09   48113.00c 2.3817E-09   48114.00c 5.5995E-09
      48116.00c 1.4598E-09   66156.00c 4.0447E-12   66158.00c 6.7412E-12
      66160.00c 1.5774E-10   66161.00c 1.2748E-09   66162.00c 1.7197E-09
      66163.00c 1.6786E-09   66164.00c 1.8997E-09   26054.00c 1.4905E-06
      26056.00c 2.3398E-05   26057.00c 5.4036E-07   26058.00c 7.1911E-08
      64152.00c 1.3932E-11   64154.00c 1.5186E-10   64155.00c 1.0310E-09
      64156.00c 1.4260E-09   64157.00c 1.0902E-09   64158.00c 1.7304E-09
      64160.00c 1.5228E-09   12024.00c 7.1203E-06   12025.00c 9.0141E-07
      12026.00c 9.9246E-07   28058.00c 1.2706E-08   28060.00c 4.8945E-09
      28061.00c 2.1276E-10   28062.00c 6.7837E-10   28064.00c 1.7276E-10
      8016.00c 8.4497E-04    8017.00c 3.2121E-07   62144.00c 2.2366E-10
      62147.00c 1.0921E-09   62148.00c 8.1889E-10   62149.00c 1.0069E-09
      62150.00c 5.3767E-10   62152.00c 1.9489E-09   62154.00c 1.6574E-09
c      Total      1.2060E-01
mt4      Be.00t  OBeO.00t
c
c ----- 7"-9" HEU Annulus -----
c ----- Part 2738 -----
m5      92234.00c 4.7317E-04   92235.00c 4.4783E-02   92236.00c 1.1489E-04
      92238.00c 2.6725E-03   47107.00c 4.3466E-07   47109.00c 4.0382E-07
      56130.00c 4.3633E-13   56132.00c 4.1575E-13   56134.00c 9.9491E-12
      56135.00c 2.7135E-11   56136.00c 3.2330E-11   56137.00c 4.6234E-11
      56138.00c 2.9513E-10   83209.00c 8.8722E-06   6000.00c 4.7064E-06

```


NEA/NSC/DOC/(95)03/II
Volume II

HEU-MET-FAST-059

```

48106.00c 6.2824E-10 48108.00c 4.4730E-10 48110.00c 6.2773E-09
48111.00c 6.4331E-09 48112.00c 1.2127E-08 48113.00c 6.1416E-09
48114.00c 1.4439E-08 48116.00c 3.7644E-09 27059.00c 9.5865E-07
24050.00c 6.6095E-08 24052.00c 1.2746E-06 24053.00c 1.4453E-07
24054.00c 3.5976E-08 29063.00c 3.0748E-06 29065.00c 1.3705E-06
19039.00c 2.6951E-08 19040.00c 3.3812E-12 19041.00c 1.9450E-09
3006.00c 1.2356E-07 3007.00c 1.5043E-06 12024.00c 1.1017E-06
12025.00c 1.3947E-07 12026.00c 1.5355E-07 25055.00c 1.1518E-05
42092.00c 8.7388E-09 42094.00c 5.4470E-09 42095.00c 9.3748E-09
42096.00c 9.8223E-09 42097.00c 5.6237E-09 42098.00c 1.4209E-08
42100.00c 5.6708E-09 11023.00c 1.3270E-05 28058.00c 1.3106E-05
28060.00c 5.0486E-06 28061.00c 2.1946E-07 28062.00c 6.9973E-07
28064.00c 1.7820E-07 51121.00c 2.0176E-06 51123.00c 1.5091E-06
22046.00c 1.9469E-08 22047.00c 1.7558E-08 22048.00c 1.7397E-07
22049.00c 1.2767E-08 22050.00c 1.2224E-08 8016.00c 1.4119E-05
8017.00c 5.3673E-09 7014.00c 2.4112E-05 7015.00c 8.9060E-08

c   Total      4.8127E-02
c
c ----- Part 2780 -----
m28  92234.00c 4.7200E-04 92235.00c 4.4663E-02 92236.00c 1.1938E-04
92238.00c 2.6706E-03 47107.00c 4.3358E-07 47109.00c 4.0282E-07
56130.00c 4.3525E-13 56132.00c 4.1472E-13 56134.00c 9.9245E-12
56135.00c 2.7068E-11 56136.00c 3.2250E-11 56137.00c 4.6120E-11
56138.00c 2.9440E-10 83209.00c 8.8503E-06 6000.00c 4.6947E-06
20040.00c 2.7278E-08 20042.00c 1.8206E-10 20043.00c 3.7988E-11
20044.00c 5.8699E-10 20046.00c 1.1256E-12 20048.00c 5.2620E-11
48106.00c 6.2704E-10 48108.00c 4.4645E-10 48110.00c 6.2654E-09
48111.00c 6.4209E-09 48112.00c 1.2104E-08 48113.00c 6.1299E-09
48114.00c 1.4412E-08 48116.00c 3.7572E-09 27059.00c 9.5682E-07
24050.00c 6.5969E-08 24052.00c 1.2721E-06 24053.00c 1.4425E-07
24054.00c 3.5907E-08 29063.00c 3.0689E-06 29065.00c 1.3679E-06
19039.00c 2.6900E-08 19040.00c 3.3748E-12 19041.00c 1.9413E-09
3006.00c 1.2332E-07 3007.00c 1.5015E-06 12024.00c 1.0996E-06
12025.00c 1.3920E-07 12026.00c 1.5326E-07 25055.00c 1.1496E-05
42092.00c 8.7221E-09 42094.00c 5.4366E-09 42095.00c 9.3569E-09
42096.00c 9.8036E-09 42097.00c 5.6130E-09 42098.00c 1.4182E-08
42100.00c 5.6600E-09 11023.00c 1.3245E-05 28058.00c 1.3081E-05
28060.00c 5.0389E-06 28061.00c 2.1904E-07 28062.00c 6.9839E-07
28064.00c 1.7786E-07 51121.00c 2.0137E-06 51123.00c 1.5062E-06
22046.00c 1.9432E-08 22047.00c 1.7524E-08 22048.00c 1.7364E-07
22049.00c 1.2743E-08 22050.00c 1.2201E-08 8016.00c 1.4092E-05
8017.00c 5.3571E-09 7014.00c 2.4066E-05 7015.00c 8.8890E-08

c   Total      4.8035E-02
c
c --- Control Cards -----
mode n
kcode 1000000 1 50 1050
ksrc  0 7.62 4 0 -7.62 4 7.62 0 4 -7.62 0 4
      0 7.62 -4 0 -7.62 -4 7.62 0 -4 -7.62 0 -4
print

```

A.1.1.2 Simple Model

```
ORALLOY (93.15 235U) METAL ANNULI WITH BERYLLIUM CORE (SIMPLE - 13")  
c  
c John Darrell Bess - Idaho National Laboratory  
c Last Updated: January 5, 2010  
c  
c  
c Cell Cards *****  
1 1 1.2065E-01 -1 imp:n=1 $ Be  
2 2 4.6923E-02 1 -2 imp:n=1 $ HEU  
3 0 0 imp:n=0 $ Void  
c  
  
c Surface Cards *****  
1 rcc 0 0 0 0 12.7 8.89  
2 rcc 0 0 0 0 12.7 16.51  
c  
  
c Data Cards *****  
c --- Material Cards -----  
c ----- Be -----  
m1 4009.00c 1.2065E-01  
c Total 1.2065E-01  
mt1 Be.00t  
c  
c ----- HEU -----  
m2 92234.00c 4.5628E-04 92235.00c 4.3740E-02 92236.00c 1.1092E-04  
92238.00c 2.6151E-03  
c Total 4.6923E-02  
c  
c  
c --- Control Cards -----  
mode n  
kcode 1000000 1 50 1050  
ksrc 0 7.62 6.35 0 -7.62 6.35 7.62 0 6.35 -7.62 0 6.35  
print
```

A.1.2 Fifteen-Inch-Diameter Annulus (Configuration 2)

A.1.2.1 Detailed Model

```
ORALLOY (93.15 235U) METAL ANNULI WITH BERYLLIUM CORE (DETAILED - 15")  
c  
c John Darrell Bess - Idaho National Laboratory  
c Last Updated: January 7, 2010  
c  
c  
c Cell Cards *****  
c ----- Be Discs -----  
1 1 1.2176E-01 1 -2 -7 imp:n=1 $ 2"  
2 2 1.2215E-01 3 -4 -7 imp:n=1 $ 1.5"  
3 3 1.2060E-01 5 -6 -7 imp:n=1 $ 0.5"  
c  
c ----- 7"-9" HEU Annulus -----  
4 4 4.8185E-02 8 -9 24 -32 imp:n=1 $ Part 2740  
5 5 4.8088E-02 10 -11 25 -33 imp:n=1 $ Part 2829  
6 6 4.8043E-02 12 -13 26 -34 imp:n=1 $ Part 2773  
7 7 4.8155E-02 14 -15 27 -35 imp:n=1 $ Part 2738  
8 8 4.8071E-02 16 -17 28 -36 imp:n=1 $ Part 2736  
9 9 4.7943E-02 18 -19 29 -37 imp:n=1 $ Part 2763  
10 10 4.8217E-02 20 -21 30 -38 imp:n=1 $ Part 2775  
11 11 4.8238E-02 22 -23 31 -39 imp:n=1 $ Part 2774  
c  
c ----- 9"-11" HEU Annulus -----  
12 12 4.8157E-02 40 -41 56 -64 imp:n=1 $ Part 2748  
13 13 4.8076E-02 42 -43 57 -65 imp:n=1 $ Part 2746  
14 14 4.8161E-02 44 -45 58 -66 imp:n=1 $ Part 2742  
15 15 4.8103E-02 46 -47 59 -67 imp:n=1 $ Part 2776  
16 16 4.8386E-02 48 -49 60 -68 imp:n=1 $ Part 2743  
17 17 4.8090E-02 50 -51 61 -69 imp:n=1 $ Part 2779
```

HEU-MET-FAST-059

```

18   18  4.7994E-02   52 -53   62 -70   imp:n=1 $ Part 2778
19   19  4.8301E-02   54 -55   63 -71   imp:n=1 $ Part 2744
c
c ----- 11"-13" HEU Annulus -----
20   20  4.8182E-02   72 -73   84 -90   imp:n=1 $ Part 2756
21   21  4.8244E-02   74 -75   85 -91   imp:n=1 $ Part 2754
22   22  4.8148E-02   76 -77   86 -92   imp:n=1 $ Part 2751
23   23  4.8145E-02   78 -79   87 -93   imp:n=1 $ Part 2757
24   24  4.8167E-02   80 -81   88 -94   imp:n=1 $ Part 2755
25   25  4.8151E-02   82 -83   89 -95   imp:n=1 $ Part 2749
c
c ----- 13"-15" HEU Annulus -----
26   26  4.8004E-02   96 -97   110 -117  imp:n=1 $ Part 2735
27   27  4.8011E-02   98 -99   111 -118  imp:n=1 $ Part 2848
28   28  4.8071E-02   100 -101  112 -119  imp:n=1 $ Part 2785
29   29  4.8153E-02   102 -103  113 -120  imp:n=1 $ Part 2761
30   30  4.8348E-02   104 -105  114 -121  imp:n=1 $ Part 2739
31   31  4.8186E-02   106 -107  115 -122  imp:n=1 $ Part 2766
32   32  4.8318E-02   108 -109  116 -123  imp:n=1 $ Part 2784
c
c ----- Void Spaces-----
33     0  1 -55 -124 #1 #2 #3 #4 #5 #6 #7 #8 #9 #10 #11 #12 #13 #14#15 #16 #17 #18
          #19 #20 #21 #22 #23 #24 #25 #26 #27 #28 #29 #30 #31 #32 imp:n=1 $ Gaps
34     0  -1:55:124                                imp:n=0 $ The Great Void

c Surface Cards ****
c ----- Be Discs -----
c ----- Horizontal Planes -----
1   pz  -5.098669 $ Bottom
2   pz  -0.018669 $ 2"
3   pz  0.000000 $ Gap (Diaphragm Location)
4   pz  3.810000 $ 1.5"
5   pz  3.812540 $ Gap
6   pz  5.082540 $ 0.5" (Top)
c ----- Outer Radii -----
7   cz  8.885460 $ All Be
c
c ----- 7"-9" HEU Annulus -----
c ----- Horizontal Planes -----
8   pz  -5.098669 $ Bottom
9   pz  -1.288669 $ Part 2740
10  pz  -1.284753 $ Gap
11  pz  -0.329078 $ Part 2829
12  pz  -0.325162 $ Gap
13  pz  -0.007662 $ Part 2773
14  pz  0.000000 $ Gap (Diaphragm Location)
15  pz  2.543048 $ Part 2738
16  pz  2.545239 $ Gap
17  pz  3.501168 $ Part 2736
18  pz  3.503359 $ Gap
19  pz  3.819081 $ Part 2763
20  pz  3.821271 $ Gap
21  pz  4.452461 $ Part 2775
22  pz  4.454652 $ Gap
23  pz  5.089652 $ Part 2774 (Top)
c ----- Inner Radii -----
24  cz  8.893175 $ Part 2740
25  cz  8.894001 $ Part 2829
26  cz  8.891905 $ Part 2773
27  cz  8.894763 $ Part 2738
28  cz  8.893302 $ Part 2736
29  cz  8.894826 $ Part 2763
30  cz  8.895080 $ Part 2775
31  cz  8.893810 $ Part 2774
c ----- Outer Radii -----
32  cz  11.425238 $ Part 2740
33  cz  11.425238 $ Part 2829
34  cz  11.426190 $ Part 2773
35  cz  11.424603 $ Part 2738
36  cz  11.424920 $ Part 2736
37  cz  11.424666 $ Part 2763
38  cz  11.425873 $ Part 2775

```

HEU-MET-FAST-059

```
39    cz  11.425555 $ Part 2774
c
c ----- 9"-11" HEU Annulus -----
c ----- Horizontal Planes -----
40    pz  -5.098669 $ Bottom
41    pz  -1.288669 $ Part 2748
42    pz  -1.288352 $ Gap
43    pz  -0.961581 $ Part 2746
44    pz  -0.961263 $ Gap
45    pz  -0.008509 $ Part 2742
46    pz  0.000000 $ Gap (Diaphragm Location)
47    pz  2.543810 $ Part 2776
48    pz  2.546572 $ Gap
49    pz  3.496532 $ Part 2743
50    pz  3.499295 $ Gap
51    pz  4.136835 $ Part 2779
52    pz  4.139597 $ Gap
53    pz  4.777137 $ Part 2778
54    pz  4.779899 $ Gap
55    pz  5.101844 $ Part 2744 (Top)
c ----- Inner Radii -----
56    cz  11.433175 $ Part 2748
57    cz  11.432223 $ Part 2746
58    cz  11.431905 $ Part 2742
59    cz  11.431905 $ Part 2776
60    cz  11.433175 $ Part 2743
61    cz  11.431905 $ Part 2779
62    cz  11.432540 $ Part 2778
63    cz  11.438255 $ Part 2744
c ----- Outer Radii -----
64    cz  13.966825 $ Part 2748
65    cz  13.965555 $ Part 2746
66    cz  13.965936 $ Part 2742
67    cz  13.965555 $ Part 2776
68    cz  13.965555 $ Part 2743
69    cz  13.966190 $ Part 2779
70    cz  13.965555 $ Part 2778
71    cz  13.965936 $ Part 2744
c
c ----- 11"-13" HEU Annulus -----
c ----- Horizontal Planes -----
72    pz  -5.098669 $ Bottom
73    pz  -2.558161$ Part 2756
74    pz  -2.558161 $ Gap
75    pz  -1.279017 $ Part 2754
76    pz  -1.279017 $ Gap
77    pz  0.000000 $ Part 2751
78    pz  0.000000 $ Gap (Diaphragm Location)
79    pz  2.543937 $ Part 2757
80    pz  2.545906 $ Gap
81    pz  3.977196 $ Part 2755
82    pz  3.979164 $ Gap
83    pz  4.937760 $ Part 2749 (Top)
c ----- Inner Radii -----
84    cz  13.974572 $ Part 2756
85    cz  13.975080 $ Part 2754
86    cz  13.971905 $ Part 2751
87    cz  13.973175 $ Part 2757
88    cz  13.973810 $ Part 2755
89    cz  13.973810 $ Part 2749
c ----- Outer Radii -----
90    cz  16.505809 $ Part 2756
91    cz  16.504031 $ Part 2754
92    cz  16.504666 $ Part 2751
93    cz  16.504920 $ Part 2757
94    cz  16.504920 $ Part 2755
95    cz  16.504285 $ Part 2749
c
c ----- 13"-15" HEU Annulus -----
c ----- Horizontal Planes -----
96    pz  -5.098669 $ Bottom
97    pz  -2.562479 $ Part 2735
```

HEU-MET-FAST-059

```

98  pz  -2.558270 $ Gap
99  pz  -1.283444 $ Part 2848
100 pz  -1.279235 $ Gap
101 pz  -0.327497 $ Part 2785
102 pz  -0.323288 $ Gap
103 pz  -0.001978 $ Part 2761
104 pz  0.000000 $ Gap (Diaphragm Location)
105 pz  2.526030 $ Part 2739
106 pz  2.538476 $ Gap
107 pz  3.968496 $ Part 2766
108 pz  3.980942 $ Gap
109 pz  4.927092 $ Part 2784 (Top)
c ----- Inner Radii -----
110 cz  16.512540 $ Part 2735
111 cz  16.513937 $ Part 2848
112 cz  16.513683 $ Part 2785
113 cz  16.511270 $ Part 2761
114 cz  16.513429 $ Part 2739
115 cz  16.511270 $ Part 2766
116 cz  16.511905 $ Part 2784
c ----- Outer Radii -----
117 cz  19.041745 $ Part 2735
118 cz  19.045428 $ Part 2848
119 cz  19.044666 $ Part 2785
120 cz  19.043333 $ Part 2761
121 cz  19.044285 $ Part 2739
122 cz  19.045555 $ Part 2766
123 cz  19.043015 $ Part 2784
c
124 cz  19.050000 $ Boundary
c

c Data Cards ****
c --- Material Cards -----
c ----- Be Discs -----
c ----- 2" -----
m1  4009.00c 1.2073E-01 13027.00c 2.4594E-05 5010.00c 2.0358E-07
    5011.00c 8.1942E-07 83209.00c 2.6461E-06 35079.00c 3.5080E-09
    35081.00c 3.4125E-09 6000.00c 1.1049E-04 48106.00c 2.4596E-10
    48108.00c 1.7513E-10 48110.00c 2.4577E-09 48111.00c 2.5187E-09
    48112.00c 4.7481E-09 48113.00c 2.4046E-09 48114.00c 5.6533E-09
    48116.00c 1.4738E-09 66156.00c 4.0835E-12 66158.00c 6.8059E-12
    66160.00c 1.5926E-10 66161.00c 1.2870E-09 66162.00c 1.7362E-09
    66163.00c 1.6947E-09 66164.00c 1.9179E-09 26054.00c 1.5048E-06
    26056.00c 2.3622E-05 26057.00c 5.4554E-07 26058.00c 7.2602E-08
    64152.00c 1.4066E-11 64154.00c 1.5332E-10 64155.00c 1.0409E-09
    64156.00c 1.4397E-09 64157.00c 1.1007E-09 64158.00c 1.7470E-09
    64160.00c 1.5374E-09 12024.00c 7.1886E-06 12025.00c 9.1006E-07
    12026.00c 1.0020E-06 28058.00c 1.2828E-08 28060.00c 4.9415E-09
    28061.00c 2.1480E-10 28062.00c 6.8489E-10 28064.00c 1.7442E-10
    8016.00c 8.5308E-04 8017.00c 3.2429E-07 62144.00c 2.2581E-10
    62147.00c 1.1026E-09 62148.00c 8.2675E-10 62149.00c 1.0165E-09
    62150.00c 5.4283E-10 62152.00c 1.9676E-09 62154.00c 1.6734E-09
c Total 1.2176E-01
mt1  Be.00t OBeO.00t
c
c ----- 1.5" -----
m2  4009.00c 1.2112E-01 13027.00c 2.4672E-05 5010.00c 2.0422E-07
    5011.00c 8.2201E-07 83209.00c 2.6545E-06 35079.00c 3.5191E-09
    35081.00c 3.4233E-09 6000.00c 1.1084E-04 48106.00c 2.4674E-10
    48108.00c 1.7556E-10 48110.00c 2.4655E-09 48111.00c 2.5267E-09
    48112.00c 4.7632E-09 48113.00c 2.4122E-09 48114.00c 5.6712E-09
    48116.00c 1.4785E-09 66156.00c 4.0965E-12 66158.00c 6.8275E-12
    66160.00c 1.5976E-10 66161.00c 1.2911E-09 66162.00c 1.7417E-09
    66163.00c 1.7000E-09 66164.00c 1.9240E-09 26054.00c 1.5096E-06
    26056.00c 2.3697E-05 26057.00c 5.4727E-07 26058.00c 7.2832E-08
    64152.00c 1.4111E-11 64154.00c 1.5381E-10 64155.00c 1.0442E-09
    64156.00c 1.4442E-09 64157.00c 1.1042E-09 64158.00c 1.7526E-09
    64160.00c 1.5423E-09 12024.00c 7.2114E-06 12025.00c 9.1295E-07
    12026.00c 1.0052E-06 28058.00c 1.2869E-08 28060.00c 4.9571E-09
    28061.00c 2.1548E-10 28062.00c 6.8706E-10 28064.00c 1.7497E-10
    8016.00c 8.5578E-04 8017.00c 3.2532E-07 62144.00c 2.2653E-10

```


A.1.2.2 Simple Model

```
ORALLOY (93.15 235U) METAL ANNULI WITH BERYLLIUM CORE (SIMPLE - 15")
c
c John Darrell Bess - Idaho National Laboratory
c Last Updated: January 5, 2010
c
c
c Cell Cards ****
1    1  1.2061E-01  -1    imp:n=1 $ Be
2    2  4.7489E-02   1  -2    imp:n=1 $ HEU
3    0                  2    imp:n=0 $ Void
c

c Surface Cards ****
1    rcc 0 0 0 0 10.16  8.89
2    rcc 0 0 0 0 10.16 19.05
c

c Data Cards ****
c --- Material Cards -----
c ----- Be -----
m1    4009.00c 1.2061E-01
c     Total      1.2061E-01
mt1    Be.00t
c
c ----- HEU -----
m2    92234.00c 4.6422E-04  92235.00c 4.4264E-02  92236.00c 1.1543E-04
      92238.00c 2.6453E-03
c     Total      4.7489E-02
c
c
c --- Control Cards -----
mode n
kcode 1000000 1 50 1050
ksrc  0 10.16 5.08 0 -10.16 5.08 10.16 0 5.08 -10.16 0 5.08
print
```

APPENDIX B: CALCULATED SPECTRAL DATA

The neutron spectral calculations provided below were obtained from the output files for the input decks provided in Appendix A and results in Section 4. The ENDF/B-VII.0, JEFF-3.1, and JENDL-3.3 neutron cross section libraries are provided here for the MCNP5 analyses. The cross sections are all continuous in the MCNP5 analyses.

B.1 MCNP-Calculated Neutron Spectral Data**B.1.1 Detailed Models**

A summary of the computed neutron spectral data using MCNP5 for the detailed benchmark models is provided in Tables B.1 and B.2 for Configurations 1 and 2, respectively.

Table B.1. Neutron Spectral Data for Detailed Benchmark Model (Configuration 1).

Neutron Cross Section Library	ENDF/B-VII.0	JEFF-3.1	JENDL-3.3
k_{eff}	0.99711	0.99519	1.00193
$\pm \sigma_k$	0.00002	0.00002	0.00002
Neutron Leakage (%)^(a)	54.03	54.07	53.70
Fission Fraction, by Energy (%)	Thermal (<0.625 eV)	0.00	0.14
	Intermediate	9.21	9.33
	Fast (>100 keV)	90.79	90.53
Fission Fraction, by Isotope (%)	^{234}U	0.73	0.75
	^{235}U	98.31	98.29
	^{236}U	0.08	0.08
	^{238}U	0.89	0.90
Average Number of Neutrons Produced per Fission		2.589	2.586
Energy of Average Neutron Lethargy Causing Fission (MeV)		0.645	0.640
			0.651

- (a) The neutron leakage is calculated using the neutron balance tables provided in the MCNP output file. The weight fraction of neutrons lost due to escaping the boundaries of the benchmark model are divided by the total weight fraction of neutron loss.

Table B.2. Neutron Spectral Data for Detailed Benchmark Model (Configuration 2).

Neutron Cross Section Library	ENDF/B-VII.0	JEFF-3.1	JENDL-3.3
k_{eff}	0.99680	0.99451	1.00125
$\pm \sigma_k$	0.00002	0.00002	0.00002
Neutron Leakage (%)^(a)	54.60	54.66	54.31
Fission Fraction, by Energy (%)	Thermal (<0.625 eV)	0.00	0.03
	Intermediate	7.21	7.39
	Fast (>100 keV)	92.79	92.57
Fission Fraction, by Isotope (%)	^{234}U	0.76	0.76
	^{235}U	98.25	98.24
	^{236}U	0.08	0.08
	^{238}U	0.91	0.92
Average Number of Neutrons Produced per Fission		2.594	2.591
Energy of Average Neutron Lethargy Causing Fission (MeV)		0.734	0.734
			0.746

- (a) The neutron leakage is calculated using the neutron balance tables provided in the MCNP output file. The weight fraction of neutrons lost due to escaping the boundaries of the benchmark model are divided by the total weight fraction of neutron loss.

B.1.2 Simple Model

A summary of the computed neutron spectral data using MCNP5 for the detailed benchmark model is provided in Table B.3 and B.4 for Configurations 1 and 2, respectively.

Table B.3. Neutron Spectral Data for Simple Benchmark Model (Configuration 1).

Neutron Cross Section Library	ENDF/B-VII.0	JEFF-3.1	JENDL-3.3
k_{eff}	0.98953	0.98772	0.99401
$\pm \sigma_k$	0.00002	0.00002	0.00002
Neutron Leakage (%)^(a)	54.40	54.43	54.09
Fission Fraction, by Energy (%)			
Thermal (<0.625 eV)	0.15	0.13	0.13
Intermediate	9.09	9.36	9.04
Fast (>100 keV)	90.76	90.54	90.82
Fission Fraction, by Isotope (%)			
^{234}U	0.73	0.73	0.75
^{235}U	98.30	98.29	98.28
^{236}U	0.08	0.08	0.08
^{238}U	0.89	0.90	0.90
Average Number of Neutrons Produced per Fission	2.589	2.587	2.594
Energy of Average Neutron Lethargy Causing Fission (MeV)	0.640	0.641	0.652

- (a) The neutron leakage is calculated using the neutron balance tables provided in the MCNP output file. The weight fraction of neutrons lost due to escaping the boundaries of the benchmark model are divided by the total weight fraction of neutron loss.

Table B.4. Neutron Spectral Data for Simple Benchmark Model (Configuration 2).

Neutron Cross Section Library	ENDF/B-VII.0	JEFF-3.1	JENDL-3.3
k_{eff}	0.99257	0.99027	0.99699
$\pm \sigma_k$	0.00002	0.00002	0.00002
Neutron Leakage (%)^(a)	54.81	54.86	54.51
Fission Fraction, by Energy (%)	Thermal (<0.625 eV)	0.04	0.03
	Intermediate	7.15	7.36
	Fast (>100 keV)	92.81	92.61
Fission Fraction, by Isotope (%)	^{234}U	0.76	0.76
	^{235}U	98.25	98.23
	^{236}U	0.08	0.08
	^{238}U	0.91	0.93
Average Number of Neutrons Produced per Fission		2.594	2.592
Energy of Average Neutron Lethargy Causing Fission (MeV)		0.734	0.736
			0.749

- (a) The neutron leakage is calculated using the neutron balance tables provided in the MCNP output file. The weight fraction of neutrons lost due to escaping the boundaries of the benchmark model are divided by the total weight fraction of neutron loss.

B.1.3 Comparison of Models

A direct comparison of the results tabulated in Tables B.1 through B.4 for the detailed and simple benchmark models, respectively, shows minimal significant difference. These differences are shown in Tables B.5 and B.6 for Configurations 1 and 2, respectively.

It should be noted, that in the calculation of the detailed model using the ENDF/B-VII.0 library, if the effects of thermal scattering from oxygen in BeO are not included, then the fission fraction by energy for the thermal and intermediate energies are approximately identical between the calculated neutron spectra from both detailed and simple models (matching those obtained from the simple models).

Table B.5. Comparison of Benchmark Model Neutron Spectral Data (Configuration 1).

Neutron Cross Section Library	ENDF/B-VII.0	JEFF-3.1	JENDL-3.3
Δk_{eff}	-0.00758	-0.00747	-0.00792
$\pm \sigma_{\Delta k}$	0.00003	0.00003	0.00003
Neutron Leakage (%)^(a)	0.38	0.36	0.38
Fission Fraction, by Energy (%)			
Thermal (<0.625 eV)	0.15	-0.01	0.00
Intermediate	-0.12	0.03	-0.02
Fast (>100 keV)	-0.02	-0.02	0.01
Fission Fraction, by Isotope (%)			
^{234}U	0.00	0.00	0.00
^{235}U	0.01	0.00	0.00
^{236}U	0.00	0.00	0.00
^{238}U	0.00	0.00	0.01
Average Number of Neutrons Produced per Fission	0.000	0.001	0.001
Energy of Average Neutron Lethargy Causing Fission (MeV)	-0.005	0.001	0.001

- (a) The neutron leakage is calculated using the neutron balance tables provided in the MCNP output file. The weight fraction of neutrons lost due to escaping the boundaries of the benchmark model are divided by the total weight fraction of neutron loss.

Table B.6. Comparison of Benchmark Model Neutron Spectral Data (Configuration 2).

Neutron Cross Section Library	ENDF/B-VII.0	JEFF-3.1	JENDL-3.3
Δk_{eff}	-0.00423	-0.00424	-0.00426
$\pm \sigma_{\Delta k}$	0.00003	0.00003	0.00003
Neutron Leakage (%)^(a)	0.22	0.21	0.21
Fission Fraction, by Energy (%)			
Thermal (<0.625 eV)	0.04	0.00	0.00
Intermediate	-0.06	-0.03	-0.03
Fast (>100 keV)	0.02	0.04	0.04
Fission Fraction, by Isotope (%)			
^{234}U	0.00	0.00	0.00
^{235}U	0.00	0.01	0.00
^{236}U	0.00	0.01	0.00
^{238}U	0.00	0.00	0.00
Average Number of Neutrons Produced per Fission	0.000	0.001	0.000
Energy of Average Neutron Lethargy Causing Fission (MeV)	0.000	0.002	0.003

- (a) The neutron leakage is calculated using the neutron balance tables provided in the MCNP output file. The weight fraction of neutrons lost due to escaping the boundaries of the benchmark model are divided by the total weight fraction of neutron loss.

APPENDIX C: BERYLLIUM MODERATOR/REFLECTOR WORTH

The effect of the beryllium moderator/reflector was determined by comparing this benchmark experiments with similar bare HEU cylinder benchmark experiments evaluated in [HEU-MET-FAST-051](#) (Configurations 17 and 18). These experiments utilized many of the same HEU annuli and had outer diameters of 13 and 15 inches (33.02 and 38.1 cm), respectively, with 7-inch-diameter (17.78 cm) HEU discs in the center. Both the beryllium-moderated/reflected experiment and the bare HEU experiment had k_{eff} eigenvalues very close to 1.0000 and a β_{eff} of 0.0066. The primary difference between the bare HEU experiments and the beryllium-reflected experiments is their approximate total stacked height. The two bare HEU experiments (Configurations 17 and 18) were approximately 3 inches (7.62 cm) high while the moderated/reflected configurations were 5 inches (12.7 cm) and 4 inches (10.16 cm) high for Configurations 1 and 2, respectively.

A comparison of the parts and total mass of the 13-inch experiments is provided in Table C.1, and a comparison of the 15-inch experiments is provided in Table C.2. There is not a moderator/reflector mass savings, however, because the annular HEU configurations with internal beryllium reflectors required more mass than their bare HEU counterparts: 13.497 kg HEU for the 13-inch experiment and 3.258 kg HEU for the 15-inch experiment. The worth of the moderator/reflector was estimated using MCNP calculations for the configurations in this report with and without the beryllium. A summary of the worth calculations using ENDF/B-VII.0, JEFF-3.1, and JENDL-3.3 neutron cross section data is provided in Tables C.3 and C.4 for Configurations 1 and 2, respectively. Their respective beryllium worth is estimated to be $8.5 \pm 0.4\$$ and $4.2 \pm 0.2\$$. Although the beryllium cores provide internal reflection to achieve criticality, they are not of sufficient worth to minimize the total quantity of fissile material needed significantly.

Table C.1. Comparison of Bare HEU Cylinder and Be-Reflected HEU Annulus (13-Inch Outer Diameter).

Bare HEU Cylinder ^(a) Part (Type) ^(b)	Mass (g)	Be-Reflected HEU Annulus Part (Type) ^(b)	Mass (g)
2728 (Disc)	4435	--	--
2729 (Disc)	4440	--	--
2730 (Disc)	6646	--	--
2733 (Disc)	17742	--	--
2736 (Annulus)	2895	2736 (Annulus)	2895
--	--	2737 (Annulus)	4336
--	--	2738 (Annulus)	7710
2740 (Annulus)	11568	2740 (Annulus)	11568
2742 (Annulus)	3617	2742 (Annulus)	3617
2743 (Annulus)	3621	2743 (Annulus)	3621
2744 (Annulus)	1223	2744 (Annulus)	1223
--	--	2745 (Annulus)	9634
2747 (Annulus)	14436	2747 (Annulus)	14436
2749 (Annulus)	4360	2749 (Annulus)	4360
--	--	2750 (Annulus)	4336
2751 (Annulus)	5822	2751 (Annulus)	5822
--	--	2752 (Annulus)	5811
--	--	2753 (Annulus)	5782
--	--	2754 (Annulus)	5826
2756 (Annulus)	11567	2756 (Annulus)	11567
2757 (Annulus)	11575	2757 (Annulus)	11575
--	--	2762 (Annulus)	7703
2768 (Disc)	1481	--	--
2773 (Annulus)	962	2773 (Annulus)	962
2774 (Annulus)	1930	--	--
2775 (Annulus)	1917	--	--
--	--	2776 (Annulus)	9644
2778 (Annulus)	2411	2778 (Annulus)	2411
2779 (Annulus)	2417	2779 (Annulus)	2417
--	--	2780 (Annulus)	1440
2782 (Annulus)	2914	--	--
2803 (Disc)	7220	--	--
2829 (Annulus)	2895	2829 (Annulus)	2895
Total	128094	Total	141591

(a) HEU-MET-FAST-051 (Configuration 14).

(b) Parts listed in numerical order.

Table C.2. Comparison of Bare HEU Cylinder and Be-Reflected HEU Annulus (15-Inch Outer Diameter).

Bare HEU Cylinder ^(a) Part (Type) ^(b)	Mass (g)	Be-Reflected HEU Annulus Part (Type) ^(b)	Mass (g)
2728 (Disc)	4435	--	--
2729 (Disc)	4440	--	--
2731 (Disc)	11841	--	--
2732 (Disc)	11814	--	--
2735 (Annulus)	13409	2735 (Annulus)	13409
2736 (Annulus)	2895	2736 (Annulus)	2895
2737 (Annulus)	4336	--	--
2738 (Annulus)	7710	2738 (Annulus)	7710
--	--	2739 (Annulus)	13461
--	--	2740 (Annulus)	11568
2742 (Annulus)	3617	2742 (Annulus)	3617
2743 (Annulus)	3621	2743 (Annulus)	3621
--	--	2744 (Annulus)	1223
2745 (Annulus)	9634	--	--
--	--	2746 (Annulus)	1238
--	--	2748 (Annulus)	14462
2749 (Annulus)	4360	2749 (Annulus)	4360
2750 (Annulus)	4336	--	--
--	--	2741 (Annulus)	5822
2754 (Annulus)	5826	2754 (Annulus)	5826
2755 (Annulus)	6514	2755 (Annulus)	6514
2756 (Annulus)	11567	2756 (Annulus)	11567
--	--	2757 (Annulus)	11575
--	--	2761 (Annulus)	1706
--	--	2763 (Annulus)	953
2766 (Annulus)	7605	2766 (Annulus)	7605
2767 (Annulus)	5410	--	--
--	--	2773 (Annulus)	962
2774 (Annulus)	1930	2774 (Annulus)	1930
2775 (Annulus)	1917	2775 (Annulus)	1917
--	--	2776 (Annulus)	9644
2778 (Annulus)	2411	2778 (Annulus)	2411
2779 (Annulus)	2417	2779 (Annulus)	2417
2784 (Annulus)	5039	2784 (Annulus)	5039
2785 (Annulus)	5043	2785 (Annulus)	5043
2820 (Disc)	6471	--	--
2821 (Disc)	6518	--	--
2829 (Annulus)	2895	2829 (Annulus)	2895
2848 (Annulus)	6748	2848 (Annulus)	6748
3104 (Thin Foil)	60.3	--	--
3105 (Thin Foil)	60.3	--	--
Total	164879.6	Total	168138

(a) [HEU-MET-FAST-051](#) (Configuration 14).

(b) Parts listed in numerical order.

Table C.3. Calculated Worth of Beryllium Moderator (Configuration 1).

Neutron Cross Section Library	Calculated Worth (ρ)	1σ
ENDF/B-VII.0	0.05596	0.00003
JEFF-3.1	0.05709	0.00003
JENDL-3.3	0.05616	0.00003
Average	0.05640	0.00060 ^(a)
Worth ($\rho\$$) ^(b)	8.55	0.44

(a) The standard deviation is of the population, and not the average of the calculated statistical uncertainties.

(b) $\beta_{\text{eff}} = 0.0066$ with an uncertainty of $\pm 5\%$.

Table C.4. Calculated Worth of Beryllium Reflector (Configuration 2).

Neutron Cross Section Library	Calculated Worth (ρ)	1σ
ENDF/B-VII.0	0.02768	0.00003
JEFF-3.1	0.02850	0.00003
JENDL-3.3	0.02772	0.00003
Average	0.02797	0.00046 ^(a)
Worth ($\rho\$$) ^(b)	4.24	0.22

(a) The standard deviation is of the population, and not the average of the calculated statistical uncertainties.

(b) $\beta_{\text{eff}} = 0.0066$ with an uncertainty of $\pm 5\%$.

APPENDIX D: Support Structure Assembly Schematics

Additional drawings were provided by the experimenter^a to preserve the dimensions of the support structure immediately surrounding the experiment. Figure D.1 represents the diaphragm and rings with its support structure. Figure D.2 represents the low-mass support structure. Both of these structures can be seen in Figure 4. These support structures were used in many other critical experiments with orraloy at ORCEF although the details of these support structures were not presented in the previous benchmarks: [HEU-MET-FAST-051](#), [HEU-MET-FAST-071](#), and [HEU-MET-FAST-076](#).

^a Personal communication with John T. Mihalczo, February 2010.

Revision: 0

Date: September 30, 2010

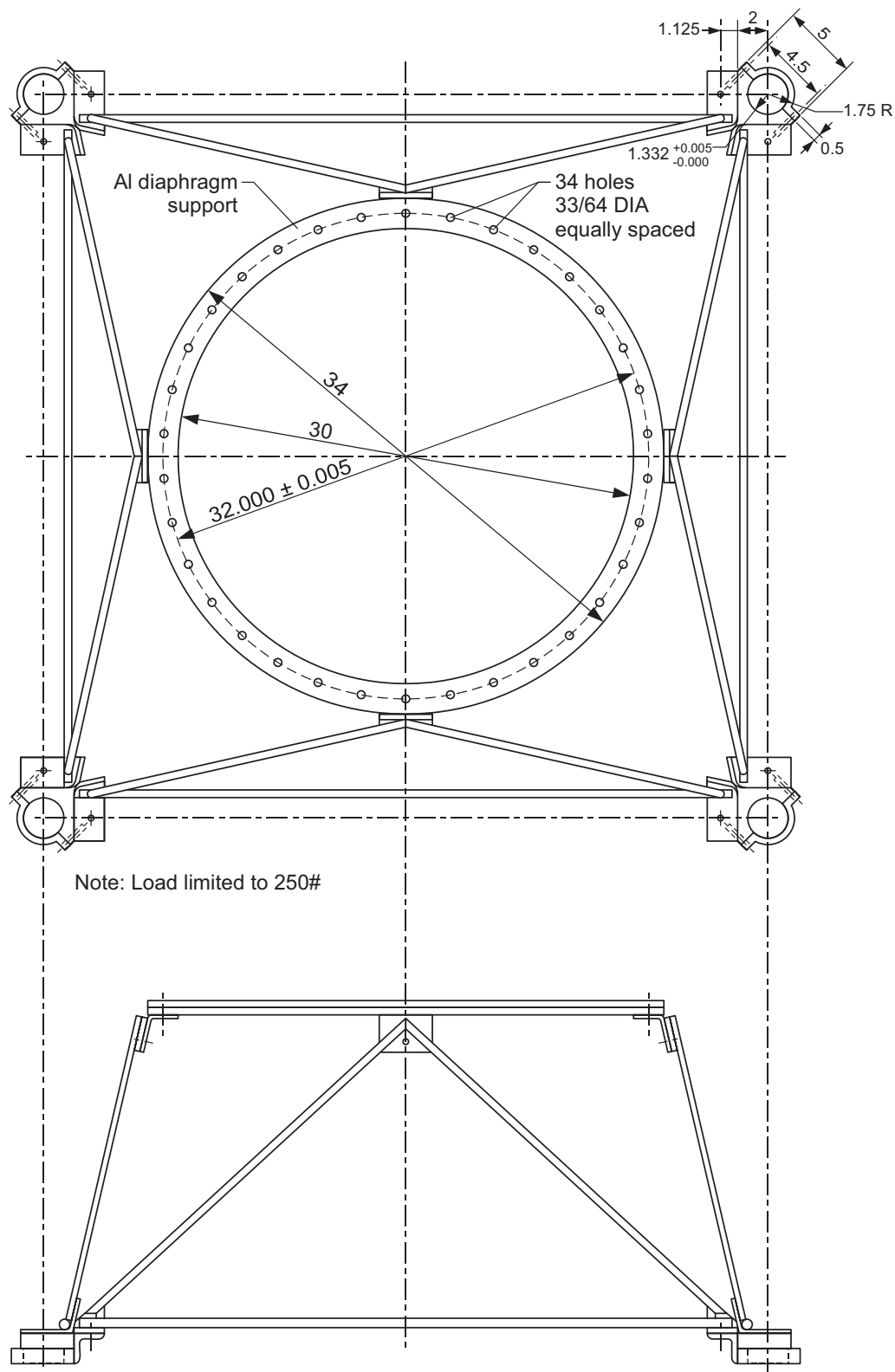
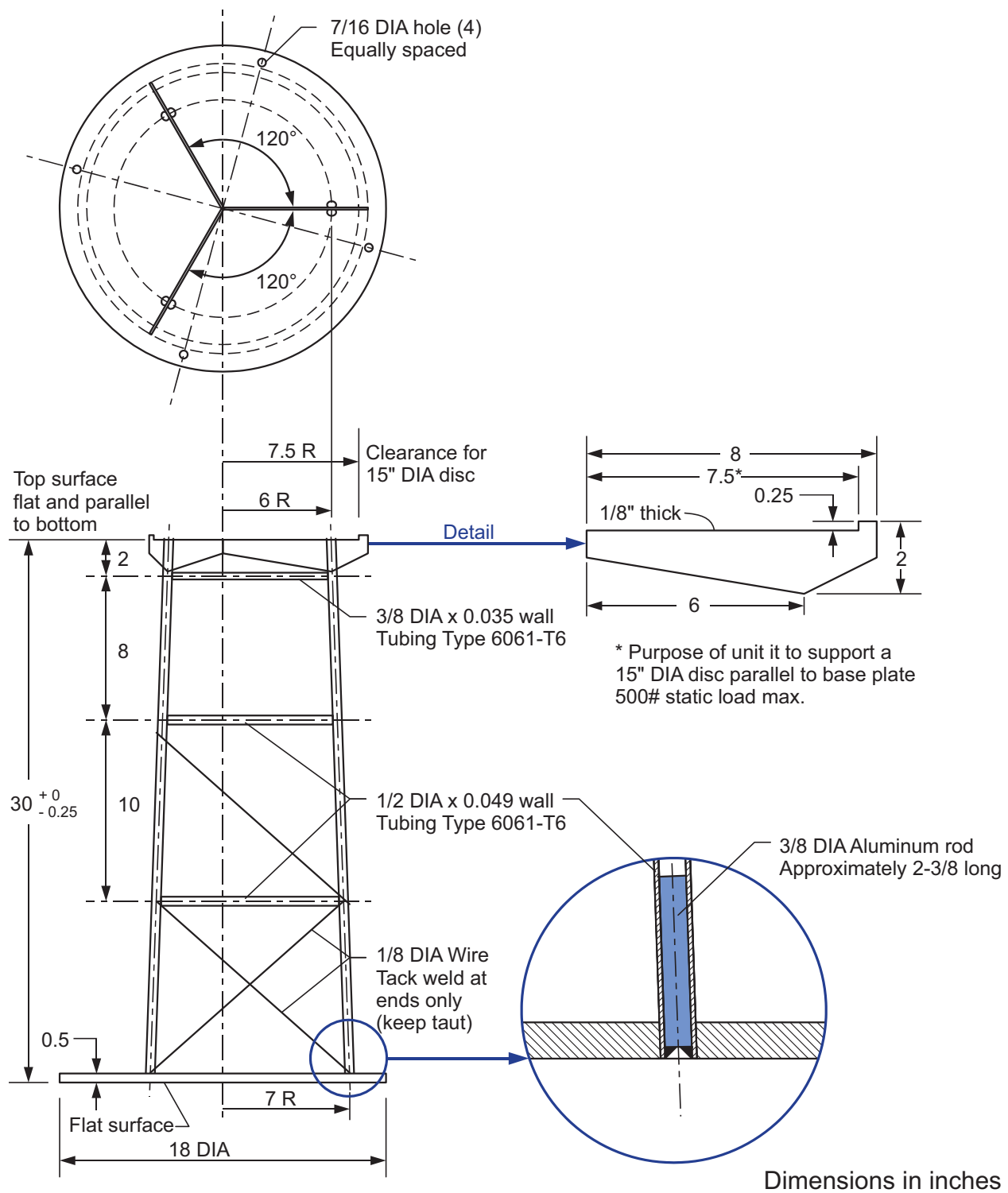


Figure D.1. Diaphragm Support Structure.



10-GA50002-73-2

Figure D.2. Low-Mass Support Structure.